JPRS-CST-87-025
10 JUNE 1987

JPRS Report

Science & Technology

China

SPECIAL NOTICE

Effective 1 June 1987 JPRS reports will have a new cover design and color, and some reports will have a different title and format. Some of the color changes may be implemented earlier if existing supplies of stock are depleted.

The new cover colors will be as follows:

CHINA.....aqua
EAST EUROPE.....gold
SOVIET UNION.....salmon
EAST ASIA.....yellow
NEAR EAST & SOUTH ASIA...blue
LATIN AMERICA.....pink
WEST EUROPE.....ivory
AFRICA (SUB-SAHARA).....tan
SCIENCE & TECHNOLOGY.....gray
WORLDWIDES.....pewter

The changes that are of interest to readers of this report are as follows:

All science and technology material will be found in the following SCIENCE & TECHNOLOGY series:

CHINA (CST)
CHINA/ENERGY (CEN)
EUROPE & LATIN AMERICA (ELS)
JAPAN (JST)
USSR: COMPUTERS (UCC)
USSR: EARTH SCIENCES (UES)
USSR: MATERIALS SCIENCE (UMS)
USSR: LIFE SCIENCES (ULS)
USSR: CHEMISTRY (UCH)
USSR: ELECTRONICS & ELECTRICAL ENGINEERING (UEE)
USSR: PHYSICS & MATHEMATICS (UPM)
USSR: SPACE (USP)
USSR: SPACE BIOLOGY & AEROSPACE MEDICINE (USB)
USSR: SCIENCE & TECHNOLOGY POLICY (UST)
USSR: ENGINEERING & EQUIPMENT (UEQ)

The USSR REPORT: MACHINE TOOLS AND METALWORKING EQUIPMENT (UMM) will no longer be published. Material formerly found in this report will appear in the SCIENCE & TECHNOLOGY/USSR: ENGINEERING & EQUIPMENT (UEQ) series.

If any subscription changes are desired, U.S. Government subscribers should notify their distribution contact point. Nongovernment subscribers should contact the National Technical Information Service, 5285 Port Royal Road, Springfield, Virginia 22161.

JPRS-CST-87-025

10 JUNE 1987

SCIENCE & TECHNOLOGY

CHINA

CONTENTS

APPLIED SCIENCES

NATIONAL DEVELOPMENTS

/9987

TWO-LASER RESONANCE ENHANCED PHOTOIONIZATION SPECTRUM OF GAS PHASE BENZENE

Shanghai GUANGXUE XUEBAO [ACTA OPTICA SINICA] in Chinese Vol 7 No 1, Jan 87 pp 1-10

[English abstract of article by Fan Junying [5400 0193 4481] of Shanghai Institute of Optics and Fine Mechanics, Chinese Academy of Sciences; G. Muller, W.E. Schmid and K.L. Kompa of Max-Planck-Institute for Quantum Optics, Munich; J.L. Lyman of Los Alamos National Laboratory, New Mexico]

[Text] This paper reports the results of a two-laser resonance enhanced photoionization experiment with benzene molecules. The excitation was provided by two frequency doubled dye lasers. The first laser pumped the molecule to a selected single state (S-1), from where it was ionized by a time delayed pulse of the second laser. The ion quantum yield depends on the intermediate vibronic state as well as on the wavelength of the ionizing laser. From the structure and intensity of the measured ion spectrum, the authors derived vibrational frequencies and molecular parameters of the ground electronic state of the ion that were highly precise. The contributions of autoionizing Rydberg levels to the ionization cross sections could be clearly distinguished from those of direct ionization. Some of these resonance peaks could be assigned to vibrations within these Rydberg states.

The work was done at Max-Planck-Institute for Quantum Optics in West Germany.

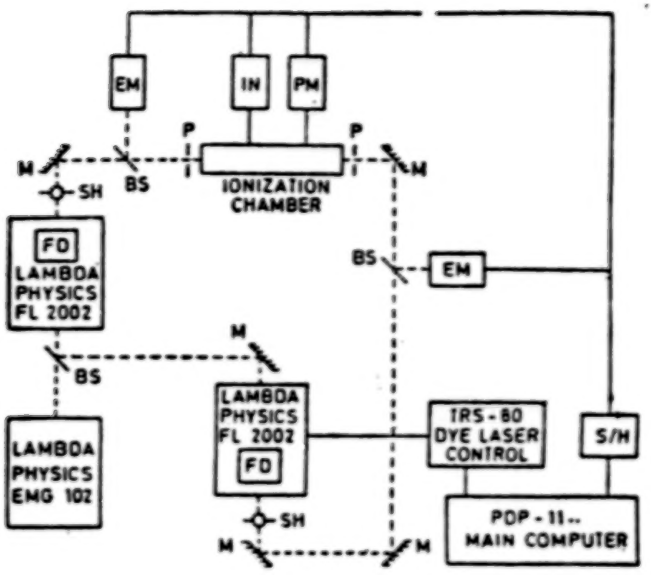

S/H: SAMPLE AND HOLD
EM: ENERGY METER R_J 7100
IN: INTEGRATOR
PM: PRESSURE METER
M: MIRROR
BS: BEAMSPLITTER
FD: FREQUENCY DOUBLING
SH: SHUTTER
P: PINHOLE

Fig. 1 The experimental arrangement

9717
CSO: 4009/39

RESONANT SELF-FOCUSING OF TWO-FREQUENCY LASER BEAMS IN PLASMAS

Shanghai GUANGXUE XUEBAO [ACTA OPTICA SINICA] in Chinese Vol 7 No 1, Jan 87 pp 27-35

[English abstract of article by Xu Tiefeng [1776 6993 1496], et al., of Shanghai Institute of Optics and Fine Mechanics, Chinese Academy of Sciences]

[Text] In this paper the authors have studied theoretically the resonant self-focusing of two-frequency laser beams in plasmas. From the plasma fluid equations, the authors have derived an expression for the nonlinear dielectric constants of plasmas driven by two-frequency laser beams, showing the effect of the ponderomotive force of the plasma waves. After presenting an approximate solution for the longitudinal electrostatic field, characteristics of resonant self-focusing are shown. Finally, the influence of resonant self-focusing on particle acceleration in a beat wave accelerator is also discussed.

9717
CSO: 4009/39

STIMULATED ELECTRONIC RAMAN SCATTERING IN SODIUM VAPOR

Shanghai GUANGXUE XUEBAO [ACTA OPTICA SINICA] in Chinese Vol 7 No 1, Jan 87 pp 17-21

[English abstract of article by Ma Zuguang [7456 4372 0342], et al., of the Laser Division, Harbin Institute of Technology]

[Text] The first observation of the 3S-4S stimulated electronic Raman scattering (SERS) in sodium vapor with infrared output tunable from 2.38 μm to 2.65 μm is reported. The calculation for the power gain factors and the measurement for the infrared output as a function of dye laser tuning are made and are in good agreement. The pumping threshold as correlated to sodium vapor pressure is measured. The photo-conversion efficiency is about 30 percent. In addition, the amplified spontaneous emission (ASE) of the Na 4S-3P transition is also observed.

9717
CSO: 4009/39

INTRACAVITY ABSORPTION SPECTROSCOPY WITH RING TRAVELING-WAVE DYE LASER

Shanghai GUANGXUE XUEBAO [ACTA OPTICA SINICA] in Chinese Vol 7 No 1, Jan 87 pp 11-16

[English abstract of article by Yong Huayong [7167 5478 5554], et al., of the Department of Physics, Sichuan University, Chengdu]

[Text] By using a cw ring traveling-wave dye laser enhancement factor up to 10^5 of the intracavity absorption, sensitivity was obtained in air even if the pump power was two times over the threshold. Using the single-frequency scanning method for the first time, a resolution of 10^{-2} angstrom was measured without sensitivity reduction. The experimental results agree with the predictions of the modified Brunner-Paul theory.

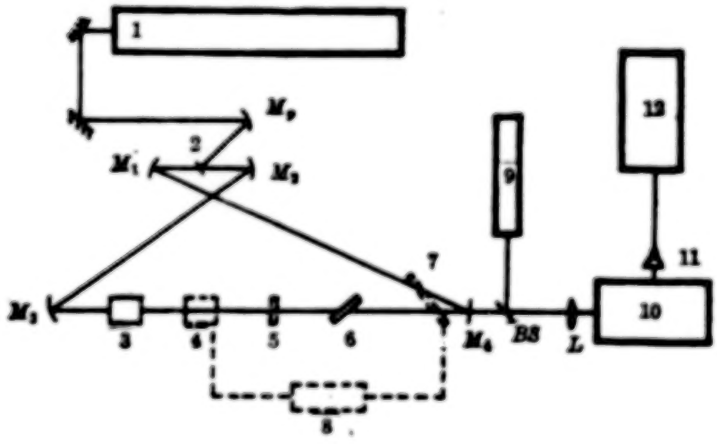

Fig. 1 Experimental set-up for broadband scanning (dashed-line represents the inserted parts in single-frequency scanning)
1—Mode 360 Argon laser, *2*—Dye jet, *3*—Unidirectional device, *4*—Thick etalon, *5*—Thin etalon, *6*—Birefringent filter, *7*—Galvanometer plate, *8*—Lock circuit standard light resource, *10*—Model CT-50 monochrometer, *11*—Photodiode, *13*—X-Y recorder

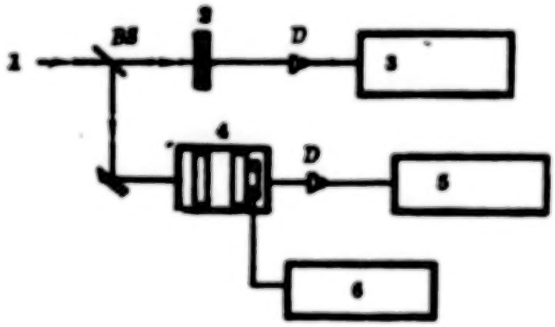

Fig. 2 Monitor and recorder for single-frequency scanning
1—Dye laser, *2*—Attenuator, *3*—X-Y recorder *4*—1.5GHz scanning etalon, *5*—CS-2100 oscilloscope, *6*—Model SMY generator

9717
CSO: 4009/39

LASER INDUCED CHEMICAL ETCHING BY A SINGLE STEP

Shanghai GUANGXUE XUEBAO [ACTA OPTICA SINICA] in Chinese Vol 7 No 1, Jan 87 pp 49-54

[English abstract of article by Li Ding [2621 0002], et al., of Shanghai Institute of Laser Technology]

[Text] The scanning etching on Si, GaAs and Zn plates with a frequency doubling Ar^+ laser at 257.3 nm is reported. The width of the smallest etched line (1.2 m) has been obtained. The dependence of the etching depth on the light intensity/scanning rate is given. The diffusion coefficient, free path of the halogen radical and scale of laser focused spot have been estimated for the first time using the laser etching technique. A threshold phenomenon has been observed and explained.

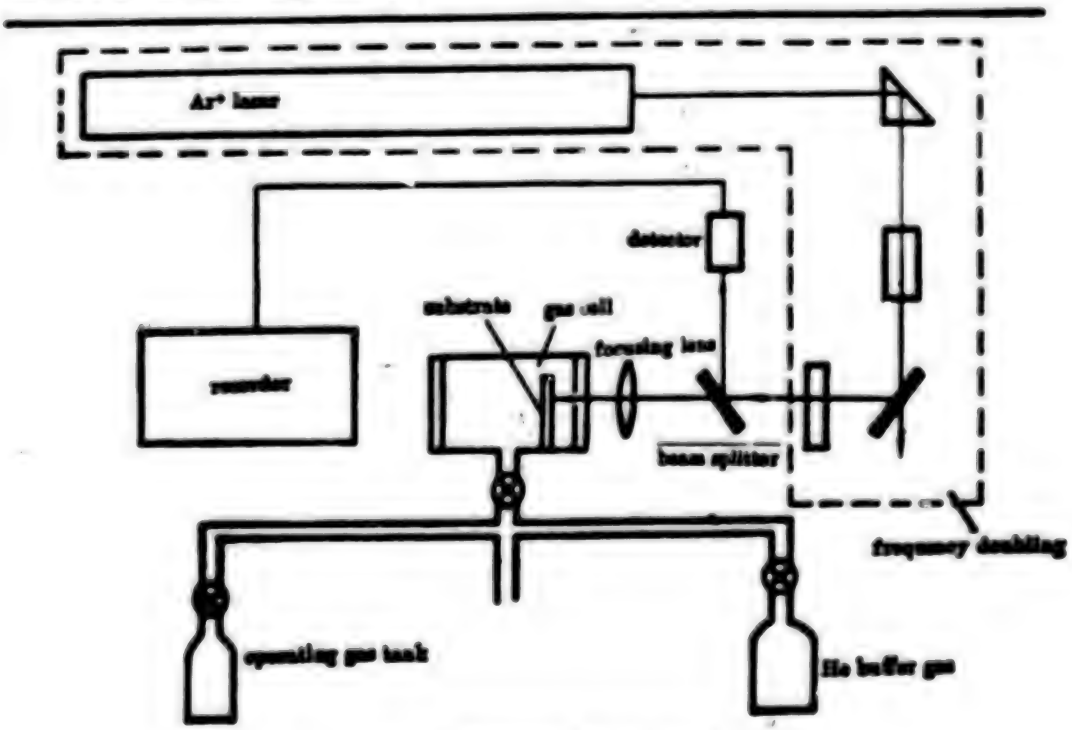

Fig. 1 Experimental arrangement

9717
CSO: 4009/39

STUDY OF IR LASER PHOTOACOUSTIC SPECTRA OF ORGANIC MOLECULES ADSORBED ON METAL SURFACE

Shanghai GUANGXUE XUEBAO [ACTA OPTICA SINICA] in Chinese Vol 6, No 12, Dec 86 pp 1057-1062

[Article by Lu Huizong [7120 1920 1350], Chen Kaitai [7115 7030 3141], He Maoqi [0149 2021 4388], and Wang Zhaoyong [3769 0340 3057] of the Department of Physics, Fudan University, Shanghai; paper received 7 Dec 1985; revised manuscript received 24 Mar 1986; this paper was read at the 1985 National Optics Annual Meeting]

[Text] Abstract]: Using a branch-tuning CW CO_2 laser in the range of 0.2 μm to 10.8 μm we studied the IR photoacoustic spectra of organic molecules adsorbed on a silver surface. The absorbed molecular spectra of four layers of arachidic acid and cellulose diacetate with different surface densities was studied. No peak shift was found in a comparison between the IR photoacoustic spectra of solid arachidic acid near 944 cm^{-1} and the corresponding IR Fourier spectra of solid archidic acid. The IR photoacoustic spectra of cellulose diacetate with $\sigma_1 = 1.4X10^{5}$ cm^{-2} and $\sigma_1 = 5.5X10^{15}$ cm^{-2} respectively was compared with the corresponding transmission spectra of solid cellulose diacetate. It was found that the peak of the former near 1054 cm^{-1} had a red shift of about 5 cm^{-1} while the peak of the latter had no obvious shift within the range of accuracy of the experiment.

I. Introduction

Study of the physical properties of surface adsorption molecules has major significance for new chemical reaction catalysts, anti-corrosiveness of materials, surface oxidation properties of semiconductors as well as for material that have special behavior and surface treatment work. For surface research there are at present several very effective means for surface detection but they all has their limitations. The photoacoustic spectrum serves as a new detection means which can supplement the other methods to more clearly and effectively study surface physics problems. This is especially so for molecular adsorption. Because the vibratory state of characteristic molecular features generally are in the infrared region, infrared laser photoacoustic spectra will be an extremely effective means for the study of surface adsorption. Since the sensitivity of

photoacoustic spectra is very high, it is entirely possible that it can be used to study monolayer and sublayer adsorbed molecules.[1,2] This paper, using cellulose diacetate molecules as example, based on the adsorption coefficient of this sort of molecule in the vicinity of 1054 cm^{-1},[3] prepared sample surfaces with densities of $\sigma_1 = 1.4X10^{15}$ cm^{-2} and celluloid series samples with specific gravity from 1.27~1.61 g cm^{-3}.[4] Experiments showed that photoacoustic spectral methods were quite sensitive when used to study the surface adsorption states.

II. Experimental Apparatus and Measuremen

The experimental apparatus was as shown in Figure 1. The light source was a homemade branch tunable CW CO_2 laser with wave length range of 9.2~10.8 μm, maximum power of 10 W, and a linearly polarized beam. The photoacoustic detector was made from a S_4 type piezoelectric ceramic transducer (PZT). One side of an optically polished slab (20 X 40 X 2) piezoelectric ceramic transducer was vapor plated in a vacuum (~10^{-6} Torr) with a high purity layer of silver about 1 μm thick. Electrodes were led respectively from its two faces forming one detector. Because the sample on the surface is thin, during measurement after the silver base on the piezoelectric ceramic itself absorbs optical energy it produces a photoacoustic signal. This signal constitutes a background that cannot be ignored with respect to the entire measurement.

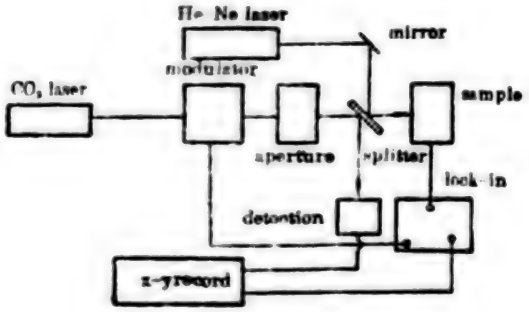

Fig. 1 Setup of the experiment

1. Preparation of adsorption state sample

In the experiment the preparation of the arachidic acid molecular sample was done with the die method to make an L-B film on the silver surface.[6] Arachidic acid molecules in a clean deionized water surface can form a very thin single layer film. If, along the direction of the film surface, there is applied a fixed surface tension, then it can form a dense monomolecular thin film.[7] The arachidic acid molecule forms a rod shaped molecule, one end of which is hydrophobic and the other hydrophilic. The hydrophobic end of the molecular film faces the outside of the solution surface. When preparing the sample, one slowly immerses the piezoelectric transducer into the solution surface and the hydrophobic ends of the arachidic acid molecules adsorb on the silver surface forming a monomolecular sample. Then, again slowly, removing transducer from the solution the first monomolecular

film adsorbs another layer of which the hydrophobic ends face outward as shown in Fig. 2. By repeating this procedure, the metallic surface forms a polymolecular film. In these experiments four layer molecular samples were prepared.

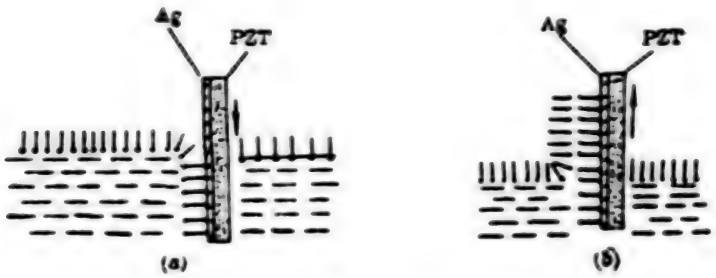

Fig. 2

(a) Arachidic acid molecules adsorbed on the surface of evaporated silver film of the detector, which is being slowly thrusted in to the molecular film

(b) Molecules adsorbed on the surface of evaporated silver film of the detector, which is being slowly lifted up from the molecular film

To prepare the cellulose diacetate molecular samples we took 18 mg of cellulose diacetate sample solution and dissolved it in an 80 mg acetone solution. The, using a micro-dropper to takeup a sample, it was dropped on the rotating silver plating surface of the piezoelectric ceramic transducer. Based on the molecular weight of this molecule and the surface area of the detector we estimated the molecular surface density of the sample on the silver surface. The surface densities of the samples prepared for the experiments were $\sigma_1 = 1.4X10^{15}$ cm^2 and $\sigma_2 = 5.5X10^{15}$ cm^{-2}.

2. Method of measurement

This paper adopted the differencing measurement method with a single light path. The laser beam was incident successively on two piezoelectric ceramic transducers as shown in Fig. 3. PZT(1) and PZT(2) are two piezoelectric ceramic transducers with the same properties, polished and silver plated under identical conditions then placed in a vacuum chamber as shown in Fig. 3. The surface of PZT(2) was prepared with the sample to be measured while no sample was prepared for the surface of PZT(1). With a p polarized laser beam incident on the sample of PZT(2) at an angle of 80°, the electrical signals produced by PZT(1) and PZT(2) were separately input to a dual channel phase locked amplifier. Doing subtractive measurements and simultaneously monitoring the power one can get

$$S(\lambda) = \frac{S_{PA}^{PZT(2)} - S_{PA}^{PZT(1)}}{S_{PA}^{PZT(1)}},$$

in which $S_{PA}^{PZT(1)}$ and $S_{PA}^{PZT(2)}$ are the respective photoacoustic signal strengths received by transducer (2).

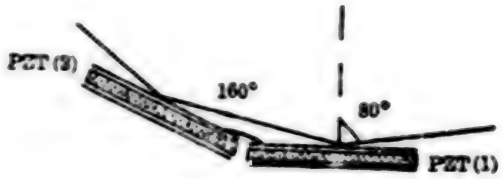

Fig. 3 Location of detectors. The angle between the two detectors is 160°

Since the samples of adsorbed molecules are very thin films, the absorption can be approximated linearly and considering that absorption of the metal itself is directly proportional to $(1 - R_{Ag})$, in the end we can get

$$S(\lambda) = \frac{2\chi\alpha(d/\cos\varphi)}{1 - R_{Ag}(\lambda, \varphi)}, \tag{1}$$

where χ is a constant related to the thermodynamic properties of the sample and the silver base, α is the absorption coefficient of the adsorbed sample, d is the thickness of the sample, and $R_{Ag}(\lambda,\phi)$ is the reflectivity of the silver base at wave length λ, and incident angle ϕ. From formula (1) we can see that $S(\lambda)$ is directly proportional to $\alpha(d/\cos\phi)$, that is in direct proportion to the sample absorption coefficient and also to the sample thickness d. Also $S(\lambda)$ is also related to $R_{Ag}(\lambda,\phi)$. However, from theoretical estimates we know that in the vicinity of absorption peaks of the sample, the variation of $(\alpha\, d/\cos\phi)$ with wave length is much greater than the variation of $[1-R_{Ag}(\lambda,\phi)]^{-1}$ with wave length. The reflectivity of metals in the infrared region and their conductivity at this time can be represented approximatley by their static values[5]

$$R_{Ag}(\lambda) = 1 - 2\sqrt{\frac{c}{\lambda\cdot\sigma}} + \cdots, \tag{2}$$

$$A(\lambda) = \frac{1}{[1 - R_{Ag}(\lambda)]} = \frac{1}{2}\sqrt{\frac{\sigma\lambda}{c}}, \tag{3}$$

in which σ is the conductivity of silver, λ is the wave length, and c is the speed of light. For the wave length range measured in our experiments, 9.2 μm~110.8 μm, the corresponding $(\Delta A/A(\bar{\lambda}))$ was

$$\Delta A/A(\bar{\lambda}) < 0.08. \tag{4}$$

From formula (4) we can see that in the wave length range used in our experiments, since the variation of $S(\lambda)$ caused by changes in $R_{Ag}(\lambda,\phi)$ was less than 8% while the absorption coefficient of general samples at

absorption peaks can be several times to several magnitudes more than at non-absorption peaks. The experimental results show that the influence of silver's basic reflectivity is very small and moreover that the change in this sort of effect with wave length is monotonic and therefore cannot have a very great influence on the spectral structure.

In our experiments the modulation frequency of the laser was 23 Hz and a small diaphragm (d = 2.0 mm) was used to obstruct a part of the edge light. The He-Ne laser in the experimental apparatus followed the same light path as the CO_2 laser beam to act as an index beam for adjusting the light path.

III. Experiment Results

The experiment measured four layers of arachidic acid. The results are as shown in Fig. 4, in which the vertical coordinate is arbitrary units representing the strength of the photoacoustic signal. Figure 5 is the infrared Fourier spectra for solid sample of arachidic acid. A comparison of Fig. 4 and Fig. 5 reveals that in the 924.90 cm^{-1} ~ 1086.84 cm^{-1} (i.e. 10.8 ~ 9.2 μm) band region, the peak at 944 cm^{-1} in the photoacoustic spectrum corresponds to the absorption peak at the same location in the Fourier spectrum. The absorption peak of arachidic acid in the vicinity of 944 cm^{-1} corresponds to the characteristic absorption of the carboxyl group cluster. Figure 6 shows the measured results of a sample of cellulose diacetate with molecular surface densities of $\sigma_1 = 1.4X10^{15}$ cm^{-2} and $\sigma_2 = 5.5X10^{15}$ cm^{-2}. Figure 7 is the infrared trnasmission spectrum of a sample of cellulose diacetate. The two spectra in Fig. 6 separately represent the photoacoustic spectra of the two samples with different molecular surface densities. From these results we see that the peak value amplitude and the surface density are in direct proportion which is in agreement with formula (1).

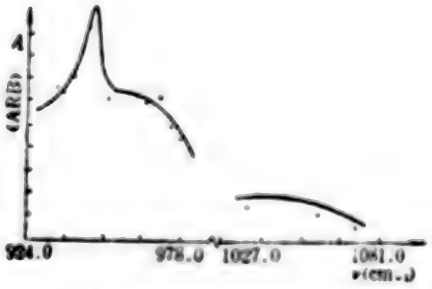

Fig. 4 IR laser photoacoustic spectrum of four layers of Arachidic acid molecules adsorded on the surface of silver. The wavenumber of the peak is 944 cm^{-1}

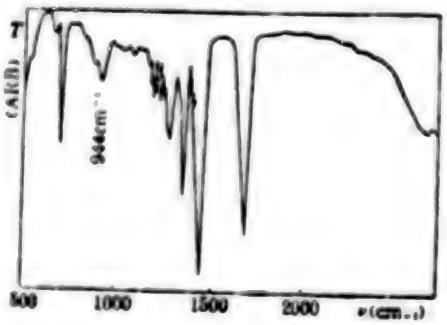

Fig. 5 Infrared Fourier transmittance spectrum of Arachidic acid

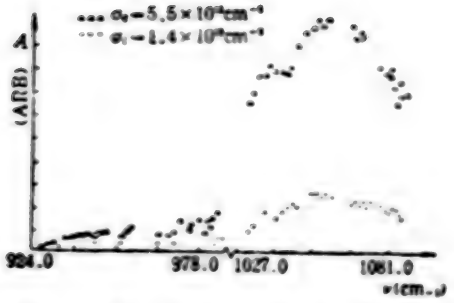

Fig. 6 IR laser photoacoustic spectra of Cellulose diacetate molecules adsorbed on the surface of silver with surface densities of $\sigma_1 = 1.4 \times 10^{15}\,cm^{-2}$ and $\sigma_1 = 5.5 \times 10^{15}\,cm^{-2}$, respectively. The wavenumbers of the peaks are $1054\,cm^{-1}$ and $1059\,cm^{-1}$, respectively

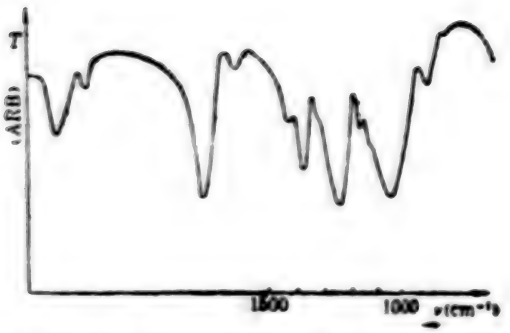

Fig. 7 IR transmittance spectrum of Cellulose diacetate. The marked peak in the spectrum is what we studied in the experiment. The wavenumber of the peak is $1059\,cm^{-1}$

The peak value positions of the photoacoustic spectra are at 1054 cm^{-1} (σ_1) and 1059 cm^{-1} (σ_2) respectively. The former has about a 5 cm^{-1} red shift and the latter has no clearly observable shift within the experiment's range of precision relative to the peak position of this location in the absorption spectrum of Fig. 7.

IV. Discussion

That there is no observable shift of the peak value of arachidic acid's photoacoustic spectrum at the 944 cm^{-1} position with respect to the absorption spectrum is possibly related to the arrangement of arachidic acid on the silver surface. Arachidic acid is a long chain molecule with one end that is hydrophilic while the other is hydrophobic so that arrangement of its molecules on the silver surface is as shown in Fig. 8. In the figure the round head of the rod shaped molecule represents the hydrophilic end while the hydrophobic end is in contact with the silver surface. The length of the molecule is 26 Å and the 944 cm^{-1} peak corresponds to the carboxyl group culster of the hydrophilic end.[8] Consequently the influence of the silver surface on the carboxyl group cluster is very small and the peak has no clear shift. On the other hand, the cellulose diacetate molecules cover the silver surface chaotically so there is always the ether and acetal structure of a portion of the molecules (corresponding to a 1059 cm^{-1} peak value) that will receive direct influence from the silver surface. When the sample is very thin this influence will be more pronounced since there is a relative increase in the molecules in direct contact with the surface causing a red shift of the spectrum at the 1059 cm^{-1} peak value.

Photoacoustic spectra are a sensitive spectroscopy technique which can easily be applied in high vacuum conditions to study adsorption questions

of several simple molecules. The high vacuum environment can effectively suppress external acoustic interference but if one further applied low temperature cooling to the sample, then the effect of thermal noise would be reduced and in a high vacuum, low temperature environment we could expect a vast increase in sensitivity of measurement. Another course to increase measurement sensitivity is to use a surface electromagnetic wave method to make the laser beam and the surface adsorbed molecules more effectively interact. We used a prism coupled exciter surface electro-magnetic wave to excite the adsorbed molecules and then examined the photoacoustic signals of the molecule, i.e. surface electro-magnetic wave photoacoustic spectroscopy. Preliminary results prove that the strength of photoacoustic signals produced with this method are several times greater than direct incidence. The detailed results of our work in this area will appear in another report.

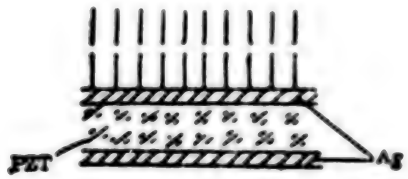

Fig. 8 Arachidic acid molecules (two layers) stand up on the surface of silver, the sticks stand for the molecules and the dot heads of the sticks stand for the parts of positive hydrotropism

We express our gratitude to our colleague, Zhao Youyuan, for providing several beneficial suggestions and much concrete assistance and to Wang Yuhang for providing the arachidic acid samples and the preparation techniques.

REFERENCES

1. F. Trager, H. Coufal, PHYS. REV. LETT., 1982, 42, No. 23 (Dec), 1720.

2. H. Coufal, F. Trager, SURFACE SCI., 1984, 145, No. 2/3 (Oct), L504.

3. K. Bhasin, D. Bryan, J. CHEM. PHYS., 1976, 64, No. 12 (Jun), 15.

4. "CRC Handbook of Chemistry and Physics", 58th ed., (CRC handbook 18901 Cranwood parkway Cleveland, Ohio 44128 U.S.A.), C242, 1977.

5. M. Bron, E. Wolf, "Principles of Optics", (Pergamon press 5th ed., 1975, Oxford), 611.

6. K. Boldgett, I. Langmuir, PHYS. REV., 1937, 51, June 1, 964.

7. Georg Hass et al. ed., PHYSICS OF THIN FILMS, Vol 7, (Academic Press, 1973), 311.

8. Wang Zongming et al., SHIYONG HONGWAI GUANGPUXUE [PRACTICAL INFRARED SPECTROSCOPY] in Chinese, (Petrochemical Industry Press, 1978), 211.

12966/9835
CSO: 4008/34

GENERATION OF IR STIMULATED RADIATION, UV VISIBLE VIOLET COHERENT RADIATION BY TWO-PHOTON RESONANCE PUMPING IN K VAPOR

Shanghai GUANGXUE XUEBAO [ACTA OPTICA SINICA] in Chinese Vol 6, No 12, Dec 86, pp 1063-1070

[Article by Wang Zugeng [3769 4371 6342], Tang Xiaoling [0781 1420 3781], Zhang Kiachang [1728 7030 2490], and Zheng Yishan [6774 0001 0810] of the Department of Physics, East China Normal University; paper received 4 Feb 1986; revised manuscript received 22 Apr 1986; first paragraph is source-supplied abstract]

[Text] Abstract: When two-photon excited potassium atoms reach the 7S energy level, a series of photo-pumped stimulated emissions and cascade stimulated emissions are observed in the infrared region. The processes of photo-pumped stimulated emission and two-photon resonance four-wave mixing of pumped light produced corresponding strong coherent emission at 6P-4S and 5P-4S. These two coherent emissions also had the function of pumped light and through a succession of four wave mixing processes produced several coherent emissions in the ultraviolet and the visible regions. This article discusses the process of generation of these observed infrared stimulated emissions as well as the ultraviolet and visible coherent emissions.

Introduction

The use of photo-puming to produce stimulated emission and new coherent emissions obtained from mixing has long aroused interest. In metal vapors, the two-photon excitation of Na, K, Ba, and Cs atoms through four-wave mixing and other processes has lead to observations of several coherent emissions.[1-5]

In our work, we used a YAG laser pumped dye laser and with dual photon excited potassium atoms from the ground state, 4S, to 7S. An infrared detector received the photo-pumped infrared emission and a series of cascade stimulated emissions from the 7S output. We used a photoelectric multiplier tube to detect these infrared stimulated emissions and the strong ultraviolet coherent emissions produced by pumped beam four-wave mixing interaction as well as to detect the ultraviolet and visible coherent emissions produced by these ultraviolet coherent emissions when acting as a pumping beam through successive four-wave mixing processes.

We identified the 10 infrared stimulated emission lines observed in the 1.18 μm to 7. 9 μm region. We also discussed the formation process for the 30-odd coherent emission lines in the 345.3 nm to 560.3 nm region.

Experiment

The experimental apparatus is as shown in Figure 1. A pulsed YAG frequency doubler laser, 1, pumps a dye laser, 2. When using DCM dye, the output energy in the vicinity of 660.0 nm is about 5 mJ and the laser output line width is about 0.01 nm.

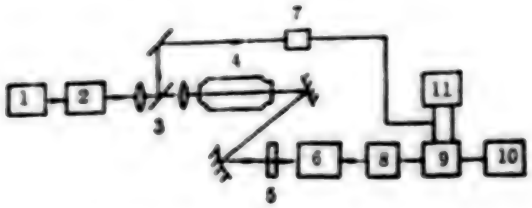

Fig. 1 Experimental setup

1—Nd:YAG laser; *2*—Dye laser; *3*—lens; *4*—heat-pipe oven; *5*—filters; *6*—grating monochromator; *7*—triggering detector; *8*—signal detector; *9*—signal processing system; *10*—Chart recorder; *11*—oscilloscope.

The dye laser beam is focused through a lens onto the center of the heat-pipe oven, 4, affixed to the potassium. The heat-pipe oven is 650 mm long, with a diameter of 25 mm, and heating region lenggh of 250 mm. The incident and emergent ends of the pipe oven are fixed separately to quartz and CaF_2 windows. Using an auto thermostat the heat pipe oven is heated to 400°C where the corresponding concentration of potassium atoms is 10^{16} cm^{-3}.[6]

The directed infrared, visible, and ultraviolet emission signal emergent forward from the heat-pipe oven displays a light spot. At about 1 meter from the center of the heat-pipe oven, the radius of the light spot is about 3 mm. After passing through the filters, 5, the stimulated emissions and coherent emissions enters the monochromator, 6, for spectroscopic analysis. Appropriate band pass optical filters are used for the different signals in the infrared, visible, and ultraviolet regions to filter out the extraneous pumped light and leave the signals in the band to be analyzed. The infrared band signals emergent from the monochromator are received by a PbS detector of a 'Gaolai' pool while after being received by a photo-electric multiplying tube, the visible and ultraviolet band signals are fed through a signal processing system, 9, and recorded by the chart recorder, 10, and observed on an oscilloscope, 11. The detector, 7, received a minute quantity of pumped light to provide the trigger signal required by the signal processing system and the oscilloscope.

II. Results and Discussion

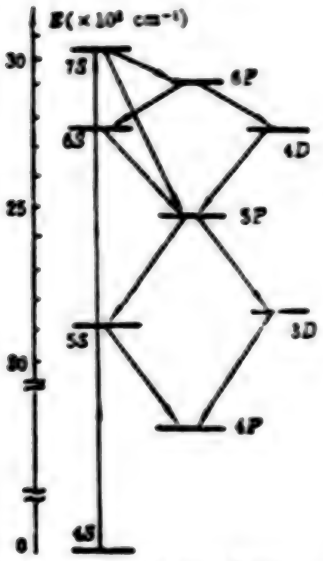

Fig. 2 Energy level diagram of potassium and two-photon pumped stimulated radiation

Figure 2 is a partial diagram of the potassium atom energy states.[7] When the output wave length, λ_L of the pumped beam is tuned to 660.45 nm, the potassium atom is excited by a two-photon resonance from the 4S ground state to the 7S state. The fixed direction emission spectral components of the forward emergent ray from the heat-pipe oven, after detailed measurement and computation can be divided into the following types based on the process of generation.

1. Two-photon Resonance Pumped Stimulated Emission

When the potassium atom is stimulated by two-photon resonance to the 7S state, population inversions form between the 7S state and 6P state and between the 7S state and the 5P state consequently producing 7.89 μm and 1.80 μm stimulated emissions. The stimulate emission coming from the 7S state also made the 6P state become largely population in turn forming population inversions between the 6P state and the 6S state and between the 6P state and the 4D state thereby producing the 6.43 μm and 6.21 μm first degree cascade stimulated emissions. Similarly, second, third, and fourth degree cascade stimulated emission also is present. In the experiment, fourth degree cascade stimulated emission was observed as shown in Figure 2 and the final state of this emission was 4P. For greater clarity, the two-photon resonance pumping, the 7S to 6P stimulated emission, and the corresponding first degree of cascade stimulated emission processes can be represented as

$$K(4S)+2\omega_L \longrightarrow K^*(7S), \qquad (1)$$

$$K_i^*(7S) \longrightarrow K^*(6P) + \omega(7S - 6P,\ 7.89\,\mu\text{m}), \tag{2}$$

$$K^*(6P) \begin{cases} K^*(6S) + \omega(6P - 6S,\ 6.43\,\mu\text{m}), & (3) \\ K^*(4D) + \omega(6P - 4D,\ 6.21\,\mu\text{m}). & (4) \end{cases}$$

Table 1 lays out the wave lengths of the 10 stimulated emissions and cascade stimulated emissions observed in the experiment as well as indicating the corresponding energy state transitions.

Table 1 Stimulated and cascade stimulated radiation and corresponding transitions by two-photon, resonant pumping

No.	corresponding transition	theor. value (μm)	exp. value (μm)
1	7S→6P	7.89534	7.89
2	6P→6S	6.42252	6.42
3	6P→4D	6.21288	6.21
4	4D→5P	3.73412	3.73
5	6S→5P	3.66227	3.66
6	5P→3D	3.14154	3.14
7	5P→5S	2.70739	2.71
8	7S→5P	1.80046	1.80
9	5S→4P	1.25256	1.25
10	3D→4P	1.17729	1.18

2. Coherent emission produced by two-photon resonance four wave mixing.

From the above recounted four-wave mixing process by the interaction of two-photon resonance stimulated emission waves with the pumping waves, ultraviolet region coherent emission was produced. The form of mixing was

$$\omega_p = 2\omega_L - \omega_s, \tag{5}$$

in which ω_L is the pumping frequency, ω_S is the frequency of two-photon resonance stimulate emission or cascade stimulated emission, and ω_p is the coherent emission frequency produced by the process. Table 2 gives the 9 coherent emission lines belonging to this sort of mixing that wer observed in the experiment. In the table, the first column is the coherent emission wave length values observed experimentally and the second column

is the values computed by formula (5). The third column gives the frequency mixing form, and the fourth column notes the relative intensities of each coherent emission. We note that intensities were greatest for the coherent emissions produced by frequency mixing of two-photon stimulated emission waves and pumping waves (numbers 1 to 4 in Table 2.); with those produced by frequency mixing of first degree cascade emission waves and pumping waves next in intensity (numbers 5 and 6 in Table 2); while the weakest were those produced by the frequency mixing of second (or third) degree waves (numbers 7 to 9 in Table 2); and the experiment did not observe any coherent emissions involving fourth degree cascade emission waves.

Table 2 UV coherent radiation generated in two-photon resonant four-wave mixing

No.	exp. value λ(nm)	theor. value λ(nm)	form of mixing	relative intensity
1	344.66	344.67	$2\omega_L-\omega_S(7S-6P_{3/2})$	80.0
2	344.76	344.74	$2\omega_L-\omega_S(7S-6P_{1/2})$	76.0
3	404.42	404.41	$2\omega_L-\omega_S(7S-5P_{3/2})$	64.0
4	404.76	404.72	$2\omega_L-\omega_S(7S-5P_{1/2})$	61.0
5	348.75	348.76	$2\omega_L-\omega_S(6P-4D)$	15.0
6	348.15	348.12	$2\omega_L-\omega_S(6P-6S)$	20.0
7	362.00	362.96	$2\omega_L-\omega_S(6S-5P)$	8.5
8	362.30	362.26	$2\omega_L-\omega_S(4D-5P)$	6.0
9	369.05	369.02	$2\omega_L-\omega_S(5P-3D)$	4.5

From the polarization theory of nonlinear optics, the polarized intensity of the $\omega_P = 2\omega_L - \omega_S$ four-wave mixing process is

$$P^{(3)}(\omega_P) = \varepsilon_0 \chi^{(3)}(-\omega_P, \omega_L, \omega_L, -\omega_S) E_L^2(\omega_L) E_S^*(\omega_S), \qquad (6)$$

Here $E_L(\omega_L)$ and $E_S(\omega_S)$ are the electric field intensity of the laser field and the stimulated emission field produced by two-photon excitation, and $\chi^{(3)}$ is the third order polarization frequency of the process

$$\chi^{(3)}(-\omega_P, \omega_L, \omega_L, -\omega_S) = K \frac{N}{\hbar^3} \sum_{ijk} \frac{R_{gi} R_{ij} R_{jk} R_{kg}}{(\Omega_i - \omega_L)(\Omega_j - 2\omega_L)(\Omega_k - \omega_P)}, \qquad (7)$$

Here N is the density of the atom, R_{ij} is the electric dipole matrix element between the ith and jth energy states, and $\Omega_i = [(E_i - E_g)/\hbar] - i\Gamma_i$ is the complex frequency. Γ_i is a quantity related to the lifetime and relaxation of the ith energy state and K is a numerical factor. From formula (6) we see that the polarization intensity of the coherent field produced by four-wave mixing is in direct proportion to the polarization frequency $\chi^{(3)}$ of this process, to the square of the laser field which participates in the frequency mixing, E_L^2, and to the stimulated emission field, E_S. For the four coherent emissions marked as 1 to 4 in Table 2, there correspond respectively two resonance strengthening terms, i.e.

$\Omega_{7S}-2\omega_L$, $\Omega_{6P_{3/2}}-\omega_P$, $\Omega_{7S}-2\omega_L$, $\Omega_{6P_{1/2}}-\omega_P$, $\Omega_{7S}-2\omega_L$, $\Omega_{6P_{1/2}}-\omega_P$, $\Omega_{7S}-2\omega_L$, $\Omega_{6P_{3/2}}-\omega_P$.

In addition, the stimulated emission fields $E_S[\omega_S(7S-6P)]$ and $E_S[\omega_S(7S-5P)]$ are the two strongest of the emissions in Table 1. Consequently these four coherent emission lines are very strong. The reason that emissions 5 and 6 in Table 2 are second is because in the expressions for $\chi^{(3)}$ we have respectively a single resonance factor, $\Omega_{7S}-2\omega_L$, and a nearly resonant factor, $\Omega_{6P}-\omega_P = 342\ cm^{-1}$ or $\Omega_{6P}-\omega_P = 292\ cm^{-1}$ and because the first degree cascade stimulated emission intensities, $E_S[\omega_S(7S-5P)]$. The last two coherent lines in Table 2 (9 and 10) are very weak because in the expression for $\chi^{(3)}$, there is only a single resonant term and because the second and third degree cascade stimulated emission fields are even weaker.

Figure 3 shows the two-photon resonance four-wave mixing form which produced the 344.6 nm ($6P_{3/2}$-4S) and 344.7 nm ($6P_{1/2}$-4S) coherent emission lines.

Fig. 3 Mixing scheme for generating 344.6 nm and 344.7 nm coherent radiation lines

3. Second Degree Frequency Mixing Coherent Emission With ω_P as the Pumping Beam

The strong coherent emission corresponding to the frequency $\omega_P = \omega(6P-4S)$ and $\omega_P' = \omega(5P-4S)$ produced by formula (5) can serve as a second degree pumping beam to produce four-wave mixing. At this time in the form of a single photon it pumps the potassium atoms and frequency mixes with the photon-pumped stimulated emission and the cascade stimulated emission described in the previous section. This produces a series of coherent emissions in the ultraviolet and visible region. The frequency mixing form is

$$\omega_0 = \omega_P - \omega_S' \mp \omega_S' \qquad (8)$$

in which ω_S' and ω_S'' are the stimulated emissions or cascade stimulated emissions listed in Table 1 and ω_c is the coherent emission produced by the second degree four wave mixing. For example, $\omega_S' = \omega_S(6P\text{-}6S)$, $\omega_S'' = \omega_S(5S\text{-}4P)$, while $\omega_P = 2\omega_L - \omega_S(7S\text{-}6P)$. Then the four-wave mixing represented by formula (8) can produce coherent emission with wave length 513.5 nm. Figure 4 shows this sort of second degree four wave mixing. The polarization intensity of this process is given by the following formulas

$$P^{(3)}_{(\omega_c)} = \varepsilon_0 \chi^{(3)}(-\omega_c, \omega_p, -\omega_s' - \omega_s'') E_p(\omega_p) E_s^*(\omega_s') E_s^*(\omega_s'') \tag{9}$$

$$\chi^{(3)}(-\omega_c, \omega_p, -\omega_s', -\omega_s'') = K' \frac{N}{h^3} \sum_{ijk} \frac{R_{gi} R_{ij} R_{jk} R_{kg}}{(\Omega_i - \omega_p)(\Omega_j - \omega_p + \omega_s')(\Omega_k - \omega_c)}. \tag{10}$$

For the frequency mixing form with a "+" in front of the ω_S'' it is only necessary in formulae (9) and (10) to change the ω_S'' to "$-\omega_S''$" and change $E_S^*(\omega_S'')$ to its complex conjugate $E_S(\omega_S'')$.

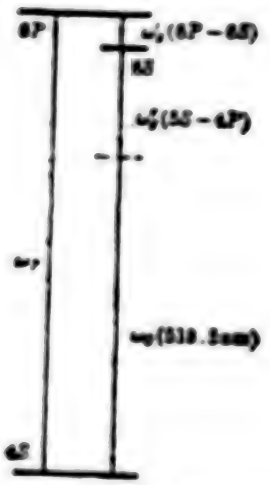

Fig. 4 Mixing scheme for generating 513.5 nm coherent radiation line

Table 3 gives the other 22 coherent emission lines observed in the experiment. There are produced by the four-wave mixing process with ω_P or ω_p as the pumping beam. The third column in thetable gives the form of the four wave mixing which corresponds to the coherent emission observed. We can see clearly that all take $\omega_S(4S\text{-}6P)$ as pumping beam. Moreover, at least one first degree cascade stimulated emission from Table 1 (i.e. $\omega_S(6P\text{-}6S)$ or $\omega_S(6P\text{-}4D)$) participates in the frequency mixing. So frequently not only are we able to observe in the experiment the corresponding second degree four-wave mixing coherent emission, but also the signal is a strong one (1 to 14 in Table 3). In fact, for conditions where $\omega_P(4S\text{-}6P)$ secondarily

pumps the sample, the ω_S(6P-6S) and ω_S(6P-4D) emissions also obtain resonance strengthening. In addition from formula (10) we know that for these 14 coherent emissions, their $\chi^{(3)}$ also have two resonance strengthening terms. The signals of the 8 coherent emissions from 15 to 22 in Table 3 are rather weak. From the frequency mixing forms to which they correspond we can see that some of them, although taking ω_p(4S-6P) as the pumping beam, a strengthened first degree cascade emission did not take part in the frequency mixing, or that the two original resonance terms in the expression for $\chi^{(3)}$ for a "+" taken in front of ω_S^H in formula (8) now has become one resonant term and one non-resonant term. Some take ω_p(4S-5P) = $2\omega_L - \omega_S$(7S-5P) as pumping beam and obviously their emissions will be much weaker than with ω_p'(4S-6P) = $2\omega_L - \omega_S$(7S-6P).

In summary, the above experimental facts are in very close agreement with theory. From formulae (9) and (10) we know that the strength of coherent emission fields produced in second degree four-wave mixing is in a direct porportion with pumping field strength and stimulated emission field strength of those that participate in the frequency mixing and with the polarization frequency of the process. If the pumping or the stimulated emission fields are weak the coherent field produced by the frequency will be weak. Also if

Table 3 Coherent radiation generated through the second four-wave mixing processes (pumping beam: $\omega_p = 2\omega_L - \omega_S(7S-6P)$ or $\omega_p' = 2\omega_L - \omega_S(7S-5P)$)

No.	exp. value λ(nm)	theor. value λ(nm)	form of mixing	relative intensity
1	365.30	365.27	$\omega_p - \omega_S(6P-4D) + \omega_S(6P-6S)$	12.0
2	381.82	381.80	$\omega_p - \omega_S(7S-6P) - \omega_S(6P-6S)$	30.0
3	382.60	382.57	$\omega_p - \omega_S(7S-6P) - \omega_S(6P-4D)$	27.5
4	386.10	386.09	$\omega_p - 2\omega_S(6P-6S)$	25.0
5	386.90	386.87	$\omega_p - \omega_S(6P-6S) - \omega_S(6P-4D)$	26.5
6	387.70	387.66	$\omega_p - 2\omega_S(6P-4D)$	25.0
7	403.60	403.55	$\omega_p - \omega_S(6P-6S) - \omega_S(4D-5P)$	25.0
8	405.25	405.29	$\omega_p - \omega_S(6P-4D) - \omega_S(6S-5P)$	25.0
9	412.00	411.96	$\omega_p - \omega_S(6P-6S) - \omega_S(5P-4P)$	15.5
10	413.90	413.86	$\omega_p - \omega_S(6P-4D) - \omega_S(5S-3D)$	14.0
11	420.82	420.79	$\omega_p - \omega_S(6P-6S) - \omega_S(5P-5S)$	13.5

[Table 3 continued on following page.]

[Table 3 continued.]

12	421.76	421.73	$\omega_p-\omega_g(6P-4D)-\omega_g(5P-5S)$	10.5
13	513.55	513.54	$\omega_p-\omega_g(6P-6S)-\omega_g(5S-4P)$	10.0
14	514.90	514.87	$\omega_p'-\omega_g(5P-5S)-\omega_g(6P-4D)$	8.0
15	373.10	373.08	$\omega_p'-\omega_g(6P-4D)+\omega_g(5P-5S)$	8.0
16	481.15	481.20	$\omega_p-\omega_g(7S-5P)-\omega_g(4D-5P)$	4.5
17	505.90	505.93	$\omega_p-\omega_g(7S-5P)-\omega_g(5P-5S)$	4.0
18	531.62	531.58	$\omega_p'-\omega_g(6S-5P)-\omega_g(5P-3D)$	8.0
19	546.45	546.49	$\omega_p-\omega_g(6S-5P)-\omega_g(5S-4P)$	8.5
20	544.90	544.92	$\omega_p'-\omega_g(5S-4P)+\omega_g(6P-4D)$	2.5
21	560.30	560.27	$\omega_p'-\omega_g(5P-5S)-\omega_g(5P-3D)$	8.0
22	376.18	376.14	$\omega_p-\omega_g(5S-4P)+\omega_g(7S-5P)$	1.5

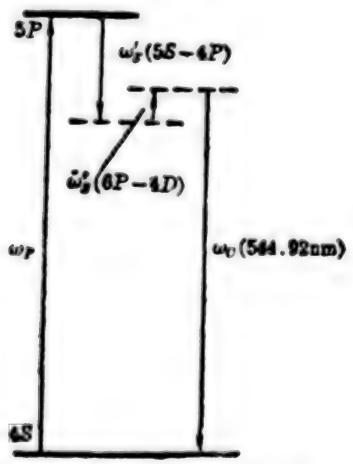

Fig. 5 Mixing scheme for generating 544.92 nm coherent radiation line

the resonance terms in the representation of the polarization frequency are few then the coherent emission field will be weak. The reverse is also true.

Figure 5 depicts the frequency mixing form producing a 544.9 nm coherent emission. Clearly, the coherent emission produced from this form of frequency mixing is weak.

Figure 6 shows the particl coherent emission lines observed. The frequency mixing form corresponding to each spectral line is also indicated in Fig. 6.

IV. Conclusion

In this work we excited potassium atoms with two-photon resonance to the 7S energy state and observed 10 two-photon resonance pumped stimulated emissions and multiple cascade stimulated emissions in the infrared region. By the process of two-photon resonance four-wave mixing, 9 ultraviolet coherent emissions were produced. Of these the two strongest coherent emissions, $\omega_P = 2\omega_L - \omega_S(7S\text{-}6)$ and $\omega_P' = 2\omega_L - \omega_S(7S\text{-}5P)$, could also serve as a pumping beam to excite the potassium atom and by the process of second degree frequency mixing we detected 22 coherent emissions in the ultraviolet and visible range.

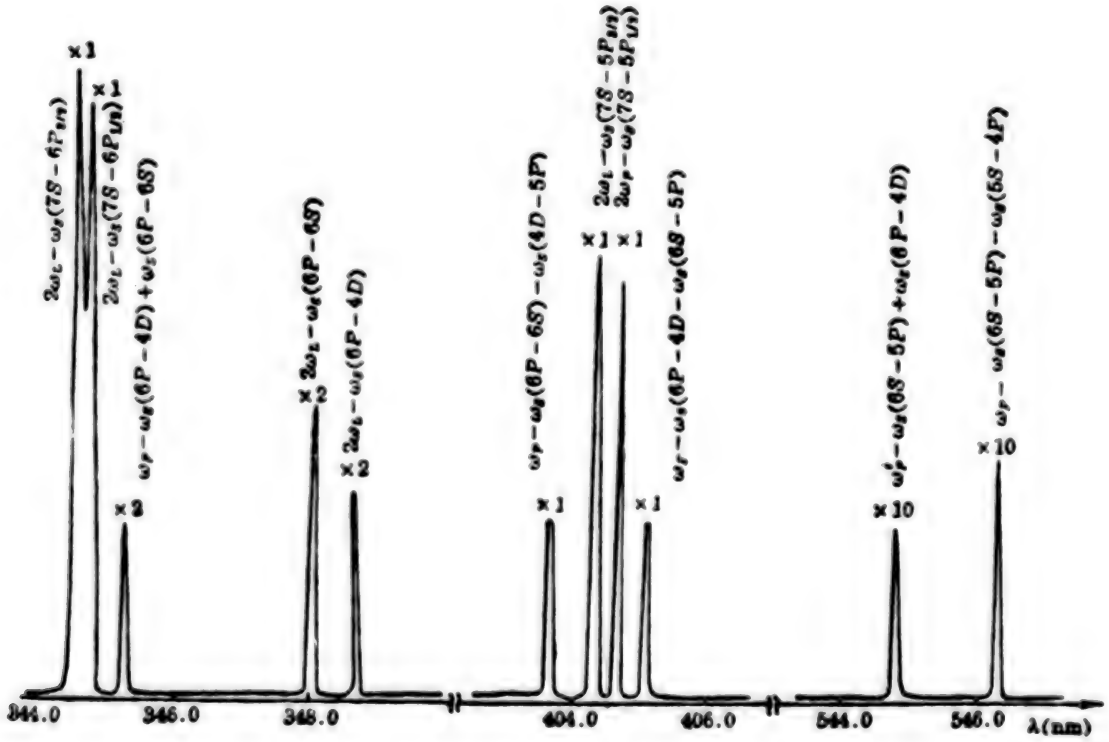

Fig. 6 Part of coherent radiation lines

REFERENCES

1. W. Hartig, APPL. PHYS., 1978, 15, No. 4 (Apr), 427.

2. P.-L. Zhang, Y.-C. Wang, A.L. Schawlow, J. O. S. A., 1984, 1, No. 1 (Mar), 9.

3. C.H. Skinner, H.P. Palenius, OPT. COMMUN., 1976, 18, No. 3 (Aug), 335.

4. J. Heinrich, W. Behmenburg, APPL. PHYS., 1980, 23, No. 3 (Nov), 333.

5. A.V. Smith, J.F. Ward, IEEE J. QUANT. ELECTRON., 1981, QE-17, No. 4 (Apr), 525.

6. A.N. Nesmyanov, "Vapor Pressure of the Chemical Elements," translated and edited by J.I. Carasso, (New York: Academic Press, 1963).

7. S. Bashkin, J.O. Stoner, Jr., "Atomic Energy-levels and Grotrian Diagrams, Vol II," (Amsterdam: North-Holland, 1978).

12966/9835
CSO: 4008/34

ULTRA-SHORT PULSE LASER SYSTEM USED FOR LAGEOS RANGE FINDING

Shanghai GUANGXUE XUEBAO [ACTA OPTICA SINICA] in Chinese Vol 6, No 12, Dec 86 pp 1092-1097

[Article by He Huijuan [0149 1979 1227], Li Yongchun [2621 3057 2504], Gu Shengru [7357 5110 1172], Qian Linxing [6929 2651 5281], and Zhao Longxing [6392 7127 5281] of the Shanghai Institute of Optics and Fine Mechanics, Chinese Academy of Science and Tan Detong [6223 1795 0681], Xiao Chikun [5135 3589 3540], Cheng Wanzhen [7115 1238 3791], and Yang Fumin [2799 4395 3046] of the Shanghai Observatory, Chinese Academy of Sciences; paper received 5 Apr 1986; first paragraph is source-supplied abstract]

[Text] Abstract: The paper reports a new Nd:YAG ultra short pulse laser system. The system's single pulse output energy at 1.06 μm wavelength is greater than 100 mJ. Through a frequency doubler, pulse outputs of 50 mJ at 0.53 μm were obtained. The system was used on a range finder with main mirror of ϕ600 mm at the Shanghai Observatory and measured the laser geodynamic satellite (LAGEOS). The ranging distance was 8000 km with an accuracy of 5 cm.

I. Introduction

Use of lasers for range finding of artificial satellites has developed from first and second generations and in the last few years, has advanced to a third generation. A major indication of this change in laser range-finding of satellites is the precision of measured distances. This precision depends on the laser pulse which acts as the emitted light source. The precision of the first generation was on the order of meters, the second was decimeters, while the third has reached centimeter magnitude. The U.S. Space Agency, NASA mobile stations all use several hundred ps locking laser third generation laser satellite range finders. The lasers used are largely active locking lasers manufactured by the Xierfaniya company. The systems are large, expensive, and the switching components' service life effects the life of the entire system. In the early eighties, pure passive, high efficiency locking lasers were already commercial products. Some stations, for example England's Greenwich Observatory and (Huoer) University cooperated[1] to use this system with a pulse width of 150 ps and single pulse

output of 30 mJ. Because a pure passive, locking pulse is constructed on the random noise of passive switching dyes in spontaneously radiated fluorescence, its locking probability is low, reproducibility is lacking, under repeated operation, the amplitude flutter between each time is large, around 150 percent, and often satellite pulses appear.

In 1974 there was reported an intracavity added active modulator to improve the stability of passive locked lasers[8] adopting a high voltage 100 MHz signal modulated Pockels cell but its use is inconvenient. In 1978 an Nd glass laser with pulse series amplitude stability improved to ±5 percent was reported.[3] Reference [4] reported a 1 Hz repetition operation Nd:YAG laser but did not provide detailed performance information.

In 1981 we constructed a repetition active-passive Nd YAG locking laser using an acoustic-optical modulator as active locking component, improving the stability of the passive locked laser making the locking probability reach 100 percent and the amplitude stability at 10 Hz reach ±2 percent. We did research on the cavity thermal stability for high repetition operation,[5] making the repeatability of the oscillator reach 30 Hz. Through a single pulse selector, single pulse outputs of 0.5 to 1.0 mJ can be obtained, and, through a two stage amplifier, at a wavelength of 1.06 μm the output can reach 100 mJ. This ultra short pulsed laser system has been incorporated into the satellite range finder with main mirror aperture of ϕ600 mm at the Shanghai Observatory as China's first third generation laser satellite range finder experimental system. Measurements with respect to laser geodynamic satellites (LAGEOS) show that its range extends to 8000 km and its accuracy approaches 5 cm.

II. Ultra Short Pulse Laser System

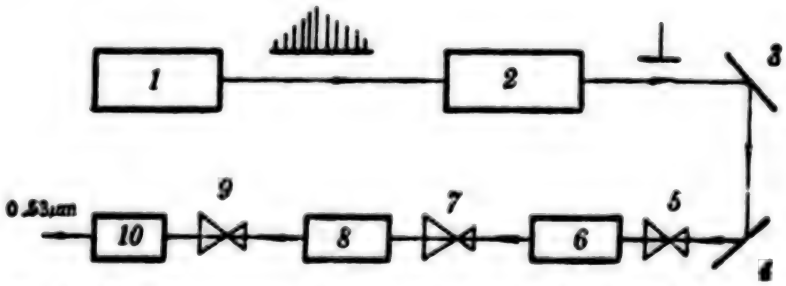

Fig. 1 Schematic diagram of repetition rate ultra-short pulse laser system
1—Ultra-short pulse oscillator, 2—Single pulse selector, 3, 4—45° mirrors, 5, 7, 9—Beam expanders, 6—First stage of amplifier 8—Second stage of amplifier 10—Harmonic generator

Our system is as shown in Fig. 1. The laser oscillator produces series of pulses from which the single pulse selector selects one to be passed through a two stage amplifier. The nonlinearity effects of a type II matching KDP crystal are used to do frequency doubling, putting out 0.53 μm green light. Three doubling beam expanders are inserted into the system. The first two

of these are to expand the laser light spot to permit the laser beam to be amplified effectively as well as to lower the power density within the beam, preventing the nonlinear destruction of the laser medium at high power. The third beam expander is used to lower the power density to prevent damage to the frequency doubling crystal as well as to perfect the directionality and increase the doubling efficiency.

The repetition ultra short pulse oscillator in the system has the features of high repeatability, high locking probability, and is highly stabile. Using the active locking set up, we performed studies of the thermal stability of the resonance cavity under locking conditions,[5] obtaining a set of computer modeled design methods that gave good agreement in experiments.

The G factor of the resonance cavity is:

$$G_1 = \frac{G_2}{2G_2^2 + 2\alpha G_2 + \alpha^2}, \tag{1}$$

in which $\alpha = a/b$. a and b, respectively are the distances from the output lens and the rear cavity lens to the internal lens. With heating, the light spot dimensions on the front and rear of the laser ...ty and at the laser beam are

$$W_1 = \frac{\lambda L}{\pi} \frac{2G_2^2 + 2\alpha G_2 + \alpha^2}{G_2 + \alpha}, \tag{2}$$

$$W_2 = \frac{\lambda L}{\pi} \frac{1}{G_2 + \alpha}, \tag{3}$$

$$W_3 = \frac{\lambda L}{\pi} \frac{[2G_2^2 + 3\alpha G_2 + \alpha^2]^2}{(1+\alpha^2)(G_2+\alpha)[2G_2 + 2\alpha G_2 + \alpha^2]}, \tag{4}$$

model volume $$V = \pi l W_2^2 = \pi l W_1^2 \left[\left(1 - \frac{d_1}{R_1}\right)^2 + \left(\frac{d_2 \lambda}{\pi W_1^2}\right)^2\right]. \tag{5}$$

Based on the major expressions above one can use a computer to make model computations and, based on the dimensions of the cavity's internal parts, select the normal operating parameters for the laser oscillator.

Using an acoustic-optic modulator and dye respectively as active locking and passive locking components, active locking operation is attained. The medium of the acoustic-optic modulator is fused quartz 21 mm long with a transducer plate of Y36° cut $LiNbO_3$. The transducer plate and the fused quartz are pressure bonded with indium. The dye is pentamethylene dissolved in ethylene dichloride solution. The dye box and the rear cavity lens comprise one unit which carries a circulation system to make the dye replacement rate satisfy the repetition frequency.

In order to lower the randomness and increase the reproducibility an active acoustic-optic modulator is inserted into the cavity to serve as a preselector. It forms an instantaneous window which has a width[6]

$$\tau=\frac{4\ln 2}{\pi\sigma}\frac{L}{\sqrt{l_2 N}}\left\{1+\frac{2-l_2}{2}\left(\frac{\pi x}{2L}\right)^2\right\}, \qquad (6)$$

in which L is the cavity length, l_2 is the maximum single pass dissipation caused by sine modulation, x is the distance between the modulator and the nearest cavity lens, and N is the number of times the laser beam goes back and forth in the linear section of the cavity. From the above we know that τ gets small as x gets small, that is the modulator ought to be as close as possible to the resonance cavity lens. According to experimental measurements, x within a few cm, will not obviously increase the laser threshold and also will not significantly lower the stability. This is because the Nd:YAG laser is in a high gain state to within a few cm the constant dissipation action caused by x is minute. Formula (6) is appropriate to continuous locking lasers. In this paper formula (6) is used for a qualitative description of the window width.

The light path of the oscillator is shown in Fig. 2. In order to accomodate the echo time of the receiving system on the laser satellite range finder the pulse width is broadened from 30 ps to 120 ps using F-P to substitute for the common sphenoidal output lens and by adding a plate of auxiliary F-P changing the F-P thickness and reflectivity and altering the pulse width.

Fig. 2 High repetition rate ultra-short pulse oscillator
1—Rear mirror contacted by dye cell with circulating system 2—Transverse mode selecting aperture 3—Xe-flash lamp 4—Front mirror

Fig. 3 Mode-locked train of pulses (Time scale: 10 ns/cm)

Figure 3 gives the envelope of a series of pulses. This is a 70 pulse repeated exposure demonstrating that the stability of the pulse series is good.

The pulse width was measured using a streak camera constructed by the Xi an Optical Institute. After the output was frequency doubled, it was split into two paths. One path was input to a high current tube producing a pulsed electrical signal to trigger the streak tube. The other path was input to the streak tube and immediately produced a streak signal. Figure 4 is the recorded curve of the streak camera. The output light spot was a model TEM_{00}. Using a (nigro) meter to do a sweep trace with respect to the field diagram photograph, the sweep trace curve shown in Fig. 5 was obtained.

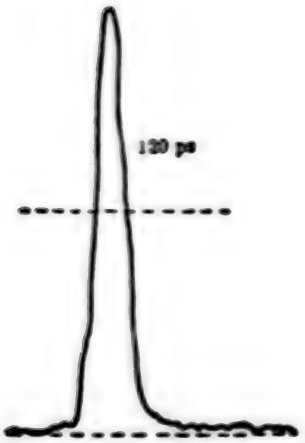

Fig. 4 Pulse duration measured by streak camera

Fig. 5 Scanning curve of output near field spot

We used an oscilloscope to measure a sample of pulse envelopes when the laser ocillator was operating at 10 Hz, revealing the pulse series envelope peak value stability. Figure 6 is a diagram obtained using a storage oscilloscope sampling 30 times at 10 Hz. From the 30 pulses in the figure the stability was computed to be about ± 2 percent.

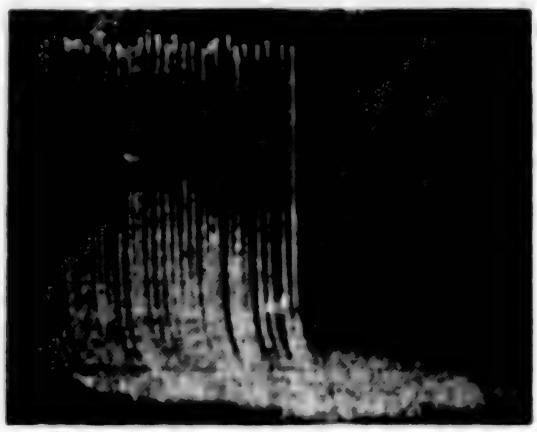

Fig. 6 Stability of pulse train (10 Hz)

The output of the ultra short pulse oscillator is a series of pulses. To get a single pulse it is necessary to go through a single pulse selector (see Fig. 7). The light path is composed of two or more right angle prisms and one $LiNbO_3$ Pockels cell. In the electrical circuit, the sequenced pulses are received by a PIN diode and after the produced signal is amplified it triggers a high voltage switching tube. A 2 ns leading high voltage pulse generated linearly by Blumlein shaping at a specially fixed instant is applied to the two electrodes of the Pockels cell. Of the sequenced pulses, the one that is jacketed by the high voltage pulse is the single pulse selected.

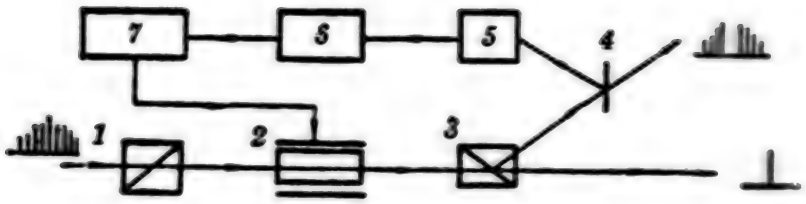

Fig. 7 Single pulse selector

1, 3—Glan prism; 2—Pockels cell; 4—Reflective mirror; 5—Photodetector; 6—Trigger-amplifier; 7—Forming network of high voltage pulse

After beam expanding, the single pulse selected above is input to a two stage amplifier given a 1.06 μm laser output up to 100 mJ. Through a type II KDP crystal frequency doubler, we can get a single pulse green laser of 50 mJ.

The output energy of the single pulse of the Nd:YAG ultra short pulse laser system is adjustable 30 to 50 mJ (0.53 μm). The pulse width is 120 ps; the type is TEM_{00}; with directionality 0.5 mrad, and repeating frequency of 1 Hz, 5 Hz, and 10 Hz.

III. Application to Laser Satellite Range Finding

The Nd:YAG ultra short pulse laser system combined with a main mirror ϕ600 mm laser satellite range finder constitutes China's first third-generation laser satellite range finder experimental system. This system first measured laser geodynamic satellite distances on 12 Dec 1985. The measured data was sent to one of the international laser data processing collection centers--the U.S. space center, Goddard Space Flight Center Laser Tracking Net (NASA/GLTN). They sent the analyzed results back electronically. Table 1 is a summary of the actual observations of the ultra short pulse laser system and our analysis results. Figures 8 and 9 give the observed distance curve on 16 Dec 1985 and Jan 8 1986 for the LAGEOS. On the entire curve there is a portion for which there is no data. This was the result of sudden malfunctions rather than any system defect. The analysis of Table 1 and 2 show that our use of the Nd:YAG ultra short pulse laser system brought the observation precision to around 5 cm thereby attaining the level of foreign third generation range finding systems.

Table 1 Summary of Observation

Observation Date	Observation Time	Length of arc	Observation Points	Internal Consistent accuracy
Dec. 12. 1985	18h40m~59m	11 M	182	6.3cm
Dec. 16. 1985	20h12m~41m	29 M	144	7.6cm
Jan. 5. 1986	17h43m~56m	13 M	133	6.1cm
Jan. 8. 1986	17h27m~37m	10 M	131	6.9cm
Jan. 9. 1986	19h16m~23m	7 M	16	5.0cm

Table 2 NASA/GLTN Analysis Results

Observation Date	Observation Time	Length of arc	Observation Points	Edited Points	Internal Consistent accuracy
Dec. 12. 1985	19h48m~59m	11 M	80	19	7.2cm
Dec. 16. 1985	20h12m~41m	29 M	50	1	4.9cm
Jan. 5. 1986	17h43m~56m	13 M	100	3	4.5cm
Jan. 8. 1986	17h27m~37m	10 M	100	0	3.5cm
Jan. 9. 1986	19h16m~23m	7 M	16	2	6.0cm

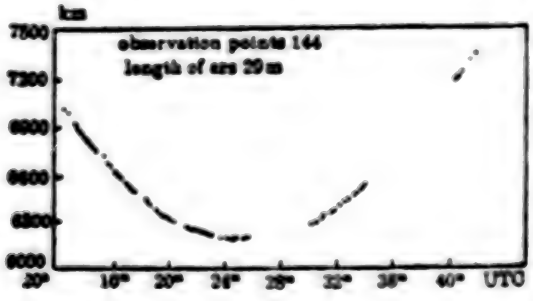

Fig. 8 Range measuring curve of LAGEOS on Dec. 16. 1985

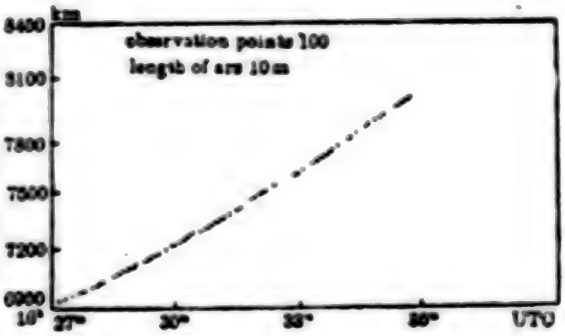

Fig. 9 Range measuring curve of LAGEOS on Jan. 8. 1986

REFERENCES

1. D.R. Hull et al., I.C.L. DIGEST, Supplement, (Guangzhou, China, 1983), 14.

2. B.C. Johnson et al., "Tech. Digest., Int. Electron Devices Meeting," 1974, p. 322.

3. W. Seka et al., JAP, 1978, 49, No. 4 (Apr), 2277.

4. B.B. Craig et al., 2nd Int. Conf. Picosecond Phenomena, (Berlin: Springer-Verlag, 1980), 253.

5. He Huijuan et al., ZHONGGUO JIGUANG [CHINESE LASERS], 1983, 10, No. 11 (Nov), 785.

6. S. Kishida et al., OPT. COMMUN., 1976, 18, No. 1 (Jul), 19.

12966/9835
CSO: 4008/34

LARGE-APERTURE HIGH-EFFICIENCY FREQUENCY DOUBLING USING TANDEM KDP CRYSTALS

Shanghai GUANGXUE XUEBAO [ACTA OPTICA SINICA] in Chinese Vol 6, No 12, Dec 86 pp 1098-1104

[Article by Cai Xijie [5591 1585 3381], Dai Meilan [2071 5019 5695], Lang Jiajun [6745 1367 0193], and Lu Ruixi [7120 3843 3556] of the Shanghai Institute of Fine Mechanics, Chinese Academy of Science and Qin Wenhua [6009 2429 7520] of the Department of Physics, Zhongshan University, Guangzhou; paper received 24 Feb 1986; revised manuscript received 7 Apr 1986; first two paragraphs are source-supplied abstract]

[Text] Abstract: This paper gives the theory of tandem frequency doubling and relative orientation requirements of two crystals. Using two 1.4 cm thick type II KDP crystals and incident base frequency laser intensity of 0.33 to 0.67 GW/cm^2, the external conversion efficiency was over 60% and the laser beam diameter 42 mm. The theoretical results matched quite well with experimental values.

We did comparisons of the experimental features of a tandem frequency doubler with $L_1 = L_2 = 1.4$ cm to those of single crystal frequency doublers with thicknesses of 3 cm and 1.4 cm. The results showed that the tandem frequency doubler had the advantages of both the thin and the thick crystal frequency doublers.

I. Introduction

Due to many factors, in frequency doubling crystals there is always a certain phase mismatch present causing some difficulty in increasing the external conversion efficiency. Especially under conditions of low power density, only relying on increasing the crystal length to get the limit of the optimal length for a high conversion efficiency, as the crystal gets longer the reception half-width of the mismatch angle gets smaller so that correcting the phase mismatch becomes more arduous. People have adopted the idea of two crystals in tandem,[1-6,8] resolving this difficulty by making the mismatch angle the same in the two crystals and the signs opposite for the mismatch quantities which they cause. This can be achieved by changing the relative orientation of the two crystals. This paper gives the detailed theory for tandem frequency doubling. Using two 1.4 cm type II KDP crystals and a power density of 0.33 to 0.67 GW/cm^2, we obtained a frequency doubling conversion efficiency of greater than 60 percent.

II. Theory

As everyone knows the coupled wave equation describing the frequency doubling process is

$$\begin{cases} \dfrac{dE_1}{dz}+\dfrac{1}{2}\gamma_1 E_1 = -iKE^*E_2\exp(-i\Delta kz), \\ \dfrac{dE_2}{dz}+\dfrac{1}{2}\gamma_2 E_2 = -iKE_1^2\exp(i\Delta kz). \end{cases} \tag{1}$$

If we ignore the absorption term, i.e. $\gamma_1 = \gamma_2 = 0$, and suppose that there is no dissipation inside the two crystals, then in a small signal approximation, we can clearly see the superiority of tanden frequency doubling.

$$\begin{aligned} E_2 &= -iKE_1^2\int_0^{l_1+l_2}\exp\left(i\int_0^z \Delta k\,dz\right)dz \\ &= -iKE_1^2\left\{\int_0^{l_1}\exp(i\Delta k_1 z)dz+\exp(i\phi)\int_{l_1}^{l_1+l_2}\exp\left(i\int_0^z \Delta k\,dz\right)dz\right\} \\ &= KE_1^2\left\{\frac{1-\exp(i\,\Delta k_1 l_1)}{\Delta k_1}+\exp\left[i(\phi+i\Delta k_2 l_1)\frac{1-\exp(i\,\Delta k_2 l_2)}{\Delta k_2}\right\}\right., \end{aligned} \tag{2}$$

in which ϕ is the phase difference between the fundamental and frequency doubled light in the crystal caused by the atmosphere and other media.

When $\Delta k_2 = -\Delta k_1$, $l_1 = l_2$,

$$E_2 = KE_1^2\left(\frac{1-\exp(i\,\Delta k_1 l_1)}{\Delta k_1}\right)[1+\exp(i\phi)]. \tag{3}$$

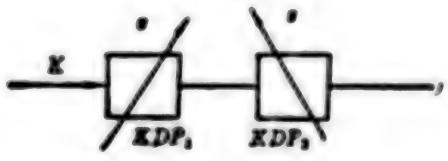

Fig. 1 Relative orientations of tandem crystals

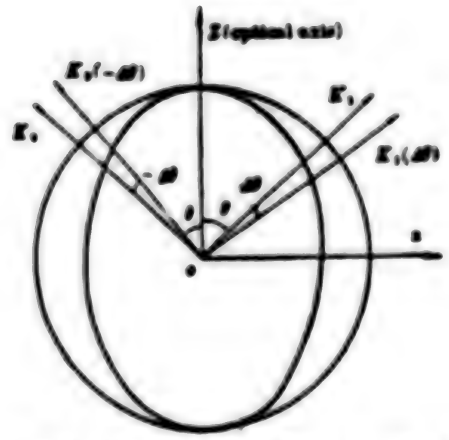

Fig. 2 Principle of change in sign of phase mismatch Δk

If $\Delta k_1 = \Delta k_2$, it is only necessary for the relative orientation of the optical axes of the two crystals to be as shown in Figure 1. Figure 2 gives the principle for the sign change of Δk. For a single mismatched ray (like on the right side of the matching direction), because the signs of the mismatch angles caused in the two crystals placed as in Fig. 1, are opposite, since $\Delta k = \beta\Delta\theta$, thus the mismatch quantities, Δk_1 and Δk_2 are oppositely signed. To obtain a very high conversion efficiency it is only necessary to adjust appropriately the separation between the two cyrstals to make $\phi = 2n\pi$ (the distance to produce $\phi = \pi$ in the atmosphere is 65 mm). At this time

(4)

Formula (4) shows that in the range of larger mismatch angles, the mismatch quantity of the first crystal is optimally offset by the second crystal. The result of the two crystals in tandem is this: the frequency doubling conversion efficiency is in direct proportion to the square of the crystals total length ($L = l_1 + l_2 = 2l_1$) while the reduction of conversion efficiency due to the phase mismatch Δk is just the same as for a single crystal l_1. This lowers the requirements for adjusting precision and increases the frequency doubler stability.

If $\phi = (2n + 1)\pi$, from formula (3) $E_2 = 0$.

That is, the difference frequency in the second crystal completely changes the doubled frequency obtained from the first crystal back to the fundamental frequency. This must be strenuously avoided.[4]

In order better to understand the features of operation under high power densities and to approach as much as possible experimental conditions, we solved formula (1) numerically and did Gaussian numerical integration with respect to the time distribution of the light pulse. We also considered that after application of a refractive matching solution to the crystal surfaces there was still a 1 percent cross sectional refraction. The other parameters are found in reference [11]. Figures 3 and 4 give respectively the characteristic curves of incident light power density versus conversion efficiency for a single 1.4 cm crystal and two 1.4 tandem type II KDP crystal

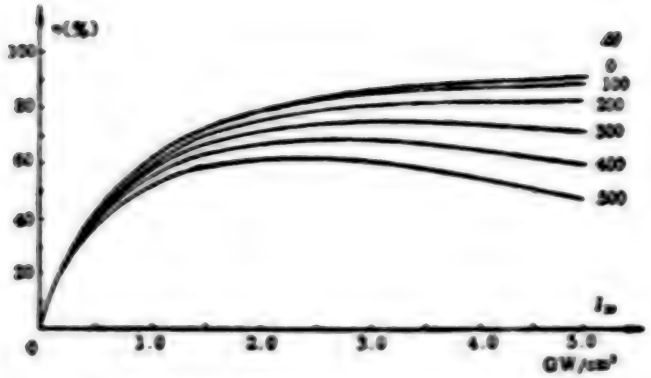

Fig. 3 Doubling characteristics of a 1.4cm type-II KDP crystal detuned 0~500 μrad from phase matching, averaged over the Gaussian temporal profile

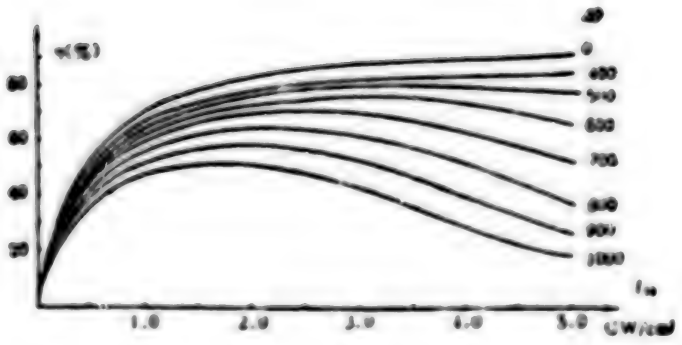

Fig. 4 Doubling characteristics of a 1.4cm type-II KDP crystals detuned 0~1000 μrad from phase matching

III. Experimental Apparatus

We selected two 1.4 cm thick type II KDP crystals to use for the tandem frequency doubling experiments. The ϕ70 mm KDP crystals were grown by the Chinese Academy of Science Fujian Structure of Matter Research Institute. In order to prevent deliquescence, the KDP crystals were sealed in a crystal cell unit. An antireflective film with respect to both the fundamental and doubled frequency was spread on the outer side of the glass window. A refractive matching solution was packed between the inner side and the crystal and to prevent destruction of the refractive matching solution at high power densities the entire KDP crystal cell units were assembled from ultra clean components. The total transmittance, $T_{1\omega}$ = 90 percent. The crystals were installed in two-dimensional servo adjustable frames with the angle adjustable to 1.5" per step.

The whole experiment was carried out at the ϕ45 mm beam amplified output of the 6-path laser table in our laboratory.[9] The laser wave length was 1.06 μm; the pulse was 250 ps, the laser spot diameter was ϕ42 mm, and with a plane wave front the directionality (measured using an array camera) was 0.5 mrad in which the energy occupied 70 percent (0.6 GW/cm^2 level). The light path of the experiment is shown in Fig. 5. We used (Ka) meters[7] 1 and 2 to detect the input and output fundamental frequency light energies, E_1 and E_1'; (Ka) meter 3 to detect the output frequency doubler light energy, E_2; filters 4 and 5, with $T_{1\omega}$ = 70 percent, $T_{2\omega}$ = 0; filter 6, with $T_{1\omega}$ = 0, $T_{2\omega}$ = 68 percent; and beam splitters 7, 8, and 9 with R = 8 percent. The external conversion efficiency, $\eta_{ext} = E_2/E_1$ and the internal conversion efficiency $\eta_{int} = E_2/(E_1' + E_2)$.

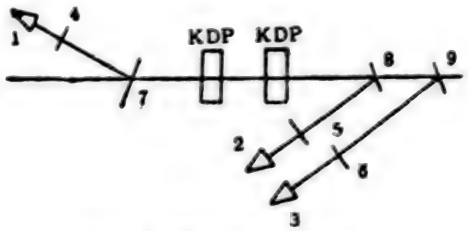

Fig. 5 Experimental setup

IV. Experiment Results and Discussion

The debugging process for the tandem frequency doubler went as follows: starting with the first KDP crystal, it was tuned to the optimal phase matching direction. Then the second crystal was introduced and an angle tuning curve was made for the tandem frequency doubler with respect to the second crystal. After finding the optimal phase matching direction, a characteristic $\eta_{ext} - I_{10}$ curve for the tandem frequency doubler was made.

Figure 6 gives the tuning curve for the angle of the first crystal, with $\Delta\theta_{FWHM} \sim 2400$ μrad, indicating that the mismatch half angle width $\Delta\theta_{FWHM}$ is rather large. Figure 7 is the characteristic curve of the fundamental frequency power density versus the frequency doubler conversion efficiency for the first KDP crystal. In the figure, the theoretically computed curves for $\Delta\theta$ = 0, 600 μrad are also included. When the power density is 1.33 GGW/cm^2, we get the highest frequency doubler conversion efficiency in this experiment of η_{ext} = 45.5 percent corresponding to η_{int} = 50.5 percent.

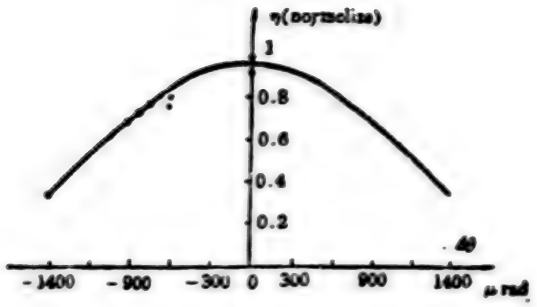

Fig. 6 Measured detuning curve of a 1.4cm type-II KDP crystal

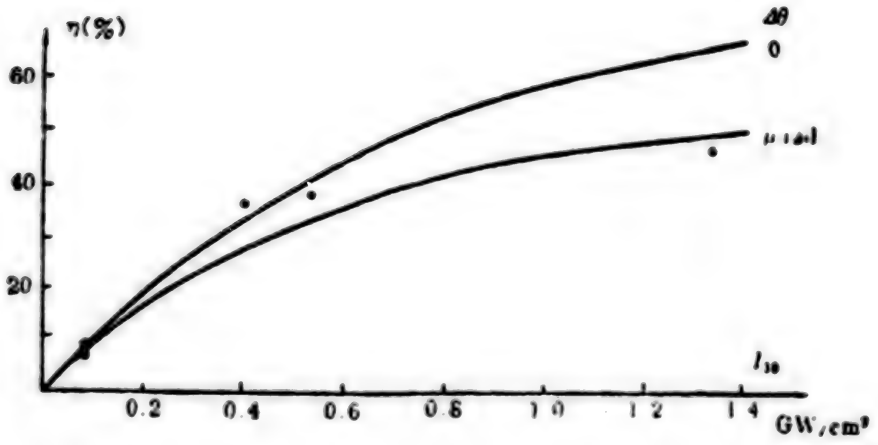

Fig. 7 Measured overall doubling energy efficiency of a 1.4-cm-thick type-II KDP crystal as a function of input intensity $I_{1\theta}$ with an aperture of 42 mm. Dashed line: theoretical calculation for phase mismatch angle $\Delta\theta = 0.600\,\mu$rad, averaged over Gaussian temporal profile

Adding the second KDP crystal according to the requirements of tandem frequency doubling, Figure 8 gives the tuning curve of the angle for the tandem frequency doubler with this second KDP crystal. We measured $\Delta\theta_{FWHM}$ = 2480 μrad and the other values were the same as for a single crystal. This proves that in the matter of angle tuning, a tandem frequency doubler has the same advantage as a single crystal, that is $\Delta\theta_{FWHM}$ is fairly large. The required tuning precision is thus lower,

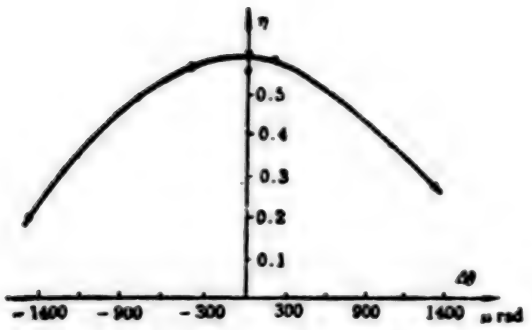

Fig. 8 Conversion efficiency of tandem KDP doubler as a function of phase mismatch angle of the second KDP crystal

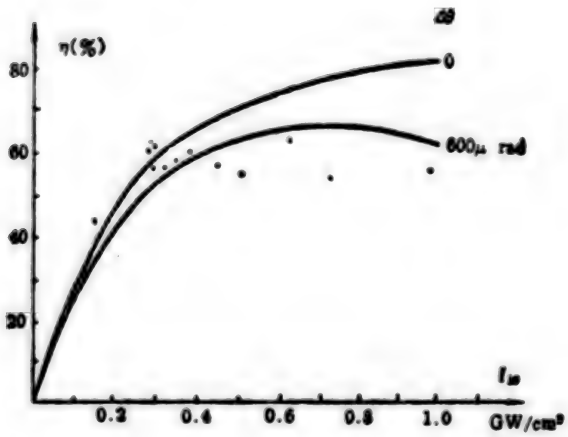

Fig. 9 Measured orerall doubling efficiency η of the tandem doubler ($L_1 = L_2 = 1.4$cm type-II KDP) as a function of input intensity I_{10} with an aperture of 42 mm. Dashed line: theoretical calculation curve for phase mismatch angle $\Delta\theta = 0.600\,\mu$rad, averaged over Gaussian temporal profile

Figure 9 gives the characteristic curve of η_{ext} for a tandem crystal frequency doubler. When $I_{10} = 0.5$ GW/cm^2, we got the greatest frequency doubling conversion efficiency, $\eta_{ext} = 63$ percent corresponding to $\eta_{int} = 77.8$ percent, achieving a ϕ42 mm wide diameter high efficiency frequency doubled output. In the range of incident power density, neither the refractive matching solution nor the KDP crystal itself suffered overload damage.

In order to see even more clearly the features of a tandem frequency doubler we have collected together in Fig. 10 the experimental curves for the 1.4 and 3.0 cm single crystal and the 1.4 cm tandem two crystal tandem frequency doublers. It is evident from this figure that the curve for the tandem

frequency doubler is better than that for the single crystal frequency doublers. At low power ($I_{10} < 0.3$ GW/cm^2), $\eta_{tandem} < \eta_{3cm}$, η_{3cm} reaches a peak value at 0.3 GW/cm^2 while η_{tandem} reaches its peak at 0.5 GW/cm^2. Both these results were theoretically predicted since the total length of the tandem frequency doubler, $L = L_1 + L_2 = 2.8$ cm, is smaller than the $L = 3$ cm for a single crystal. The maximum conversion efficiencies η_{tandem} and η_{3cm} were very close. However, it is noteworthy that in the higher power region ($I_{10} > 0.5$ GW/cm^2), $\eta_{tandem} > \eta_{single}$. This is because the tandem frequency doubler has the capability of offsetting the phase mismatch so that the fall in the conversion efficiency comes later for the tandem frequency doubler than for a single crystal of the same length. If we define the dynamic range of the conversion efficiency η_0 to be $\Omega(\eta_0) = I_{10upperlimit}/I_{10lower-limit}$, where the definition of $I_{10upperlimit}$ and $I_{10lowerlimit}$ is just for I_{10} in the region $I_{10upperlimit} \geq I_{10} \geq I_{10lowerlimit}$, $\eta > \eta_0$. From Figure 10 we know that $\Omega_{3cm}(55 \text{ percent}) = 3$ while $\Omega_{tandem}(55 \text{ percent}) = 4$ so obviously the dynamic range of the tandem frequency doubler is greater than for the 3cm crystal. The actual performance of the tandem frequency doubler is good. By comparison with the 3cm single crystal experimental curve,[10] we can also see that the tandem frequency doubling, in addition to maintaining the rather high conversion efficiency advantage of a single thick crystal at low power, it also has a rather large mismatch angle reception half width making the output of the frequency doubler more stable and the dispersion point smaller.

Of special note is that the single 1.4cm crystal and two 1.4cm crystal tandem type II KDP freuqncy doublers both operate at $\Delta\pi \sim 60$ μrad or even larger phase mismatch states but a single 3cm KDP crystal operates at a state of $\Delta\pi \sim 270$ μrad so the difference between them is really quite large. However the tandem frequency doubler can still attain the same level of conversion efficiency, a point which completely explains why the phase mismatch offset capability of the tandem frequency doubler makes it require less than the single thick crystal frequency doubler with respect to laser performance, crystal material, and adjusting precision. A single 1.4cm KDP crystal, because it is thinner, at lower power density the conversion efficiency is not very high but at high power densities the conversion efficiency maintains a rising tendency.

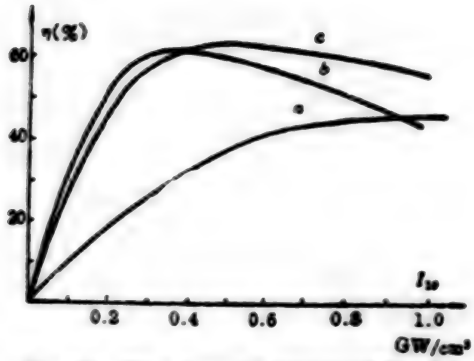

Fig. 10 Experimental characteristics for three kinds of doublers

a—L=1.4cm type-II KDP(840402), $\Delta\theta$: 600 μrad~700 μrad; b—L=3.0cm type-II KDP (840901), $\Delta\theta$: 270 μrad; c—$L_1=L_2$=1.4cm type-II KDP tandem crystals (840402), $\Delta\theta$: 600 μrad~700 μrad

Finally, through comparison of these experimental data we reach the following conclusions:

1. Single-thick crystals, although able at low power to attain high conversion efficiencies, at rising power density quickly exhibit a tendency for falling conversion efficiency. Moreover, since the conversion efficiency is more sensitive to the mismatch angle, the entire frequency doubler output is not stable.

2. The conversion efficiency of single thin crystals, although not high at low power densities, in a wider power density range still maintain a rising tendency, are not sensitive to the mismatch angle, and thus have more stable frequency doubler outputs.

3. Tandem frequency doublers combine the advantages of single thin crystals and single thick crystals. Not only do they attain high conversion efficiency at low power, they also maintain this high conversion efficiency with rising power density. Their frequency doubler output is also more stable.

This work was undertaken with the good will and support of Professor Deng Ximing. The KDP crystals used in this work were provided by the Chinese Academy of Science Fujian Structure of Matter Research Institute. At that institute, Li Qingguo constructed the crystal box window multilayer film, Luo Yongshan designed the crystal box, and Fan Dianyuan provided the type number for the refractive matching solution. We extend our gratitude to all of these individuals.

Also participating in the work were Shu Meizhong, Huang Kuixi, and Ge Xiaping.

REFERENCES

1. A.G. Akhmanov, Thesis for candidateo Degree, (Moscow State University, 1969).

2. D.G. Gonzalez et al., IEEE JQE, 1973, QE-9, No. 1 (Jan), 23-26.

3. V.G. Dmitriev et al., Sov. JQE, 1975, 4, No. 9 (Sep), 1083.

4. V.D. Volsov et al., Sov. JQE, 1976, 6, No. 10 (Oct), 1163.

5. M.A. Summers et al., Digest of Conference of Lasers and Electro-Optics, (Optical Society of America, Washington, D.C., 1981), 30.

6. LLNL 1981 Annual Report, 1981, 7-4.

7. Lin Kangchun et al., ZHONGGUO JIGUANG [CHINESE LASERS] in Chinese, 1983, 10, No. 3 (Mar), 186.

8. В. В. Бокуть, и др.; ЖПС, 1982, 37, No. 5, 748.

9. Xie Ximing et al., GUANGXUE XUEBAO [ACTA OPTICA SINICA] in Chinese, 1985, 5, No. 3 (Mar), 211.

10. Cai Xijie et al., GUANGXUE XUEBAO [ACTA OPTICA SINICA] in Chinese, 1985, 5, No. 11 (Nov), 975.

11. R.S. Craxton et al., IEEE JQE, 1981, QE-7, No. 9 (Sep), 1782.

12966/9835
CSO: 4008/34

GENERALIZED HYBRID VARIATIONAL PRINCIPLE, CORRESPONDING FINITE ELEMENT MODEL

Chongqing YINGYONG SHUXUE HE LIXUE [APPLIED MATHEMATICS AND MECHANICS] in Chinese Vol 7 No 5, May 86 pp 443-449

[Article by Chen Wanji [7115 8001 0679] of the Dalian Institute of Technology; paper received 5 April 1985]

[Text] Abstract: Based on the more generalized variational principle proposed by Professor Qian Weichang [6929 0251 7022], this paper provides an even more generalized hybrid variational principle suited for use in finite element methods. From this, a new general hybrid model is established.

Further, with varying thickness thin plate bending elements as an example, a comparison is made of various hybrid elements as established based on different general variational principles.

I. A More Generalized Extended Variational Principle in Elastic Mechanics

Recently, Professor Qian Weichang proposed high order Lagrange multipliers and established a more generalized extended variational principle in elastic theory[1] and consequently progressively unified and promoted study of a generalized variational principle.

There are two places of insufficiency in the generalized variational principle established in elastic mechanics using general Lagrange multipliers. The first is that one cannot from the potential energy principle directly obtain the Reissner principle. The second is that from the surplus-energy principle one cannot directly get the Hu Haichang [5170 3189 2490]-Jiujin [7750 3160] generalized variational principle. Evidently, the generalized variational principle set up using the former Lagrange multiplier method is limited.

The high order Lagrange multiplier method proposed by Professor Weichang further developed Lagrange multiplier methods, overcoming the difficulties present in using traditional Lagrange multiplier methods to establish a variational principle. He also further established a still more general extended variational principle.

The high order Lagrange multiplier terms proposed for Professor Weichang can also be introduced by penalty functions. This way is more direct and augments the physical explanation for the high order multiplier terms.

When establishing a more generalized extended variational principle in elastic mechanics, the interior stress strain relationship is introduced as high order multiplier terms. In elastic mechanics, the stress strain relationship can be represented as:

$$\varepsilon = a\sigma \tag{1.1}$$

or

$$\sigma = A\varepsilon \tag{1.2}$$

or

$$\sigma^T\varepsilon - \frac{1}{2}\varepsilon^T A\varepsilon - \frac{1}{2}\sigma^T a\sigma = 0 \tag{1.3}$$

in which ε, σ are, respectively, the stress and strain. a and A, respectively, are the flexibility and the elastic coefficient matrices and $a^{-1} = A$.
It is not difficult to prove

$$\sigma^T\varepsilon - \frac{1}{2}\varepsilon^T A\varepsilon - \frac{1}{2}\sigma^T a\sigma = \frac{1}{2}(\varepsilon - a\sigma)^T(\sigma - A\varepsilon) = -\frac{1}{2}(\sigma - A\varepsilon)^T a(\sigma - A\varepsilon) = -(\varepsilon - a\sigma)^T A(\varepsilon - a\sigma)/2.$$

That is to say formula (1.3) is equivalent to using the stress grain coefficient restrictions which are represented by the high order terms.

We take formula (1.3) to serve as a pnealty function and directly introduce it into a functional. Combined with the Lagrange multiplier method we can derive two equivalent more general extended variational principles from the potential energy and surplus energy principles respectively. For the detailed derivation see reference (1). Their functionals are

$$\Pi_{P\lambda} = \Pi_{\sigma 1} + \iiint_V \lambda\left(\sigma^T\varepsilon - \frac{1}{2}\varepsilon^T A\varepsilon - \frac{1}{2}\sigma^T a\sigma\right)dV \tag{1.4}$$

and

$$\Pi_{C\lambda} = \Pi_{\sigma 1} - \iiint_V \lambda\left(\sigma^T\varepsilon - \frac{1}{2}\varepsilon^T A\varepsilon - \frac{1}{2}\sigma^T a\sigma\right)dV \tag{1.5}$$

in which

$$\Pi_{\sigma 1} = \iiint_V \left[\frac{1}{2}\varepsilon^T A\varepsilon - \sigma^T(\varepsilon - D^T u) - \bar{F}^T u\right]dV - \iint_{S_\sigma} \bar{T}^T u\,dS - \iint_{S_\sigma} T^T(u-\bar{u})\,dS \tag{1.6}$$

$$\Pi_{\sigma 1} = \iiint_V \left[\sigma^T\varepsilon - \frac{1}{2}\varepsilon^T A\varepsilon + (D\sigma + \bar{F})^T u\right]dV - \iint_{S_\sigma} (T-\bar{T})^T u\,dS - \iint_{S_\sigma} T^T\bar{u}\,dS \tag{1.7}$$

in which D is the differential operator corresponding to the equilibrium equation, T is the boundary strength, u is the displacement, $\bar{F}$ is the given volume strength, $\bar{T}$ and $\bar{u}$, respectively, are given boundary strength and boundary displacement on the boundaries S_σ and S_u, and λ is any given constant.

Further, it can be proved that from $\delta\Pi_{P\lambda} = 0$ or $\delta\Pi_{C\lambda} = 0$, the variational equations corresponding to λ taken as any constant are all equivalent to the elastic mechanics general basic equations.

Obviously, $\Pi_{P\lambda} = -\Pi_{C\lambda}$.

$\Pi_{P\lambda}$ and $\Pi_{C\lambda}$ are entirely unrestricted more general variational principles. Present general variational principles, including the Hu Haichang-Jiujin general variational principle, are special cases of this.

Corresponding to different values of λ, we can get various variational principles.

(1) When $\lambda = 0$, denote $\Pi_{P\lambda}$ and $\Pi_{C\lambda}$ as Π_{P0} and Π_{C0}. Obviously, this is equivalent to the Reissner principle. Because $\Pi_{P\lambda}$ is directly derived from the surplus energy principle, these sorts of methods also are used to overcome another problem of the Lagrange multiplier method.

(3) When $\lambda = 1/2$, denote $\Pi_{P\lambda}$ and $\Pi_{C\lambda}$ as $\Pi_{P\frac{1}{2}}$ and $\Pi_{C\frac{1}{2}}$. Then we have

$$\Pi_{P\frac{1}{2}}=\iiint_V\left\{\frac{1}{2}\left[\frac{1}{2}\varepsilon^T A\varepsilon-\frac{1}{2}\sigma^T a\sigma-\sigma^T\varepsilon+2\sigma^T(D^T u)\right]-\bar{F}^T u\right\}dV$$

$$-\iint_{S_\sigma}\bar{T}^T u\,dS-\iint_{S_u}T^T(u-\bar{u})\,dS \tag{1.8}$$

$$\Pi_{C\frac{1}{2}}=-\Pi_{P\frac{1}{2}}$$

This variational principle cannot be derived from the Hu Haichang-Jiujin variational principle. If in formula (1.8) we substitute the restriction $\varepsilon = D^T u$ then

$$\Pi_{P\frac{1}{2}}=\iiint_V\left\{\frac{1}{2}\left[\frac{1}{2}\varepsilon^T A\varepsilon-\frac{1}{2}\sigma^T a\sigma+\sigma^T(D^T u)\right]-\bar{F}^T u\right\}dV-\iint_{S_\sigma}\bar{T}^T u\,dS-\iint_{S_u}T^T(u-\bar{u})\,dS \tag{1.9}$$

This is the general variational principle given by Liang Guoping [4731 0948 1627] and Fu Zizhi [0102 1311 2535].[2]

If in formula (1.9) we substitute

$$\iiint_V\sigma^T(D^T u)\,dV=\iint_{S_\sigma+S_u}T^T u\,dS-\iiint_V(D\sigma)^T u\,dV$$

and also satisfy the restriction $D\sigma = 0$, and do not count the volume strength $\bar{F}$,

$$\Pi_{P\frac{1}{2}}=\frac{1}{2}\left[\iiint_V\left(\frac{1}{2}\varepsilon^T A\varepsilon-\frac{1}{2}\sigma^T a\sigma\right)dV-\iint_{S_\sigma}u^T(2\bar{T}-T)\,dS-\iint_{S_u}T^T(2\bar{u}-u)\,dS\right] \tag{1.10}$$

This is just the mixed variational principle used in reference (3).

(4) When $\lambda = -1$, denote Π_{P_λ} and Π_{C_λ} as Π_{P-1} and Π_{C-1}. Then we have

$$\Pi_{P-1}=\iiint_V\left[\varepsilon^T A\varepsilon-2\sigma^T\varepsilon+\sigma^T(D^Tu)+\frac{1}{2}\sigma^T a\sigma-\bar{F}^Tu\right]dV-\iint_{S_\sigma}\bar{T}^Tu\,dS-\iint_{S_\varepsilon}T^T(u-\bar{u})dS \tag{1.11}$$

This variational principle also cannot be directly derived from the Hu Haichang-Jiujin general variational principle. If we substitute into formula (1.10) the restriction $\varepsilon = D^Tu$ (inthe interior), $u = \bar{u}$ (on the boundary S_u) we get

$$\Pi_{P-1}=\iiint_V\left[(D^Tu)^TA(D^Tu)+\frac{1}{2}\sigma^Ta\sigma-\sigma^T(D^Tu)-\bar{F}^Tu\right]dV-\iint_{S_\sigma}\bar{T}^Tu\,dS \tag{1.12}$$

This is just the basic structure-potential energy principle given by Oden.[4]

When λ is taken as different constants, one will get various new generalized variational principles thus making the various variational principles have a more unified framework. If we understand λ to be the penalty function factor of the stress strain relationship restriction, then by the properties of penalty functions we know that when $\lambda \to \infty$, the stress strain restriction will be satisfied. This way $\Pi_{P\lambda}$ and $\Pi_{C\lambda}$ will degenerate into the Reissner principle, the same as for $\lambda = 1$. In approximation computations, the effect of different λ values on the approximation precision is a subject awaiting further research. This paper will use an arithmetic example in the finite element method to discuss this question.

II. A More General Hybrid Extended Variational Principle in the Finite Element Method

When $\Pi_{P\lambda}$ and $\Pi_{C\lambda}$ are directly used in establishing a finite element model, in order to ensure convergence, commonly we must take into account the conformal requirements in $\Pi_{P\lambda}$ with respect to u or the conformal requirements in $\Pi_{C\lambda}$ with respect to σ. This is based on the fact that if $\Pi_{P\lambda}$ or $\Pi_{C\lambda}$ use nonconformal element functions, the establishment of finite element models is very inconvenient. If we relax the conformal restriction between elements for the Lagrange multipliers corresponding to $\Pi_{P\lambda}$ or $\Pi_{C\lambda}$, then we can establish a generalized variational principle appropriate to the finite element method. According to the method of reference (5), we can establish two kinds of hybrid variational principles directly from $\Pi_{P\lambda}$ and $\Pi_{C\lambda}$.

$$\Pi_{mP\lambda}=\sum_e\iiint_{V_e}\left[\frac{1}{2}\varepsilon^TA\varepsilon-\sigma^T(\varepsilon-D^Tu)-\bar{F}^Tu+\lambda(\sigma^T\varepsilon-\frac{1}{2}\varepsilon^TA\varepsilon-\frac{1}{2}\sigma^Ta\sigma)\right]dV$$

$$-\sum_e\iint_{\partial V_e}T^T(u-\bar{u})dS-\iint_{S_\sigma}\bar{T}^Tu\,dS \tag{2.1}$$

or
$$\Pi_{mC\lambda}=\sum_{e}\iiint_{V_e}\Big[-\frac{1}{2}\varepsilon^T A\varepsilon+\sigma^T\varepsilon+(D\sigma+\bar{F})^T u-\lambda\Big(\sigma^T\varepsilon-\frac{1}{2}\varepsilon^T A\varepsilon$$

$$-\frac{1}{2}\sigma^T a\sigma\Big)\Big]dV-\sum_{e}\iint_{\partial V_e}T^T\tilde{u}dS+\iint_{S_\sigma}\bar{T}^T\tilde{u}dS \tag{2.2}$$

in which $\tilde{u}$ is the displacement interpolation function on the element boundary ∂V_e. It has two methods of construction. The first way is make $\tilde{u}$ be uniquely determined from common parameters between elements. This is the hybrid method normally seen. The second way is to make $\tilde{u} = (\beta u^a + \alpha u^b)/(\alpha + \beta)$, in which α, β are any constants ($\alpha + \beta = 0$), with u^a and u^b being the displacement of the nonconformal element functions of the two sides of the element intersection boundary at the intersecting boundary. When α and β are taken with different values, i.e., $\alpha = \beta$ or $\alpha = 0$, or $\beta = 0$ they are also frequently called partitioned general variational principles.[3,7,8]

III. A More General Hybrid Model

Based on the $\Pi_{mP\lambda}$ or $\Pi_{mC\lambda}$ established models, we can call them a more general hybrid model.

In the elements, suppose

$$\left.\begin{aligned}&\varepsilon=N\alpha\\&\sigma=P\beta\ \text{then}\ T=R\beta\\&u=Bq\\&\tilde{u}=Lq\end{aligned}\right\} \tag{3.1}$$

in which α, β are independent parameters in the elements, q is a nodal parameter, N, P, B, L are the corresponding interpolation functions, and R is related to P. Substituting $\Pi_{mC\lambda}$ in we get:

$$\Pi_{mC\lambda}=\sum_{e}\Big[-\frac{1}{2}\alpha^T H\alpha+\beta^T D\alpha+\beta^T Wq-\lambda\Big(-\frac{1}{2}\alpha^T H\alpha$$

$$-\frac{1}{2}\beta^T C\beta+\beta^T D\alpha\Big)-\beta^T Gq\Big]+q^T Q$$

in which
$$H=\iiint_{V_e}N^T AN dV \tag{3.2}$$

$$D=\iiint_{V_e}P^T N dV$$

$$C=\iiint_{V_e}P^T aP dV$$

$$W=\iiint_{V_e} P_1^T B\,dV$$

$$G=\iint_{\partial V_e} R^T L\,dS$$

$$q^T Q=\sum_e \iiint_{V_e} \bar{F}^T C q\,dV+\iint_{S_\sigma} \bar{T}^T L q\,dS$$

From $\frac{\partial \Pi_{mc1}}{\partial \alpha}=0$ get $$\sum_e -H\alpha+D^T\beta+\lambda(H\alpha-D^T\beta)=0 \tag{3.3}$$

From $\frac{\partial \Pi_{mc1}}{\partial \beta}=0$ get $$\sum_e D\alpha+(W-G)q+\lambda(C\beta-D\alpha)=0 \tag{3.4}$$

From $\frac{\partial \Pi_{mc1}}{\partial q}=0$ get $$\sum_e (G-W)^T\beta=Q \tag{3.5}$$

From (3.3) we get $$\alpha=H^{-1}D^T\beta \tag{3.6}$$

Substitute (3.6) in (3.4) to get $$\beta=[(1-\lambda)DH^{-1}D^T+\lambda C]^{-1}(G-W)q \tag{3.7}$$

Substitute (3.7) in (3.5) to get $$\sum_e K^e q=Q \tag{3.8}$$

in which the element rigidity matrix K^e is:

$$K^e=(G-W)^T[(1-\lambda)DH^{-1}D^T+\lambda C]^{-1}(G-W) \tag{3.9}$$

When $\lambda = 0$ we get the general hybrid element. When $\lambda = 1$ we get the general hybrid stress element. As expected, this time the assumed stress satisfied the equilibrium equation in the elements giving the hybrid stress element.

IV. A More General Hybrid Model for Various Thickness Bended Plates

The hybrid elements relaxed the conformal requirement with respect to the element functions. Consequently, we can select a heuristic function from a broader range and make the performance of the elements be improved as much as possible. The general hybrid elements within the elements increased the number of variables and also relaxed as much as possible the restrictions on these variables. For example, the equilibrium condition within the elements, the continuity condition, the relationship of stress and strain, and the conformal condition among the elements further improves the performance of the hybrid elements.

For variable thickness plate elements, hybrid stress is inconvenient, making for the emergence of difficulties in the precise computation of the C matrix. Also seeking an inverse operation for the C matrix cannot be avoided. However, the use of general hybrid elements can get [illegible]d these problems.[6]

For the more general hybrid element, we give here a triangular thin plate element with linearly varying thickness and use a computational example to illustrate the effect of the λ value on precision.

The element nodal parameters were a single transverse displacement and two direction corners (Figure 1).

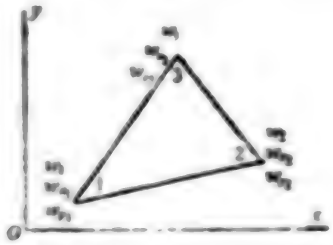

Figure 1

The stress and strain within the element used linear interpolated values expressed by area coordinates.

The displacement between elements used interpolation functions constructed from common nodal parameters between elements. The displacement ω was a third degree function. The normal derivative $\partial\omega/\partial n$ was a linear function.

From this we can derive the **C**, **W**, **D** matrix displays in the element rigidity matrix and $\mathbf{H}^{-1}\,\mathbf{C}$ can be gotten through numerical integration.

As a numerical example we computed for a cantilever plate with finite width and linearly varying thickness receiving a uniform load with dimensions as shown in Figure 2. The elastic constant was $E = 2 \times 10^6$ kg/cm^2, $\nu = 0.3$.

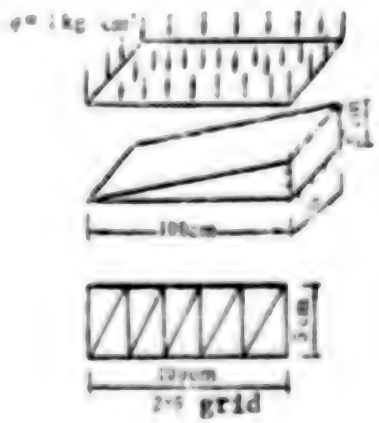

Figure 2.

Different values of λ corresponded to different hybrid models. When $\lambda = 1$, it was a hybrid stress element (the element stress field satisfied

equilibrium; when $\lambda = 0$, it was a general hybrid element; when $\lambda = 1/2$, it was a hybrid element corresponding to the variational principle given in reference (2); when $\lambda = -1$, it was the hybrid element corresponding to the variational principle given in reference (3). In Figure 3 these are respectively denoted as R, H, L, and O.

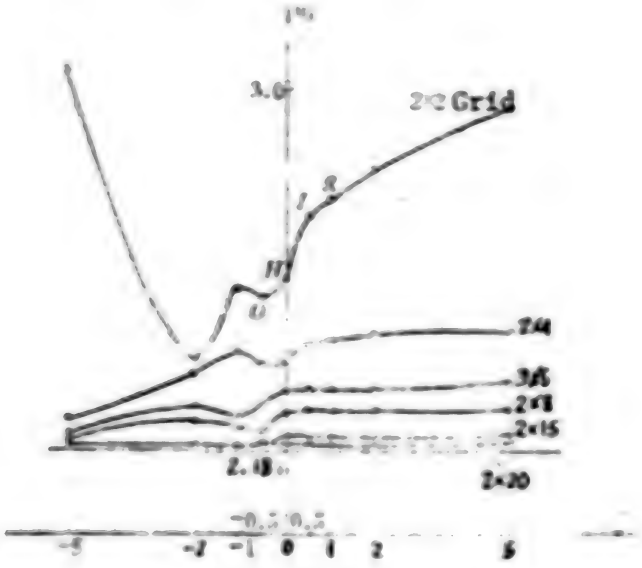

Figure 3

For the computed results of the deflection for point A, see Table 1 and Figure 3. From Figure 3 we see that when the grid reaches a certain density, for different λ values, the hybrid elements have nealry the same precision. For this type of element, if computational efficiency and saving of computer time is considered, the general hybrid element (H) is more easily implemented. From formula (3.8) we can see that for general hybrid element ($\lambda = 0$) seeking the inversion operator can be avoided but for the other λ values this step cannot be avoided.

Table 1. Deflection of Point A (cm). Beam analytical solution $w_A = 2.184$ cm

Grid / λ	2×2	2×4	2×6	2×8	2×16	2×20
0	2.555	2.279	2.211	2.274	2.219	2.206
1	2.725	2.428	2.328	2.271	2.216	2.205
−1	2.637	2.398	2.256	2.240	2.208	2.200
0.5	2.690	2.422	2.321	2.272	2.216	2.204
−0.5	2.511	2.371	—	2.228	2.204	2.197
2	2.782	2.448	2.323	2.273	2.216	2.206
−2	2.585	2.389	2.280	2.252	2.209	2.199
5	2.930	2.471	2.338	2.284	2.223	2.210
−5	3.069	2.254	2.239	2.211	2.200	2.196

REFERENCES

1. Qian Weichang, "High Order Lagrange Multipliers and a More General Variational Principle in Elastic Theory," YINGYONG SHUXUE YU LIXUE Vol 4 No 2, 1983.

2. Liang Guoping [4731 0948 1627] and Fu Zizhi [0102 1311 2535], "A New Method for Construction Elements," PROCEEDINGS OF THE INTERNATIONAL CONFERENCE ON FINITE ELEMENT METHODS, Shanghai 2-6 August 1982, pp 593-599.

3. Michael, L. Day and Yang, T.Y., "A Mixed Variational Principle for Finite Element Analysis," INT. J. NUM. METHODS ENGNG., No 8, 1982, pp 1212-1230.

4. Oden, J.T., "The Classical Variational Principles of Mechanics," ENERGY METHODS IN FINITE ELEMENT ANALYSIS, edited by R. Glowinsk, E.Y. Rodin, and O.C. Zienkiewicz, 1979, pp 1-31.

5. Chen Wanji, "Hybrid General Variational Principles and Hybrid Models," DALIAN GONGXUE XUEBAO [DALIAN ENGINEERING ACADEMY JOURNAL], No 4, 1983.

6. Ibid., "Varying Thickness Thin Plates and Shell General Hybrid Methods," LIXUE XUEBAO [ACTA MECHANICA SINICA], (forthcoming).

7. Qian Weichang, "Variational Methods and Finite Elements," Science Publishers, 1980.

8. Long Yuqiu [7893 7457 3808], "Partitioned General Variational Principle in Elastic Mechanics," SHANGHAI LIXUE [SHANGHAI MECHANICS], No 2, 1981.

12966/9365
CSO: 4008/1068

COMPACTNESS OF QUASI-CONFORMING ELEMENT SPACES, CONVERGENCE OF QUASI-CONFORMING ELEMENT METHOD

Chongqing YINGYONG SHUXUE HE LIXUE [APPLIED MATHEMATICS AND MECHANICS] in Chinese Vol 7 No 5, May 86 pp 409-423

[Article by Zhang Hongqing [1728 7703 1987] and Wang Ming [3769 7686] of the Dalian Institute of Technology, Department of Applied Mathematics; paper received 5 March 1985; first paragraph is source-supplied abstract]

[Text] Abstract: This paper first discusses the compactness of quasi-conformal element space, generalizing the Rellich compactness theorem to quasi-conformal element space sequences with certain properties then it extends the generalized Poincare, Friedrichs, and Poincare-Friedrichs inequality formulae to quasi-conformal element space. Then the convergence and error approximation of the quasi-conformal element method is discussed. The paper proves that if a quasi-conformal element space is approximate and strongly continuous, satisfies the element order condition and passes the IPT test, then the approximate solution is convergent. As examples, we show that convergence precision of 6, 9, 12, 15, 18, and 21 parameter quasi-conformal elements under the $L^{2,2}(\Omega)$ norm respectively are $O(h_\tau)$, $O(h_\tau)$, $O(h_\tau^2)$, $O(h_\tau^2)$, $O(h_\tau^3)$, and $O(h_\tau^4)$ order of magnitude.

I. Introduction

The mathematical foundations of the quasi-conformal element method were established in reference (1), where its convergence was summed up in three parts: 1) uniform positivity of the energy functional; 2) the approximability of quasi-conformal element space; and 3) quasi-conformal element space passes the extended part interval test. Reference (1) discussed 2) and 3), but not 1). This problem will be discussed here. To reach this goal, we examine the compactness of quasi-conformal element space, generalizing the well-known Rellich compactness theorem to quasi-conformal element space sequences and extending Poincare, Friedrichs, and Poincare, Friedrichs inequality formulae to quasi-conformal element space. This way when utilizing quasi-conformal elements to solve plate bending problems we can ensure uniform positivity of the energy functional. In addition, we improved the results of reference (1) concerning the approximation and interval parts test, proving that under rather broad conditions, the quasi-conformal element method converges as well as providing an error estimate. As example, 6, 9, 12, 15, 18, and 21 parameter quasi-conformal plate elements converge.

As in reference (1), we take the fixed perimeter thin plate bending as an example to summarize our results.

Let Ω be a bounded polygon in R^2. Denote $L^{2,2}(\Omega) = \{u = (u^{00}, u^{10}, u^{01}, u^{20}, u^{11}, u^{02}) \mid u^{ij} \in L^2(\Omega),\ 0 \leqslant i + j \leqslant 2\}$, then $L^{2,2}(\Omega)$ according to the norm below $\|\cdot\|_{L^{2,2}(\Omega)}$ is a Hilbert space:

$$u \in L^{2,2}(\Omega),\quad |u|^2_{L^{2,2}(\Omega)} = \sum_{0 \leqslant i+j \leqslant 2} \int_\Omega |u^{ij}|^2 dx$$

For $\forall\, w \in H^2(\Omega)$, define $Ew = (w, \partial_{x_1} w, \partial_{x_2} w, \partial^2_{x_1 x_1} w, \partial^2_{x_1 x_2} w, \partial^2_{x_2 x_2} w)$, then $EH^2(\Omega)$ becomes a closed subspace of $L^{2,2}(\Omega)$. On the space $L^{2,2}(\Omega)$ define a bilinearity continuous functional $a(\cdot,\cdot)$ as below

$$u, v \in L^{2,2}(\Omega),\quad a(u,v) = \int_\Omega (u^{20}v^{20} + 2u^{11}v^{11} + u^{02}v^{02})\,dx \tag{1.1}$$

For $\forall\, f \in (L^{2,2}(\Omega))'$, consider the variation problem:

$$u_0 \in H^1_0(\Omega),\quad a(Eu_0, Ev) = f(Ev) \qquad (\forall v \in H^1_0(\Omega)) \tag{1.2}$$

Pick $U_\tau (\tau = 1, 2, \cdots)$ to be a finite dimension subspace of $L^{2,2}(\Omega)$, then the variation problem below

$$u_\tau \in U_\tau,\quad a(u_\tau, v) = f(v) \qquad (\forall v \in U_\tau) \tag{1.3}$$

is the multiple set function finite element approximation of (1.2). If U_τ is constructed according to the quasi-conformal element method, then (1.3) is the quasi-conformal element method to solve (1.2) (see reference (1)).

For $\tau = 1, 2, \cdots$, let K_τ be a finite element dissection of Ω with the following properties:

K_1 : for $\forall K \in K_\tau$, K is a triangle (or a parallelogram), and $\bar{\Omega} = \bigcup_{K \in K_\tau} K$ $(\tau = 1, 2, \cdots)$,

K_2 : the intersection or null OR of any two distinct elements in K_τ is a common edge or is a common apex;

K_3 : denotes ρ_K to be the diameter of the maximum inscribed circle, h_K is the outer diameter of K, $h_\tau = \sup_{K \in K_\tau} h_K$ $(\tau = 1, 2, \cdots)$ then $\lim_{\tau \to \infty} h_\tau = 0$ and there exists a positive number $\eta > 0$ unrelated to τ such that $\eta h_\tau \leqslant \rho_K (\forall K \in K_\tau)$.

Quasi-conformal elements construct U_τ according to the following procedure.[1,2,3,4,5]

First, given an integer t > 0, for $\forall K \in K_T$, given linear interpolation operators $\Pi_K^{00}: H^1(K) \to H^2(K)$, $\Pi_{0E}: H^1(K) \to L^2(\partial K)$, $\Pi_{1E}: H^1(K) \to L^2(\partial K)$ and $\Pi_{2E}^{N}: H^1(K) \to L^2(\partial K)$ and the finite dimension subspace $N_K^{i\ j}$ constructed from a multiple term formula, $0 < i + j < 2$. Next, define operator $\Pi_K^{i\ j}: H^1(K) \to N_K^{i\ j}$, $0 \le i + j \le 2$. For $\forall \omega \in H^t(K)$, $\Pi_K^{i\ j}\omega$ is determined by the following equations.

$$\forall P \in N_K^{10},\ \int_K P\Pi_K^{10}\omega dx = \int_{\partial K} P\Pi_{0E}\omega N_1 ds - \int_K \partial_{x_1} P\,\Pi_K^{00}\omega dx \tag{1.4}$$

$$\forall P \in N_K^{01},\ \int_K P\Pi_K^{01}\omega dx = \int_{\partial K} P\Pi_{0E}\omega N_2 ds - \int_K \partial_{x_2} P\,\Pi_K^{00}\omega dx \tag{1.5}$$

$$\forall P \in N_K^{20},\ \int_K P\Pi_K^{20}\omega dx = \int_{\partial K} P(N_1^2\Pi_{0E}^{N}\omega - N_1N_2\Pi_{1E}\omega)\,ds - \int_K \partial_{x_1} P\Pi_K^{10}\omega dx \tag{1.6}$$

$$\forall P \in N_K^{11},\ 2\int_K P\Pi_K^{11}\omega dx = \int_{\partial K} P[2N_1N_2\Pi_{0E}^{N}\omega + (N_1^2 - N_2^2)\Pi_{1E}\omega]ds - \int_K (\partial_{x_1} P\Pi_K^{01}\omega + \partial_{x_2} P\Pi_K^{10}\omega)dx \tag{1.7}$$

$$\forall P \in N_K^{02},\ \int_K P\Pi_K^{02}\omega dx = \int_{\partial K} P(N_2^2\Pi_{0E}^{N}\omega + N_1N_2\Pi_{1E}\omega)\,ds - \int_K \partial_{x_2} P\Pi_K^{01}\omega dx \tag{1.8}$$

in which $N = (N_1, N_2)^T$ is the unit external vector of ∂K.

Finally, define operator $\Pi_h: H^1(\Omega) \to L^{1,2}(\Omega)$, for $\forall u \in H^1(\Omega)$, $\Pi_h u$ is determined by the following formula:

$$(\Pi_h u)^{ij}\Big|_E = \Pi_E^{ij}(u|_E) \qquad (i+j \le 2,\ K \in K_h) \tag{1.9}$$

With respect to problem (1.2), make $U_h = \Pi_h(H^1(\Omega) \cap H_0^1(\Omega))$. This is the quasi-conformal element method.

According to reference (1), we say that $\{U_h\}$, $H_0^1(\Omega)$ (or $H^1(\Omega)$) possess approximability, if for $\forall w \in H_0^1(\Omega)$ (or $H^2(\Omega)$), we have

$$\lim_{h \to 0} \inf_{v_h \in U_h} \|Ew - v_h\|_{1,1,\Omega} = 0$$

We say that $\{U_h\}$, $H_0^1(\Omega)$ (or $H^1(\Omega)$) passes the extended part interval test if when $v_h \in U_h$ $(r = 1, 2, \cdots)$, and $\sup_r \|v_r\|_{1,1,\Omega} < \infty$, for $\forall \varphi \in C_0^\infty(R^2)$ (or $\forall \varphi \in C_0^\infty(\Omega)$) we have $\lim_{r \to \infty} T_{i,j}(\varphi, v_r) = 0$ $(i = 0, 1, 2, j = 1, 2)$. Here

$$T_{0,1}(\varphi,v_\tau)=\int_\Omega(\partial_{x_1}\varphi\, v_\tau^{01}+\varphi v_\tau^{10})\,dx$$

$$T_{0,2}(\varphi,v_\tau)=\int_\Omega(\partial_{x_2}\varphi\, v_\tau^{01}+\varphi v_\tau^{01})\,dx$$

$$T_{1,1}(\varphi,v_\tau)=\int_\Omega(\partial_{x_1}\varphi\, v_\tau^{10}+\varphi v_\tau^{20})\,dx$$

$$T_{1,2}(\varphi,v_\tau)=\int_\Omega(\partial_{x_1}\varphi\, v_\tau^{10}+\varphi v_\tau^{11})\,dx$$

$$T_{2,1}(\varphi,v_\tau)=\int_\Omega(\partial_{x_1}\varphi\, v_\tau^{01}+\varphi v_\tau^{11})\,dx$$

$$T_{2,2}(\varphi,v_\tau)=\int_\Omega(\partial_{x_2}\varphi\, v_\tau^{01}+\varphi v_\tau^{02})\,dx$$

With regard to the convergence of the solution of (1.3) we have the following theorem (1,6).

Theorem 1. Let $a(\cdot,\cdot)$ be uniformly positive definite, that is there exists a positive constant, α unrelated to τ such that

$$\forall v_\tau\in U_\tau,\ \alpha\|v_\tau\|^2_{L^{1,1}(\Omega)}\leqslant a(v_\tau,v_\tau) \tag{1.10}$$

for $\tau = 1, 2, \cdots$ is uniformly established, then for $\forall F\in(L^{2,2}(\Omega))'$, the necessary and sufficient condition for the solution u_τ of (1.3), under the meaning of $|\cdot|_{L^{2,2}(\Omega)}$ to converge on the solution of (1.2) Eu_0 is that $\{U_\tau\}$ and $H_0^2(\Omega)$ is approximate and passes the extended part interval test.

In the second section we prove the compactness theorem for conditions where $\{U_\tau\}$ possesses consistency and then prove the generalized Poincare inequality. In the third section for quasi-conformal element spaces with consistency, we prove that element order is able, under some conditions, to derive consistency and even stronger results. The major idea is the concept of normal affine continuous groups. The fourth section will discuss approximation and the extended part interval test, providing convergence theorems and precision estimates for the quasi-conformal element method. Last, section five will give proofs of the theorems in section three and section four.

II. Compactness Theorems

Let $\{U_\tau\}$ be a series of subspaces of $L^{2,2}(\Omega)$. We say that $\{U_\tau\}$ consistency if there exists an integer $r > 0$ and a constant c unrelated to K and τ such that: a) for $\forall v_\tau\in U_\tau$, $\forall\tau$, $v_\tau^{i,j}|_K\in P_\tau(K)$ for $\forall K\in K_\tau$ $(0\leq i+j\leq 2)$ is established; b) the inequality below

$$l=0,1,\ \sum_{i+j=l}|v_\tau^{i,j}|_{0,K}\leqslant c\left\{\sum_{m+s=l+1}|v_\tau^{m,s}|_{0,K}+h_\tau^{l-1}\sum_{m+s=1}|v_\tau^{m,s}|_{0,K}\right\} \tag{2.1}$$

for $\forall v_\tau\in U_\tau$, $\forall K\in K_\tau$, $\forall\tau$ is uniformly established; c) the inequality below

$$i+j\leqslant 1,\ |(v_\tau^{i,j})^{K'}(x)-(v_\tau^{i,j})^{K''}(x)|\leqslant c\left\{h_\tau\sup_{K\subset K_0(x)}\sup_{y\in\xi}\sum_{m+s=i+j+1}|v_\tau^{m,s}(y)|\right. \tag{2.2}$$

$$\left.+h_\tau^{i+j-1}\sup_{K\subset K_0(x)}\sup_{y\in\xi}\sum_{m+s=1}|v_\tau^{m,s}(y)|\right\}$$

is uniformly established for $\forall K'$, $K'\in K_\tau(x)$, $\forall x\in\Omega$, $\forall v_\tau\in U_\tau$ and $\forall\tau$. Here $(v_\tau^{ij})^{K'}$, $(v_\tau^{ij})^{K''}$ are the continuous extensions of $v_\tau^{ij}|_{\underline{K}'}$, $v_\tau^{ij}|_{\underline{K}''}$ on K' and K'', $K_\tau(x) = \{K \mid x\in K, K\in K_\tau\}$, $\underline{K}'$, $\underline{K}''$, $\underline{K}$ are respectively the internal set of points of K', K'', and K.

We know that although U_τ is not necessarily contained in $EH^2(\Omega)$, it will be near $EH^2(\Omega)$ or its subspace. Therefore, the elements of U_τ must possess weaker properties similar to those of the elements of $EH^2(\Omega)$. Consistency is exactly what marks off these properties. The inequality (2.1) has in mind the relationship between the elements' various components and inequality (2.2) pays attention to concinuity through interior boundaries. When U_τ is not a quasi-conformal element space, the weak discontinuity in reference (7) and the weak continuity in reference (8) both are able to lead to consistency. The conditions for establishing consistency will be discussed below. Now we set up the compactness theorems.

Theorem 2. If $\{U_\tau\}$ possesses consistency, then the following two conclusions are true:

1) If $v_\tau\in U_\tau$ ($\tau = 1, 2\cdots$) and under the meaning of $L^{2,2}(\Omega)$ it weakly converges to 0, then we have $\lim\limits_{\tau\to\infty}\sum\limits_{i+j\le 1}\|v_\tau^{ij}\|_{L^2(\Omega)}=0$,

2) If $\{U_\tau\}$ and $H^2(\Omega)$ (or $H_0^2(\Omega)$) possess approximability and pass the extended part interval test, then for any bounded sequence $\{v_\tau\}$ in $L^{2,2}(\Omega)$, $v_\tau\in U_\tau$, there exists a subsequence $\{v_{\tau'}\}$ of $\{v_\tau\}$ and $v_0\in H^2(\Omega)$ (or $H_0^2(\Omega)$) such that $v_{\tau'}$ weakly converges to Ev_0 and $\lim\limits_{\tau'\to\infty}\sum\limits_{i+j\le 1}\|v_{\tau'}^{ij}-(Ev_0)^{ij}\|_{L^2(\Omega)}=0$.

This theorem is the extension of the Rellich compactness theorem on the multiple set function space U_τ and is also the generalization of the work in reference (8). Its proof entirely parallels the method in reference (8) so it is omitted here. Similarly, the methods of reference (8) can also give the theorems below.

Theorem 3. If $\{U_\tau\}$ possesses consistency then the following conclusions are true:

1) If $\{U_\tau\}$ and $H_0^2(\Omega)$ possess approximability and pass the extended part interval test, then there exist constants c, γ such that the generalized Poincare-Friedrichs inequality

$$\|v_\tau\|^2_{L^{2,2}(\Omega)}\le c\sum_{i+j=2}\|v_\tau^{ij}\|^2_{L^2(\Omega)}\quad(\forall v_\tau\in U_\tau) \tag{2.3}$$

is uniformly established for $\tau > \gamma$.

2) If $\{U_\tau\}$ and $H^2(\Omega)$ possess approximability and pass the extended part interval test, then there exist constants c, γ such that the generalized Poincare inequality

$$|v_\tau|^2_{L^2,2(\Omega)} \leqslant c\left\{ \sum_{i+j=2} |v_\tau^{ij}|^2_{L^2(\Omega)} + \sum_{i+j<2} \left(\int_\Omega v_\tau^{ij} dx \right)^2 \right\} \tag{2.4}$$

and the extended Friedrichs inequality

$$|v_\tau|^2_{L^2,2(\Omega)} \leqslant c\left\{ \sum_{i+j=2} |v_\tau^{ij}|^2_{L^2(\Omega)} + \int_{\partial\Omega} |v_\tau^{00}|^2 ds \right\} \tag{2.5}$$

are uniformly established for $\forall v_\tau \in U_\tau$, $\forall \tau \geqslant \nu$.

III. Element Order Conditions

From here on we pick U_τ to be constructed by the quasi-conformal element method (see Section I). In this section we discuss the conditions for $\{U_\tau\}$ to possess consistency. We begin from the definition of element order conditions and a normal affine continuous group.

Element order conditions. We say $\{U_\tau\}$ satisfies element order conditions if for $\forall w \in H^t(K)$, $\forall K \in K_\tau$, $(t = 1, 2, \cdots)$, from $\Pi_K^{10} w = \Pi_K^{11} w = \Pi_K^{01} w = 0$ we are able to derive $\Pi_K^{10} w, \Pi_K^{01} w \in P_0(K)$, $\Pi_K^{00} w \in P_1(K)$, and $\Pi_{\partial K} w - \Pi_K^{00} w|_{\partial K} = \Pi_{\partial K}^{\tau} w - \dfrac{\partial}{\partial s} \Pi_K^{00} w|_{\partial K} = \Pi_{\partial K}^{N} w - \dfrac{\partial}{\partial N} \Pi_K^{00} w|_{\partial K} = 0$.

The physical meaning of element order condition is "the zero energy mode is only able to be rigid body displacement" and the verification of this is the testing of the order of a matrix, so we call it the element order condition.

Now we will discuss further the operators Π_K^{00}, $\Pi_{\partial K}$, etc. For any element K, let there exist continuous functionals $\phi_{1,K}, \phi_{2,K}, \cdots, \phi_{M,K}$, which are continuous and unique on $H^t(K)$ as well as a set of polynomials $G_{1,K}, \cdots, G_{M,K}$ and a set of functions $g_{j,K}$, $g^{\tau}_{j,K}$, $g^{N}_{j,K}$, $1 \leqslant j \leqslant M$, in the space $\{g \mid g \in L^2(\partial K)$, when F is a side of K, $g|_F$ is a polynomial on F$\}$ such that for $\forall w \in H^t(K)$, we have

$$\left.\begin{aligned} \Pi_K^{00} w &= \sum_{j=1}^{M} \phi_{j,K}(w) G_{j,K} \\ \Pi_{\partial K} w &= \sum_{j=1}^{M} \phi_{j,K}(w) g_{j,K} \\ \Pi_{\partial K}^{\tau} w &= \sum_{j=1}^{M} \phi_{j,K}(w) g^{\tau}_{j,K} \\ \Pi_{\partial K}^{N} w &= \sum_{j=1}^{M} \phi_{j,K}(w) g^{N}_{j,K} \end{aligned}\right\} \tag{3.1}$$

and when $\Pi_K^{00}w=0, \Pi_{\partial K}w=\Pi_{\partial K}^1 w=\Pi_{\partial K}^N w=0$ 时 $\phi_{j,K}(w)=0, 1\leqslant j\leqslant M$. We say $\phi_{j,K}$ is a parameter of Π_K^{00}, $\Pi_{\partial K}$, $\Pi_{\partial K}^1$, $\Pi_{\partial K}^N$.

We selected a fixed reference element $\hat{K}$ (a triangle or rectangle). For all elements, K, there exists an affine transform $F_K\hat{x} = B_K\hat{X} + b_K$, B_K is a 2 x 2 nonsingular matrix, $b_K \in R^2$, such that $K = F_K\hat{K}$. Thereupon for any function ω defined on K (or ∂K), denote

$$\hat{w}(\hat{x})=w(F_K\hat{x}) \qquad (\forall \hat{x}\in\hat{K}(\text{或}\partial\hat{K})) \tag{3.2}$$

For the linear function $\phi_{j,K}$, we define a linear function $\hat{\phi}_{j,K}$ on $H^t(\hat{K})$ as follows:

$$\forall \hat{w}\in H^t(\hat{K}),\ \hat{\phi}_{j,K}(\hat{w})=\phi_{j,K}(w) \tag{3.3}$$

in which $\hat{\omega}$, ω correspond to the form of formula (3.2). We say the operator order $\{\Pi_K^{00}, \Pi_{\partial K}, \Pi_{\partial K}^1, \Pi_{\partial K}^N\}=\{(\Pi_K^{00}, \Pi_{\partial K}, \Pi_{\partial K}^1, \Pi_{\partial K}^N)\,|\,K\in K_r, r=1,2,\cdots\}$ is a normal affine continuous group when: (1) if for a set of elements $\{K_m\}_{m=1}^{\infty}$ there is a B_{K_m} in the matrix norm sense converging to B_{K_0}. Then for $j=1,\cdots,M$, $\hat{\phi}_{j,K_m}$ converges to $\hat{\phi}_{j,K_0}$ under the norm of the dual spaces of $H^t(\hat{K})$, $\hat{G}_{j,K_m}$ uniformly converges to $\hat{G}_{j,K_0}$, while $\hat{g}_{j,K_m}$, $\hat{g}_{j,K_m}^s$, and $\hat{g}_{j,K_m}^N$, with the sense of $L^2(\partial K)$, converge respectively to $\hat{g}_{j,K_0}$, $\hat{g}_{j,K_0}^s$, and $\hat{g}_{j,K_0}^N$; (2) for any element K and constant θ, denote $\bar{K}=\{\bar{x}\,|\,\bar{x}=\theta x, \forall x\in K\}$, and for any function ω defined on K (or ∂K), denote $\bar{w}(\bar{x})=w(\theta^{-1}\bar{x}), \bar{x}\in\bar{K}$ (或$\partial\bar{K}$), then we have $(\Pi_K^{00}w)(x)=(\Pi_{\bar{K}}^{00}\bar{w})(\theta x)$, $(\Pi_{\partial K}w)(x)=(\Pi_{\partial\bar{K}}\bar{w})(\theta x)$, $(\Pi_{\partial K}^1 w)(x)=\theta(\Pi_{\partial\bar{K}}^1\bar{w})(\theta x)$, $(\Pi_{\partial K}^N w)(x)=\theta(\Pi_{\partial\bar{K}}^N\bar{w})(\theta x)$, $x\in K$(或∂K), $w\in H^t(K)$.

If the interpolation operators, Π_K^{00}, $\Pi_{\partial K}$, $\Pi_{\partial K}^1$, $\Pi_{\partial K}^N$ only use functions of the interpolation points and their derivative values, and if certain kinds of integral average values of the functions and derivatives act as parameters, and if the relative positions of the interpolation points on K are affine invariant, then $\{\Pi_K^{00}, \Pi_{\partial K}, \Pi_{\partial K}^1, \Pi_{\partial K}^N\}$ is a normal affine continuous group. This demonstrates that commonly used interpolation operators are normal affine continuous groups. It is not difficult to see that this is a generalization of affine groups.[9]

We say that $\{N_K^{ij}\}=\{N_K^{ij}\,|\,K\in K_r, r=1,2,\cdots\}$ is normal affine continuous if (1) for any element K there exists a group base $P_{l,K}(1 \leq l \leq L_{ij})$, of N_K^{ij} such that when $B_{K_m}\to B_{K_0}$, we have $\hat{P}_{l,K_m}$ converges uniformly to $\hat{P}_{l,K_0}$ $(1\leq l\leq L_{ij})$; (2) for any element K and constant θ, if we denote $\bar{K}=\{\bar{x}\,|\,\bar{x}=\theta x, \forall x\in K\}$, then $P_{l,K}(x)=P_{l,\bar{K}}(\theta x)$, $(\forall x\in K,\ 1\leqslant l\leqslant L_{ij})$.

One special situation of $\{N^{ij}\}$ being normal affine continuous is just that it be affine, that is that there exists an N_K^{ij} such that for any element K, $N_K^{ij} = \{P \mid P(x) = \hat{P}(F_K^{-1}x),\ \forall \hat{P} \in N_{\hat{K}}^{ij}\}$.

We say that $\{U_\tau\}$ possesses strong continuity if for every boundary F of any element K, there exist continuous functions q_F, q_F^s, q_F^N on the polynomial space which is defined on F. They have these properties $q_\tau(1)q_\tau^s(1)q_\tau^n(1) \neq 0$, and $\{q_\tau\} = \{q_\tau \mid F \subset \partial K, K \in K_\tau, \forall \tau\}$, $\{q_\tau^s\} = \{q_\tau^s \mid F \subset \partial K, K \in K_\tau, \forall \tau\}$ $\{q_\tau^n\} = \{q_\tau^n \mid F \subset \partial K, K \in K_\tau, \forall \tau\}$ respectively are affine groups such that when $F = K \cap K'$ is a side, for $\forall w \in H^1(\Omega)$, $q_\tau(\Pi_{\tau K} w|_\tau) = q_\tau(\Pi_{\tau K'} w|_\tau)$, $q_\tau^s(\Pi_{\tau K}^s w|_\tau) = -q_\tau^s(\Pi_{\tau K'}^s w|_\tau)$, $q_\tau^n(\Pi_{\tau K}^n w|_\tau) = -q_\tau^n(\Pi_{\tau K'}^n w|_\tau)$, when $F = K \cap \partial\Omega$, for $\forall w \in H^1(\Omega) \cap H_0^1(\Omega)$, $q_\tau(\Pi_{\tau K} w|_\tau) = q_\tau^s(\Pi_{\tau K}^s w|_\tau) = q_\tau^n(\Pi_{\tau K}^n w|_\tau) = 0$. We say $\{q_F\}$ is an affine group to indicate that if $F = F_K \hat{F}$, then for any polynomial P on F, we have $q_F(P) = q_{\hat{F}}(\hat{P})$, and similarly for the others.

If for $\forall w \in H^1(K)$, $\Pi_{\tau K} w|_\tau$ is used at the function interpolation points of ω in F, $\Pi_{\tau K}^s w|_\tau$ and $\Pi_{\tau K}^n w|_\tau$ are respectively used at tangential and normal derivative points when $\{U_\tau\}$ is strongly continuous; If $\Pi_{\tau K} w|_\tau$ is used at function interpolation points of ω in F, and the integral average of $\Pi_{\tau K}^s w|_\tau$, $\Pi_{\tau K}^n w|_\tau$ on F are uniquely determined by parameters of ω on F, then $\{U_\tau\}$ is also strongly continuous, which is to say that the common spaces $\{U_\tau\}$ all are strongly continuous.

Having the above concepts we can provide the conditions for establishing consistency.

Theorem 4. Let the three following conditions be established:

1) $\{\Pi_K^0, \Pi_{\tau K}, \Pi_{\tau K}^s, \Pi_{\tau K}^n\}$ is a normal affine continuous group and for $\forall P \in P_l(K)$, $\Pi_K^0 P = P$, $\Pi_{\tau K} P = P|_{\tau K}$, $\Pi_{\tau K}^s P = \frac{\partial P}{\partial s}|_{\tau K}$, $\Pi_{\tau K}^n P = \frac{\partial P}{\partial N}|_{\tau K}$;

2) $\{N_K^{ij}\}$ is normal affine continuous and N_K^{ij} contains a constant space $(0 < i + j < 2)$;

3) $\{U_\tau\}$ possesses strong continuity.

Then from the establishment of element order we can assert that $\{U_\tau\}$ possesses consistency, moreover there exists a constant unrelated to F, K, and τ such that the inequalities

$$l = 0, 1, \quad \sum_{i+j=l} |\Pi_K^{ij} w|_{i,\infty,K} \leq c \sum_{m+s=l} |\Pi_K^{ms} w|_{m,K} \tag{3.4}$$

$$|\partial_{x_1}\Pi_K^{s_0}w-\Pi_K^{t_0}w|_{0,K}+|\partial_{x_2}\Pi_K^{s_0}w-\Pi_K^{s_1}w|_{0,K}\leqslant c\,h_K\sum_{i+j=2}|\Pi_K^{i,j}w|_{0,K} \tag{3.5}$$

$$|\Pi_K^{s_0}w-\Pi_{eK}w|_{0,eK}\leqslant ch_K^{\frac{1}{2}}\sum_{m+s=2}|\Pi_K^{m,s}w|_{0,K} \tag{3.6}$$

$$|\Pi_{eK}^{t}w-\frac{\partial}{\partial S}\Pi_K^{s_0}w|_{0,eK}+|\Pi_{eK}^{n}w-\frac{\partial}{\partial N}\Pi_K^{s_0}w|_{0,eK}\leqslant c\,h_K^{\frac{1}{2}}\sum_{m+s=2}|\Pi_K^{m,s}w|_{0,K} \tag{3.7}$$

for $\forall w\in H^2(K)$, $\forall K\in\mathcal{K}_h$, and $\forall\tau$ are uniformly established and when $F=K\cap K'$ is a side, the inequalities

$$|\Pi_{eK}w-\Pi_{eK'}w|_{0,F}\leqslant c\,h_F^{\frac{1}{2}}\sum_{m+s=2}\left(|\Pi_K^{m,s}w|_{0,K}+|\Pi_{K'}^{m,s}w|_{0,K'}\right) \tag{3.8}$$

$$|\Pi_{eK}^{t}w-\Pi_{eK'}^{t}w|_{0,F}+|\Pi_{eK}^{n}w-\Pi_{eK'}^{n}w|_{0,F}\leqslant ch_F^{\frac{1}{2}}\sum_{m+s=2}\left(|\Pi_K^{m,s}w|_{0,K}+|\Pi_{K'}^{m,s}w|_{0,K'}\right) \tag{3.9}$$

are established for $\forall w\in H^2(\Omega)$ and when $F=K\cap\partial\Omega$ is a side, the inequalities

$$|\Pi_{eK}w|_{0,F}\leqslant ch_F^{\frac{1}{2}}\sum_{m+s=2}|\Pi_K^{m,s}w|_{0,K} \tag{3.10}$$

$$|\Pi_{eK}^{t}w|_{0,F}+|\Pi_{eK}^{n}w|_{0,F}\leqslant ch_F^{\frac{1}{2}}\sum_{m+s=2}|\Pi_K^{m,s}w|_{0,K} \tag{3.11}$$

are established for $\forall w\in H^2(\Omega)\cap H_0^1(\Omega)$.

Because these three conditions of this theorem are not indexed and commonly used elements satisfy these conditions, the element order condition can replace the consistency condition. The verification of the element order condition can be summed up as an examination of a matrix order.

For $\forall w\in H^2(K)$, in $N_K^{i,j}(i+j=2)$ select a group base, denote the coordinate of $\Pi_K^{i,j}w$ in this group base as $\beta_K^{i,j}(w)$ and make

$$\begin{aligned}&\beta_K(w)=((\beta_K^{2,0}(w))^T,(\beta_K^{1,1}(w))^T,(\beta_K^{0,2}(w))^T)^T\\&\phi_K(w)=(\phi_{1,K}(w),\phi_{2,K}(w),\cdots,\phi_{M,K}(w))^T\end{aligned} \tag{3.12}$$

$$L=L_{20}+L_{11}+L_{02} \tag{3.13}$$

in which L_{ij} is the dimension of $\beta_K^{i,j}(w)$. Then (3.6)$\sim$(3.8) can be written as

$$A_K\beta_K(w)=Q_K\phi_K(w) \tag{3.14}$$

in which A_K is an L x L nonsingular matrix and Q_K is an L x M matrix.

Theorem 5. Let N_K^{10}, N_K^{01} contain a constant space and for $\forall P\in P_1(K)$, $\Pi_E^{01}P=P$, $\Pi_{eE}P=P|_{eE}$, $\Pi_{eE}^{t}P=\dfrac{\partial P}{\partial t}|_{eE}$, $\Pi_{eE}^{n}P=\dfrac{\partial P}{\partial N}|_{eE}$. Then the establishment of the element order condition is equivalent to the order of Q_K being M - 3.

IV. Conditions for Quasi-Conformal Element Convergence

In the foregoing section we resolved the problm of consistency. Now we discuss approximation and extended part interval convergence. First, the approximation result for affine groups (9) is extended to normal affine continuous groups.

Theorem 6. Let $\{\Pi_E^{01}, \Pi_{eE}, \Pi_{eE}^{t}, \Pi_{eE}^{n}\}$ be a normal affine continuous group and $\{N_K^{ij}\}$ be normal affine continuous, $0 \le i + j \le 2$. If there exists an integer $r_i \ge 2$ $(1 \le i \le 5)$, such that $\Pi_E^{01}, H^{r_1,r_2+1}(K)\to H^m(K)(0\le m\le r_1+1)$, $\Pi_{eE}, H^{r_3,r_4+1}(K)\to L^2(\partial K)$, $\Pi_{eE}^{t}, H^{r_3,r_4+1}(K)\to L^2(\partial K)$, $\Pi_{eE}^{n}, H^{r_3,r_4+1}(K)\to L^2(\partial K)$ are continuous and for $\forall P\in P_{r_1}(K)$ we have $\Pi_E^{01}P=P$, for $\forall P\in P_{r_2}(K)$ we have $\Pi_{eE}P=P|_{eE}$, for $\forall P\in P_{r_3}(K)$ we have $\Pi_{eE}^{t}P=\dfrac{\partial P}{\partial t}|_{eE}$, for $\forall P\in P_{r_4}(K)$ we have $\Pi_{eE}^{n}P=\dfrac{\partial P}{\partial N}|_{eE}$, and $P_{r_5,r_5+1}(K)\subset N_K^{ij}(0\le i+j\le 2)$, then there exists a constant $c > 0$ unrelated to K and τ such that

$$0\le l\le m,\ |v-\Pi_E^{01}v|_{l,E}\le ch_E^{r_1+1-l}|v|_{r_1+1,E} \tag{4.1}$$

$$|v-\Pi_{eE}v|_{e,eE}\le ch_e^{r_2+\frac{1}{2}}|v|_{r_2+1,E} \tag{4.2}$$

$$\left|\frac{\partial v}{\partial t}-\Pi_{eE}^{t}v\right|_{e,eE}\le ch_e^{r_3-\frac{1}{2}}|v|_{r_3+1,E} \tag{4.3}$$

$$\left|\frac{\partial v}{\partial N}-\Pi_{eE}^{n}v\right|_{e,eE}\le ch_e^{r_4-\frac{1}{2}}|v|_{r_4+1,E} \tag{4.4}$$

are uniformly established for $\forall v\in H^r(K), \forall K\in K_\tau$, $r=1,2,\cdots$ and

$$|Ev-\Pi_\tau v|_{L^2(\Omega)}\le c\sum_{e=1}^{6}h_e^{r_5-1}|v|_{r_5+1,\Omega} \tag{4}$$

is uniformly established for $\forall v\in H^r(\Omega)\cap H^r(\Omega)$, $\forall r=1,2,\cdots$. Here $r=\max\limits_{1\le i\le 5}(r_i+1)$.

Because, under this theorem's conditions $\{U_\tau\}$ is approximate and these conditions are rather broad, from now on we take the condition that $\{U_\tau\}$ constructed using the quasi-conformal element method satisfies theorem 6 to mean that it is approximate.

Although under conditions of the energy functionals being positive and $\{U_\tau\}$ is approximate, passing the extended part interval test is a sufficient and necessary condition of convergence, its verification is not easy. Below we give an easier condition of verification--IPT testing.

IPT Testing: For $\forall K\in K$, there exists interpolation operators $\tilde{\Pi}^{v}_{\cdot K}$, $\tilde{\Pi}^{n}_{\cdot K}$ such that $\{\Pi^{m}_{I}, \Pi_{\cdot K}, \tilde{\Pi}^{v}_{\cdot K}, \tilde{\Pi}^{n}_{\cdot K}\}$ are also a normal affine continuous group and the parameters of Π^{m}_{I}, $\Pi_{\cdot K}$, $\tilde{\Pi}^{v}_{\cdot K}$, $\tilde{\Pi}^{n}_{\cdot K}$ are a linear combination of the parameters of Π^{m}_{I}, $\Pi_{\cdot K}$, $\Pi^{v}_{\cdot K}$, $\Pi^{n}_{\cdot K}$ and for $\forall P\in P_{r_0}(K)$, $\tilde{\Pi}^{v}_{\cdot K}P=\left.\frac{\partial P}{\partial s}\right|_{\cdot K}$, $\tilde{\Pi}^{n}_{\cdot K}P=\left.\frac{\partial P}{\partial N}\right|_{\cdot K}$. If there exists $r_0>2$ such that the following two conditions are established:

a) For $\forall u\in H^{r}(\Omega)\cap H^{1}_{0}(\Omega)$, when $F=K\cap K'$ is a side we have

$$\forall P\in P_{r_0-2}(F),\quad \int_{F}P\begin{bmatrix}\tilde{\Pi}^{v}_{\cdot K}u\\ \tilde{\Pi}^{n}_{\cdot K}u\end{bmatrix}ds=-\int_{F}P\begin{bmatrix}\tilde{\Pi}^{v}_{\cdot K'}u\\ \tilde{\Pi}^{n}_{\cdot K'}u\end{bmatrix}ds \tag{4.6}$$

when $F=K\cap\partial\Omega$ is a side we have

$$\forall P\in P_{r_0-2}(F),\quad \int_{F}P\tilde{\Pi}^{v}_{\cdot K}u\,ds=\int_{F}P\tilde{\Pi}^{n}_{\cdot K}u\,ds=0 \tag{4.7}$$

b) For $\forall w\in H^{r}(K)$, $\forall K\in K$, $(r=1,2,\cdots)$ we have

$$\forall P\in P_{r_0-2}(K),\ \int_{\cdot K}P\begin{bmatrix}N^{1}_{1}(\Pi^{n}_{\cdot K}-\tilde{\Pi}^{n}_{\cdot K})w-N_1N_2(\Pi^{v}_{\cdot K}-\tilde{\Pi}^{v}_{\cdot K})w\\ 2N_1N_2(\Pi^{n}_{\cdot K}-\tilde{\Pi}^{n}_{\cdot K})w+(N^{2}_{1}-N^{1}_{1})(\Pi^{v}_{\cdot K}-\tilde{\Pi}^{v}_{\cdot K})w\\ N^{1}_{1}(\Pi^{n}_{\cdot K}-\tilde{\Pi}^{n}_{\cdot K})w+N_1N_2(\Pi^{v}_{\cdot K}-\tilde{\Pi}^{v}_{\cdot K})w\end{bmatrix}ds=0 \tag{4.8}$$

then we say $\{U_\tau\}$ has passed the IPT test.

Theorem 7. If $\{U_\tau\}$ possesses approximability and strong continuity, satisfies the element order condition and passes the IPT test, then for any $f\in(L^{2,1}(\Omega))'$, the solution of (1.3) converges to the solution of (1.2): $\lim_{\tau\to 0}|Eu_\tau-u_\cdot|_{L^{2,1}(\Omega)}=0$.

Theorem 8. Let $\{U_\tau\}$ possess approximability and strong continuity, satisfy the element order condition and pass the IPT test. If when $F=K\cap K'$ is a side for $\forall u\in H^{r}(\Omega)$, we have

$$\forall P\in P_{r_0-3}(F),\quad \int_{F}\Pi_{\cdot K}uP\,ds=\int_{F}\Pi_{\cdot K'}uP\,ds \tag{4.9}$$

established and when $F=K\cap\partial\Omega$ for $\forall u\in H^{r}(\Omega)\cap H^{1}_{0}(\Omega)$ we have

$$\forall P\in P_{r_0-3}(F),\quad \int_{F}P\Pi_{\cdot K}u\,ds=0 \tag{4.10}$$

established then there exists a constant c, unrelated to u_0, τ such that when taking $f(v)=\int_{\Omega}fv^{m}dx$, $f\in L^{1}(\Omega)$, if $u_\cdot\in H^{r}(\Omega)\cap H^{1}_{0}(\Omega)$ then

$$|Eu_\tau-u_\cdot|_{L^{2,1}(\Omega)}\leq c\left\{\sum_{i=1}^{k}h_i^{r-1}|u_\cdot|_{r+1,\Omega}+h_i^{r-1}|u_\cdot|_{r,\Omega}\right\} \tag{4.11}$$

is uniformly established for $\forall_T = 1, 2, \cdots$. Here $r' = \max\{r_i + 1, 4\}$, $P_{r-1}(F) = \{0\}$, $r = \max_{1 \le i \le s}\{r_i + 1, 4\}$. If for $\forall K \in \Lambda_h$, $\forall r$, $\Pi_{Ks} w = \Pi_K^m w|_{\partial K}$, $\forall w \in H^r(K)$ $\forall w \in H^r(\Omega) \cap H_0^1(\Omega)$, $(\Pi_h w)^m \in \{v \mid v \in C(\bar{\Omega}), v|_{\partial\Omega} = 0\}$, then $r' = r_0 + 1$, $r = \max_{1 \le i \le s}\{r_i + 1\}$.

It is not difficult to verify that 6, 9, 12, 15, 18, and 21 parameter quasi-conformal elements satisfy the conditions of theorem 7 (1-5). This proves that they are convergent when used to solve plate bending problems. Table 1 provides their convergence precisions.

Table 1.

Number of parameters	$\|E_{hm} - w\|_{l,2,\Omega}$	Regularity requirements	Number of parameters	$\|E_{hm} - w\|_{l,2,\Omega}$	Regularity requirements
6	$O(h_e)$	$w \in H^2(\Omega)$	15	$O(h_e^3)$	$w \in H^4(\Omega)$
9	$O(h_e)$	$w \in H^2(\Omega)$	18	$O(h_e^3)$	$w \in H^4(\Omega)$
12	$O(h_e^2)$	$w \in H^4(\Omega)$	21	$O(h_e^3)$	$w \in H^4(\Omega)$

V. Theorem Proofs

Now we provide the proofs of the theorems in Sections III and IV. First we establish a lemma.

Lemma 1. Let $\{\Pi_K^m, \Pi_{Ks}, \Pi_{Ks}^*, \Pi_{Ks}^*\}$ be a normal affine continuous group and $\{N_K^{ij}\}$ be normal affine continuous. Then for a series of elements $\{K_m\}_{m=0}^{\infty}$ and $w_m \in H^r(K_m)$ $(m = 0, 1, \cdots)$ if $\lim_{m\to\infty} |\phi_{K_m}(w_m) - \phi_{K_0}(w_0)| = \lim_{m\to\infty} |B_{K_m} - B_{K_0}| = 0$, we can assert that for $0 \le i + j \le 2$, $(\Pi_{K_m}^{ij} w_m)(F_{K_m} \hat{x})$ uniformly converges to $(\Pi_{K_0}^{ij} w_0)(F_{K_0} \hat{x})$. Here $|\cdot|$ respectively are the Euclidean norm of the vector and the norm of the matrix to which it corresponds.

Proof. Since $\{\Pi_K^m, \Pi_{Ks}, \Pi_{Ks}^*, \Pi_{Ks}^*\}$ is normal affine continuous, the conclusion of the lemma when $i + j = 0$ is obvious. For $m = 0, 1, \cdots$, in (1.4) make the coordinate conversion $x = B_{K_m} \hat{x} + b_{K_m}$, then use the differentiation chain rule and sum the following equalities

$$dx = |\det B_{K_m}| d\hat{x}, \quad ds = |\det B_{K_m}| |B_{K_m}^{-1} \hat{N}| d\hat{s}, \quad N = \frac{B_{K_m}^{-1} \hat{N}}{|B_{K_m}^{-1} \hat{N}|} \tag{5.1}$$

and we can get:

$$\begin{aligned} 1 \le l \le L_{ij}, \quad & \int_{\hat{s}} \hat{P}_{l,K_m} (\Pi_{K_m}^{ij} w_m)(F_{K_m} \hat{x}) |\det B_{K_m}| d\hat{s} \\ &= \int_{\partial\hat{s}} \hat{P}_{l,K_m} (\Pi_{Ks,m} w_m)(F_{K_m} \hat{x}) (B_{K_m}^{-1} \hat{N})_s |\det B_{K_m}| d\hat{s} \\ &\quad - \int_{\hat{s}} \Big(\sum_{p=1}^{i} b_{K_m}^{pj} \partial_i \hat{P}_{l,K_m} \Big) (\Pi_{K_m}^{ij} w_m)(F_{K_m} \hat{x}) |\det B_{K_m}| d\hat{s} \end{aligned} \tag{5.2}$$

in which $B_{K_m}^{-1} = (b_{K_m}^{ij})_{2\times 2}$.

If denoting $\Pi^{\nu}_{k_m} u_m = \sum_{i=1}^{L_m} \beta_{i,m} P_{i,x_m}$, $A^{ij}_m = \int_{\hat{k}} \hat{P}_{i,\hat{x}} \cdot \hat{P}_{j,\hat{x}} |\det B_{k_m}| d\hat{x}$, R^i_m to be the right side term of (5.2), $1 \leq 1$, $j \leq L_{1 0}$, make

$$A_m = (A^{ij}_m)_{L_m \times L_m}, \quad \beta_m = (\beta_{i,m})_{L_m \times 1}, \quad R_m = (R^i_m)_{L_m \times 1}$$

then (5.2) can become the following equality

$$A_m \beta_m = R_m$$

since $\{\Pi^{\nu}_k, \Pi_{ok}, \Pi^1_{ok}, \Pi^{\alpha}_{ok}\}$ is a normal affine continuous group and $\{K^{10}_K\}$ is normal affine continuous, therefore, by the hypothesis of the lemma, when $m \to \infty$ $A_m \to A_0$, $R_m \to R_0$, and A_0 is nonsingular so $\beta_m \to \beta_0$. From this we immediately derive that $(\Pi^{\nu}_{k_m} u_m)(F_m \hat{x})$ uniformly converges to $(\Pi^{\nu}_{k_0} u_0)(F_{k_0} \hat{x})$. Similarly, other situations can be verified and the lemma is proved.

Proof of Theorem 4: Proof of the longer parts is done in several steps.

a) For $\forall \xi > 0$, we prove that if the set $J_\xi = \{K | K$ is a triangle of the same area as K (or plane quadrilateral), $h_K < \xi\}$ is not empty, then there exists a constant related to ξ such that

$$l = 0, 1, \quad \sum_{i+j=l} |\Pi^{\nu}_k w|_{i,j,K} \leq c(\xi) \sum_{\alpha+\beta=1} |\Pi^{\alpha\beta}_k w|_{0,K} \tag{5.3}$$

$$|\partial_{x_1} \Pi^{\nu}_k w - \Pi^{\nu}_k w|_{0,K} + |\partial_{x_2} \Pi^{\nu}_k w - \Pi^{\nu}_k w|_{0,K} \leq c(\xi) \sum_{\alpha+\beta=1} |\Pi^{\alpha\beta}_k w|_{0,K} \tag{5.4}$$

$$\begin{aligned} &|\Pi^{\nu}_k w - \Pi_{ok} w|_{0,\partial K} + \left| \frac{\partial}{\partial s} \Pi^{\nu}_k w - \Pi^{1}_{ok} w \right|_{0,\partial K} \\ &+ |\Pi^{\alpha}_{ok} w - \frac{\partial}{\partial N} \Pi^{\nu}_k w|_{0,\partial K} \leq c(\xi) \sum_{\alpha+\beta=1} |\Pi^{\alpha\beta}_k w|_{0,K} \end{aligned} \tag{5.5}$$

are uniformly established for $\forall w \in H^{\nu}(K)$, $\forall K \in J_\xi$. We suppose that the above conclusions are not true. Then for $m = 1, 2, \cdots$, there exists $K_m \in J_\xi$ and $w_m \in H^{\nu}(K_m)$, such that

$$\begin{aligned} &|\Pi^{\nu}_{k_m} w_m|_{0,K_m} + \sum_{i+j=1} |\Pi^{ij}_{k_m} w_m|_{0,K_m} + |\partial_{x_1} \Pi^{\nu}_{k_m} w_m - \Pi^{\nu}_{k_m} w_m|_{0,K_m} \\ &+ |\partial_{x_2} \Pi^{\nu}_{k_m} w_m - \Pi^{\nu}_{k_m} w_m|_{0,K_m} + |\Pi^{\nu}_{k_m} w_m - \Pi_{ok_m} w_m|_{0,\partial K_m} \\ &+ |\Pi^{\alpha}_{ok_m} w_m - \frac{\partial}{\partial s} \Pi^{\nu}_{k_m} w_m|_{0,\partial K_m} + |\Pi^{\alpha}_{ok_m} w_m - \frac{\partial}{\partial N} \Pi^{\nu}_{k_m} w_m|_{0,\partial K_m} \\ &> m \sum_{i+j=1} |\Pi^{ij}_{k_m} w_m|_{0,K_m} \end{aligned} \tag{5.6}$$

is established. Since for $P\in P_1(K_m)$, $\Pi^{00}_{K_m}P=P$, $\Pi^{10}_{K_m}P=\partial_{x_1}P$, $\Pi^{01}_{K_m}P=\partial_{x_2}P$, $\Pi^{s}_{\partial K_m}P=\left.\frac{\partial P}{\partial s}\right|_{\partial K_m}$, $\Pi^{N}_{\partial K_m}P=\left.\frac{\partial P}{\partial N}\right|_{\partial K_m}$, $\Pi^{20}_{K_m}P=\Pi^{11}_{K_m}P=\Pi^{02}_{K_m}P=0$, $\Pi_{\partial K_m}P=P|_{\partial K_m}$, and these operators are all linear operators, for m = 1, 2, ··· we can let there be

$$|\phi_{K_m}(w_m)|=1,\ \phi_{K_m}(w_m)\perp\phi_{K_m}(P)\qquad(\forall P\in P_1(K_m)) \tag{5.7}$$

Since $\{K_m\}\subset J_\zeta$, from reference (9) we know that $\{B_{K_m}\}$ is a bounded set. Therefore there exist series $\{\phi_{K_m}(w_m)\}$, $\{B_{K_m}\}$ (still denoted as $\{\phi_{K_m}(w_m)\}$, $\{B_{K_m}\}$) and element K_0 and $w_0\in H^1(K_0)$ satisfying.

$$\lim_{m\to\infty}|\phi_{K_m}(w_m)-\phi_{K_0}(w_0)|=\lim_{m\to\infty}|B_{K_m}-B_{K_0}|=0,\ |\phi_{K_0}(w_0)|=1 \tag{5.8}$$

because $B_{K_m}\to B_{K_0}$, $\hat{\phi}j,K_m\to\hat{\phi}j,K_0$. Thus for j = 1, ···, M we have $\lim_{m\to\infty}\hat{\phi}_{j,K_m}(1)=\hat{\phi}_{j,K_0}(1)$, $\lim_{m\to\infty}\hat{\phi}_{j,K_m}\left(\sum_{i=1}^{2}(B_{K_m}\hat{x})_i\right)=\hat{\phi}_{j,K_0}\left(\sum_{i=1}^{2}(B_{K_0}\hat{x})_i\right)(i=1,2)$ here $B_{K_m}=(b^{ij}_{K_m})_{2\times 2}$. Consequently, from (5.7) we can get

$$\phi_{K_0}(w_0)\perp\phi_{K_0}(P)\qquad(\forall P\in P_1(K_0)) \tag{5.9}$$

On the other hand, from the fact that $\{\Pi^{00}_K,\ \Pi_{\partial K},\ \Pi^{s}_{\partial K},\ \Pi^{N}_{\partial K}\}$ is a normal affine continuous group and lemma 1, we know the left side of (5.6) is uniformly bounded. Thus $\lim_{m\to\infty}\sum_{i+j=2}|\Pi^{ij}_{K_m}w_m|_{\partial K_m}=0$, that is $(\Pi^{ij}_{K_m}w_m)(F_{K_m}\hat{x})$ uniformly converges to 0, i + j = 2. Using lemma 1 again we get

$$\Pi^{ij}_{K_0}w_0=0\qquad(i+j=2) \tag{5.10}$$

From the element order condition we get $\Pi^{10}_{K_0}w_0$, $\Pi^{01}_{K_0}w_0\in P_0(K_0)$, $\Pi^{00}_{K_0}w_0\in P_1(K_0)$, $\Pi_{\partial K_0}w_0-\Pi^{00}_{K_0}w_0|_{\partial K_0}=0$, $\Pi^{s}_{\partial K_0}w_0-\frac{\partial}{\partial\delta}\Pi^{00}_{K_0}w_0|_{\partial K_0}=\Pi^{N}_{\partial K_0}w_0-\frac{\partial}{\partial N}\Pi^{00}_{K_0}w_0|_{\partial K_0}=0$. That is, if we make $P_0=\Pi^{00}_{K_0}w_0$, then we have $\Pi^{00}_{K_0}w_0=\Pi^{00}_{K_0}P_0$, $\Pi_{\partial K_0}w_0-\Pi_{\partial K_0}P_0=\Pi^{s}_{\partial K_0}w_0-\Pi^{s}_{\partial K_0}P_0=\Pi^{N}_{\partial K_0}w_0-\Pi^{N}_{\partial K_0}P_0=0$. Thereupon we get $\phi_{K_0}(w_0)=\phi_{K_0}(P_0)$. Again from (5.9) we get $\phi_{K_0}(w_0)=0$, but this contradicts $|\phi_{K_0}(w_0)|=1$. Therefore, (5.3) (5.5) are established.

b) For $\forall K\in K_\tau$, denote θ_K = (area of $\hat{K}$/area of K)$^{1/2}$, $\tilde{K}=\{\tilde{x}\,|\,\tilde{x}=\theta_K x,\ x\in K\}$. Then K has the same area as $\hat{K}$ and there exist constants c_1, c_2 > 0 and unrelated to K, τ such that

$$c_2h_{\tilde{K}}^{-1}\leqslant\theta_K\leqslant c_1h_{\tilde{K}}^{-1},\ h_{\tilde{K}}\leqslant c_1 \tag{5.11}$$

for $\forall w\in H^1(K)$, denoting $\hat{w}(\tilde{x}) = w(\theta_K^{-1}\tilde{x})$. $\forall\tilde{x}\in\tilde{K}$. Then since $\{\Pi_K^{ij}, \Pi_{\partial K}, \Pi_{\partial K}^{s}, \Pi_{\partial K}^{n}\}, \{N_K^{ij}\}$ all are normal affine continuous, we have

$$\left.\begin{aligned}
&(\Pi_K^{ij} w)(x) = \theta_K^{i+j} (\Pi_{\tilde{K}}^{ij} \hat{w})(\theta_K x) \qquad (\forall i+j\leqslant 2, x\in K)\\
&(\Pi_{\partial K} w)(x) = (\Pi_{\partial\tilde{K}} \hat{w})(\theta_K x) \qquad (\forall x\in\partial K)\\
&(\Pi_{\partial K}^{s} w)(x) = \theta_K (\Pi_{\partial\tilde{K}}^{s} \hat{w})(\theta_K x) \qquad (\forall x\in\partial K)\\
&(\Pi_{\partial K}^{n} w)(x) = \theta_K (\Pi_{\partial\tilde{K}}^{n} \hat{w})(\theta_K x) \qquad (\forall x\in\partial K)
\end{aligned}\right\} \tag{5.12}$$

are established and this way from (5.11) and(5.3)$\sim$(5.5) we can derive (3.4)$\sim$(3.7). Again, from (3.5) we know that (2.1) is established.

c) Now we prove that for $\xi > 1$, there exists a constant $c(\xi)$ which is related only to ξ such that the following inequality

$$\begin{aligned}
&|\Pi_{\partial K} w - \Pi_{\partial K'} w|_{0,F} + |\Pi_{\partial K}^{s} w - \Pi_{\partial K'}^{s} w|_{0,F} + |\Pi_{\partial K}^{n} w - \Pi_{\partial K'}^{n} w|_{0,F}\\
&\leqslant c(\xi) \sum_{i+j=1} \{ |\Pi_K^{ij} w|_{0,F} + |\Pi_{K'}^{ij} w|_{0,K'} \}
\end{aligned} \tag{5.13}$$

is uniformly established for $\forall w\in H^1(K\cup K')$ and this sort of K and K': $F = K\cap K'$ is a side, K and $\hat{K}$ are the same area, $h_K\leqslant\xi$, $h_{K'}\leqslant\xi$, $\rho_{K'}\geqslant\xi^{-1}h_{K'}$.

If (5.13) is true then using a method similar to b) we can prove (3.8)$\sim$(3.9). Now suppose (5.13) is not established, then for m = 1, 2, $\cdots$ there exists K_m, K'_m possessing the properties $K_m\cap K'_m = F_m$ is a side, K_m and $\hat{K}$ are the same area, $h_{K_m}\leqslant\xi$, $h_{K'_m}\leqslant\xi$, $\rho_{K'_m}\geqslant\xi^{-1}h_{K'_m}$ $\exists\, w_m\in H^1(K_m\cup K'_m)$ such that

$$\begin{aligned}
&|\Pi_{\partial K_m} w_m - \Pi_{\partial K'_m} w_m|_{0,F_m} + |\Pi_{\partial K_m}^{s} w_m - \Pi_{\partial K'_m}^{s} w_m|_{0,F_m} + |\Pi_{\partial K_m}^{n} w_m\\
&- \Pi_{\partial K'_m}^{n} w_m|_{0,F_m} > m\Big\{ \sum_{i+j=1} [\,|\Pi_{K_m}^{ij} w_m|_{0,K_m} + |\Pi_{K'_m}^{ij} w_m|_{0,K'_m}\,] \Big\}
\end{aligned} \tag{5.14}$$

and, like a), we suppose for m = 1, 2, $\cdots$, we have

$$\begin{aligned}
&|\phi_{K_m}(w_m|_{K_m})|^2 + |\phi_{K'_m}(w_m|_{K'_m})|^2 = 1,\ \phi_{K_m}(w_m|_{K_m}) \perp \phi_{K_m}(P|_{K_m}),\\
&\qquad\qquad \forall P\in P_1(K_m\cup K'_m)
\end{aligned} \tag{5.15}$$

and there exist K_0, K'_0, and $w_0\in H^1(K_0\cup K'_0)$, $F_0 = K_0\cap K'_0$ is a side, such that when $m\to\infty$

$$\left.\begin{aligned}
&\phi_{K_m}(w_m|_{K_m})\to\phi_{K_0}(w_0|_{K_0}),\ \phi_{K'_m}(w_m|_{K'_m})\to\phi_{K'_0}(w_0|_{K'_0})\\
&B_{K_m}\to B_{K_0},\ B_{K'_m}\to B_{K'_0}
\end{aligned}\right\} \tag{5.16}$$

and we have

$$\Pi_{K_0}^{ij} w_0 = 0,\ \Pi_{K'_0}^{ij} w_0 = 0 \qquad (i+j=2) \tag{5.17}$$

Thus, we have $\phi_{K_0}(w_0|_{K_0})=0$, $\Pi^{00}_{K'_0} w_0 \in P_1(K'_0)$, $\Pi_{\partial K'_0} w_0 - \Pi^{00}_{K'_0} w_0|_{\partial K'_0} = \Pi^{0'}_{\partial K'_0} w_0 - \frac{\partial}{\partial s'}\Pi^{00}_{K'_0} w_0|_{\partial K'_0} = \Pi^{n'}_{\partial K'_0} w_0 - \frac{\partial}{\partial N'}\Pi^{00}_{K'_0} w_0|_{\partial K'_0} = 0$. From strong continuity we know $q^0_{r_0}(\Pi^{0'}_{\partial K'_0} w_0|_{\partial_0}) = q^{n'}_{r_0}(\Pi^{n'}_{\partial K'_0} w_0|_{\partial_0}) = 0$, thus, $\Pi^{00}_{K'_0} w_0 \in P_0(K'_0)$, and $q_{\partial_0}(\Pi_{\partial K'_0} w_0|_{\partial_0}) = 0$, so $\Pi^{00}_{K'_0} w_0 = 0$. That is $\phi_{K'_0}(w_0) = 0$, which is in contradiction with $|\phi_{K_0}(w_0|_{K_0})|^2 + |\phi_{K'_0}(w_0|_{K_0})|^2 = 1$. Therefore, (5.13) is established whence (3.8) and (3.9) are established.

Using (3.5)$\sim$(3.9) we can prove that when $F = K \cap K'$ is a side, the inequality

$$h_*^{-\frac{1}{2}} |\Pi^{00}_K w - \Pi^{00}_{K'} w|_{0,F} + h_*^{-\frac{1}{2}} \sum_{i+j=1} |\Pi^{ij}_K w - \Pi^{ij}_{K'} w|_{0,F} \leqslant c \sum_{m+n=1} [|\Pi^{mn}_K w|_{0,K} + |\Pi^{mn}_{K'} w|_{0,K'}] \tag{5.18}$$

is uniformly established for $\forall w \in H^1(\Omega)$. Here c is unrelated to K, K' and K, K' $\in K_T$. Using (5.18) and the lemma of reference (1) with the method of reference (8), we can prove formula (2.2).

d) Last, using a method similar to that employed above, (3.10), (3.11) can be proved and theorem 4 is validated.

Proof of Theorem 5: First suppose that the element order condition is established. Obviously by the theorem hypothesis $Q_K \phi_K(P) = 0, \forall P \in P_1(K)$ and $\phi_K(1)$, $\phi_K(x_1)$, $\phi_K(x_2)$ are linear independent. Thus, the order of Q_K is at most M - 3. If $u \in H^1(K)$ and $\phi_K(u)$ satisfy the equation

$$Q_K \phi_K(u) = 0 \tag{5.19}$$

then as a consequence of the element order condition we draw out $\Pi^{00}_K u \in P_1(K)$, $\Pi_{\partial K} u = \Pi^{00}_K u|_{\partial K}$, $\Pi^{s}_{\partial K} u = \frac{\partial}{\partial s}\Pi^{00}_K u|_{\partial K}$, $\Pi^{n}_{\partial K} u = \frac{\partial}{\partial N}\Pi^{00}_K u|_{\partial K}$, thus, $\phi_K(u) = \phi_K(\Pi^{00}_K u)$. Then from $R^M = \{\phi_K(u) | u \in H^1(K)\}$, we know the order of Q_K is M - 3.

Conversely, assume the order of Q_K tc be M - 3, then the solution space of (5.19) is $\{\phi_K(P) | P \in P_1(K)\}$. Consequently, if $u \in H^1(K)$, $\Pi^{00}_K u = \Pi^{10}_K u = \Pi^{01}_K u = 0$. Then $\phi_K(u)$ is a solution of (5.19). Thereupon there exists $P \in P_1(K)$ such that $\phi_K(u) = \phi_K(P)$, therefore $\Pi^{00}_K u = P$, $\Pi_{\partial K} u = P|_{\partial K}$, $\Pi^{s}_{\partial K} u = \left.\frac{\partial P}{\partial s}\right|_{\partial K}$, $\Pi^{n}_{\partial K} u = \left.\frac{\partial P}{\partial N}\right|_{\partial K}$, and from this we can get $\Pi^{10}_K u, \Pi^{01}_K u \in P_0(K)$. This demonstrates the element order condition is established. Theorem 5 is proved.

Proof of Theorem 6: We first prove (4.1). Make J_ξ be a set defined in proof a) of theorem 4. We proved that there existed a constant $c(\xi)$ such that

$$|\Pi^{00}_K w|_{m,\xi} \leqslant c(\xi) |w|_{r_1+1,\xi} \tag{5.20}$$

is uniformly established for $\forall w \in H^{r_1+1}(K)$, $\forall K \in J_\xi$. From reference (9) we know that (5.20) is equivalent to

$$\forall \hat{w} \in H^{r_1+1}(\hat{K}),\ |\Pi_{\hat{K}}^{\hat{P}} \hat{w}|_{m,\hat{K}} \leq c(\xi) |\hat{w}|_{r_1+1,\hat{K}} \tag{5.21}$$

uniformly established for $\forall K \in J_\xi$. Here $w(x) = \hat{w}(F_K^{-1} x)$, $\forall x \in K$.

For $\forall \hat{w} \in H^{r_1+1}(\hat{K})$, the set $\{\Pi_K^P w | K \in J_\xi\}$ is a bounded set in $H^m(\hat{K})$. Otherwise, for n = 1, 2, ···, there exists $K_n \in J_\xi$ such that

$$|\Pi_{K_n}^{\hat{P}} w|_{m,\hat{K}} > n \tag{5.22}$$

and $\{B_{Kn}\}$ is a bounded set, so there exists a series $\{B_{Kn'}\}$ and element K_0 of $\{B_{Kn}\}$ such that $B_{Kn'} \to B_{K_0}$ and thus $\hat{\Phi}_{j,Kn'} \to \hat{\Phi}_{j,K_0}$, $\hat{G}_{j,Kn'}$ uniformly converges to $\hat{G}_{j,K}$. Consequently, in $H^m(\hat{K})$, $\hat{G}_{j,Kn'} \to \hat{G}_{j,K_0}$, $1 \leq j \leq M$. Therefore $\Pi_{K_n}^{\hat{P}} w$ in $H^m(\hat{K})$ converges to $\Pi_{K_0}^{\hat{P}} w$. That is $\{\Pi_{K_n}^{\hat{P}}\}$ is bounded which is in contradiction to it being unbounded. Thus, $\{\Pi_K^P w | K \in J_\xi\}$ is a bounded set in $H^m(\hat{K})$. Moreover, for $\forall K \in J_\xi$, from the theorem conditions there exists a c(K) such that

$$\forall \hat{w} \in H^{r_1+1}(\hat{K}),\ |\Pi_K^{\hat{P}} \hat{w}|_{m,\hat{K}} \leq c(K) |\hat{w}|_{r_1+1,\hat{K}}$$

Consequently from the resonance theorem (reference (10)) we know that (5.21) is established which is the same as (5.20) being established.

Separately, using affine transform techniques we know (9) there exists a constant $c(\xi)$ such that $\forall w \in H^{r_1+1}(K)$, $\forall K \in J_\xi$ we have

$$\inf_{P \in P_{r_1}(K)} |w - P|_{r_1+1,K} \leq c(\xi) |w|_{r_1+1,K} \tag{5.23}$$

From (5.20) obviously we have established for $\forall w \in H^{r_1+1}(K)$, $\forall K \in J_\xi$, the inequality

$$|w - \Pi_K^P w|_{m,K} \leq c(\xi) |w|_{r_1+1,K} \tag{5.24}$$

Note that the conditions of the theorem have

$$|w - \Pi_K^P w|_{m,K} = \inf_{P \in P_{r_1}(K)} |(w-P) - \Pi_K^P (w-P)|_{m,K}$$

$$\leq c(\xi) \inf_{P \in P_{r_1}(K)} |w - P|_{r_1+1,K} \leq c(\xi) |w|_{r_1+1,K}$$

that is the inequality

$$|w - \Pi_K^P w|_{m,K} \leq c(\xi) |w|_{r_1+1,K} \qquad \forall w \in H^{r_1+1}(K) \tag{5.25}$$

is uniformly established for $\forall K \in J_\xi$.

For $\forall K\in K_\tau$, use the notation of proof b) of theorem 4. From (5.25) for $\forall w\in H^{r_1+1}(K)$, $l=0,1,\cdots,m$, we have

$$|w-\Pi_K^{r_1}w|_{l,K}=\theta_K^{l-1}|\tilde{w}-\Pi_{\tilde{K}}^{r_1}\tilde{w}|_{l,\tilde{K}}\leqslant c\theta_K^{l-1}|\tilde{w}|_{r_1+1,\tilde{K}}$$
$$=c\theta_K^{l-1}\theta_K^{l-(r_1+1)}|w|_{r_1+1,K}=c\theta_K^{l-(r_1+1)}|w|_{r_1+1,K}$$

and again using (5.11) we can get (4.1).

Similarly (4.2)$\sim$(4.4) can be proved and using methods similar to reference (1) we can get (4.5). Theorem 6 is proved.

Proof of Theorem 7: From theorem 1, theorem 3, and theorem 4, we need only prove: if $v_\tau\in U_\tau(\tau=1,2,\cdots)$ and $\sup_\tau|v_\tau|_{L^2,\tau(\Omega)}<\infty$, then for $\forall\varphi\in C_0^\infty(R^2)$,

$$\lim_{\tau\to\infty}T_{i,j}(\varphi,v_\tau)=0\quad(i=0,1,2,\ j=1,2).$$

Denote $v_\tau=\Pi_\tau w_\tau$, $w_\tau\in H^1(\Omega)\cap H_0^1(\Omega)$, then using the partial integration formula we can get

$$2T_{1,2}(\varphi,v_\tau)=2\sum_{K\in K_\tau}\int_K(\varphi\Pi_K^{r_1}w_\tau+\partial_{x_1}\varphi\,\Pi_K^{r_2}w_\tau)dx$$
$$=\sum_{K\in K_\tau}\Big\{\int_K\varphi(2\Pi_K^{r_1}w_\tau-\partial_{x_1}\Pi_K^{r_2}w_\tau-\partial_{x_2}\Pi_K^{r_2}w_\tau)dx$$
$$+\int_{\partial K}\varphi\big[(\Pi_K^{r_1}w_\tau-\Pi_{\partial K}^{r_2}w_\tau N_1+\Pi_{\partial K}^{r_1}w_\tau N_2)N_1$$
$$+(\Pi_K^{r_1}w_\tau-\Pi_{\partial K}^{r_2}w_\tau N_2-\Pi_{\partial K}^{r_1}w_\tau N_1)N_2\big]ds$$
$$+\int_K\partial_{x_1}\varphi\,(\Pi_K^{r_1}w_\tau-\partial_{x_1}\Pi_K^{r_2}w_\tau)dx+\int_{\partial K}\partial_{x_1}\varphi\,(\Pi_K^{r_1}w_\tau-\Pi_{\partial K}w_\tau)N_1ds$$
$$-\int_K\partial_{x_1}\varphi\,(\Pi_K^{r_1}w_\tau-\partial_{x_1}\Pi_K^{r_2}w_\tau)dx-\int_{\partial K}\partial_{x_1}\varphi\,(\Pi_K^{r_1}w_\tau-\Pi_{\partial K}w_\tau)N_1ds\Big\}$$
$$+\sum_{K\in K_\tau}\Big\{\int_{\partial K}\varphi[2N_1N_2\Pi_{\partial K}^{r_1}w_\tau+(N_1^2-N_2^2)\Pi_{\partial K}^{r_1}w_\tau]ds$$
$$+\int_{\partial K}\Pi_{\partial K}w_\tau(\partial_{x_1}\varphi N_1-\partial_{x_2}\varphi N_2)ds\Big\}$$

For a nonnegative integer ℓ, denote P_K^ℓ: $L^2(K)\to P_\ell(K)$ to be an orthogonal projection operator, P_F^ℓ: $L^2(F)\to P_\ell(F)$ to be an orthogonal projection operator. Using formulae (1.4), (1.5), and (1.7) and the fact that (U_τ) passed the IPT test, we have

$$
\begin{aligned}
2T_{1,2}(\varphi,v_h)=\sum_{K\in K_h}\Big\{&\int_K(\varphi-P_K^0\varphi)(2\Pi_K^{11}w_h-\partial_{x_2}\Pi_K^{10}w_h\partial_{x_1}\Pi_K^{01}w_h)\,dx\\
&+\int_{\partial K}(\varphi-P_K^0\varphi)\big[(\Pi_K^{10}w_h-\Pi_{\partial K}^{n}w_hN_1+\Pi_{\partial K}^{\tau}w_hN_2)N_2\\
&+(\Pi_K^{01}w_h-\Pi_{\partial K}^{n}w_hN_2-\Pi_{\partial K}^{\tau}w_hN_1)N_1\big]ds\\
&+\int_K\big[\partial_{x_1}\varphi(\Pi_K^{10}w_h-\partial_{x_1}\Pi_K^{00}w_h)+\partial_{x_1}\varphi(\Pi_K^{01}w_h-\partial_{x_2}\Pi_K^{00}w_h)\big]dx\\
&+\int_{\partial K}(\partial_{x_1}\varphi N_1-\partial_{x_1}\varphi N_2)(\Pi_K^{00}w_h-\Pi_{\partial K}w_h)\,ds\Big\}\\
&+\sum_{K\in K_h}\int_{\partial K}\Pi_{\partial K}w_h(\partial_{x_1}\varphi N_1-\partial_{x_1}\varphi N_2)ds\\
&+\sum_{K\in K_h}\sum_{F\subset\partial K}\int_F(\varphi-P_F^0\varphi)\big[2N_1N_2\bar{\Pi}_{\partial K}^{n}w_h+(N_1^2-N_2^2)\bar{\Pi}_{\partial K}^{\tau}w_h\big]ds\\
&+\sum_{K\in K_h}\int_{\partial K}(\varphi-P_K^0\phi)\big[2N_1N_2(\Pi_{\partial K}^{n}-\bar{\Pi}_{\partial K}^{n})w_h\\
&+(N_1^2-N_2^2)(\Pi_{\partial K}^{\tau}-\bar{\Pi}_{\partial K}^{\tau})w_h\big]ds
\end{aligned}
$$

Utilizing the Schwartz inequality, the interpolation inequality (reference (1)), the inequalities (3.4)$\sim$(3.11), and the inequalities below

$$
\begin{aligned}
&|\Pi_K^{10}w_h-(\Pi_{\partial K}^{n}w_hN_1-\Pi_{\partial K}^{\tau}w_hN_2)|_{0,\partial K}+|\Pi_K^{01}w_h-(\Pi_{\partial K}^{n}w_hN_2+\Pi_{\partial K}^{\tau}w_hN_1)|_{0,\partial K}\\
&\qquad\leqslant ch_K^{\frac{1}{2}}\sum_{i,j=1}|\Pi_K^{ij}w_h|_{0,K}
\end{aligned}
\tag{5.26}
$$

$$
|\Pi_{\partial K}^{n}w_h-\bar{\Pi}_{\partial K}^{n}w_h|_{0,\partial K}+|\Pi_{\partial K}^{\tau}w_h-\bar{\Pi}_{\partial K}^{\tau}w_h|_{0,\partial K}\leqslant ch_K^{\frac{1}{2}}\sum_{i,j=1}|\Pi_K^{ij}w_h|_{0,K}
\tag{5.27}
$$

$$
\forall\Phi\in H^1(K),\quad |\Phi|_{0,\partial K}\leqslant ch_K^{-\frac{1}{2}}|\Phi|_{1,K}
\tag{5.28}
$$

we can obtain

$$
|T_{1,2}(\varphi,v_h)|\leqslant ch_K|\varphi|_{2,\Omega}|v_h|_{L^2,h}(\Omega)
\tag{5.29}
$$

Consequently, $\lim_{h\to 0}T_{i,j}(\varphi,v_h)=0$. Similarly, we can prove for $\forall i=0,1,2,j=1,2$. $\lim_{h\to 0}T_{i,j}(\varphi,v_h)=0$ the inequality (5.26) can be gotten from (3.5) and (3.7). (5.27) can be arrived at using methods similar to the proof of theorem 4. For (5.28) see reference (7). Theorem 7 is proved.

Proof of Theorem 8: Under the conditions of the theorem, $a(\cdot,\cdot)$ is uniformly positive. Consequently, there exists a constant c unrelated to τ, such that the following inequality is established

$$
\tau=1,2,\cdots,\quad |Eu_h-u_h|_{L^2,h}(\Omega)\leqslant c\Big\{\min_{v_h\in U_h}|Eu_h-v_h|_{L^2,h}(\Omega)+\sup_{0\neq v_h\in U_h}\frac{|a(Eu_h,v_h)-f(v_h)|}{|v_h|_{L^2,h}(\Omega)}\Big\}
\tag{5.30}
$$

From (4.5) we know that for $\tau = 1, 2, \cdots$, uniformly

$$\min_{v_\tau \in U_\tau} |Eu_0 - v_\tau|_{L^2,\Omega} \leqslant c \sum_{i=1}^{k} h_\tau^{r_i - 1} |u_0|_{r_i+1,\Omega}. \tag{5.31}$$

For the second term of the left side of (5.30), using a method similar to the proof of theorem 7, we can get for $\forall v_\tau \in U_\tau$, the inequality

$$|a(Eu_0, v_\tau) - f(v_\tau)| \leqslant c|v_\tau|_{L^2,\Omega} \left\{ \sum_{i=1}^{k} h_\tau^{r_i - 1} |u_0|_{r_i+1,\Omega} + h_\tau^{r'-1} |u_0|_{r',\Omega} \right\} \tag{5.32}$$

to be established, in which c is a constant unrelated to u_0, τ. In this way we obtained (4.11). Theorem 8 is proved.

REFERENCES

1. Zhang Hongqing [1728 7703 1987] and Wang Ming [3769 7686], "Multiple Set Function Limiting Element Approximation and Quasi-Conformal Plate Elements," YINGYONG SHUXUE YU LIXUE [APPLIED MATHEMATICS AND MECHANICS] Vol 6 No 1, 1985, pp 41-52.

2. Ibid., "Finite Element Approximations With Multiple Sets of Functions and Quasi-Conforming Elements," Diwuci Guoji Shuangwei Huiyi (DD5) Lunwen Ji [Collected papers from the Fifth International Double Differentiation Conference (DD5), Beijing, 1984.

3. Tang Limin [0781 4539 3046], Cheng Wanji [7115 8001 0679], and Liu Yingxi [0491 6601 2569], "Quasi-Conformal Elements in Limited Element Analysis," DALIAN GONGXUE XUEBAO [DALIAN ENGINEERING ACADEMY JOURNAL], Vol 19 No 2, 1980, pp 16-35.

4. Cheng Wanji, Liu Yingxi, and Tang Limin, "Quasi-Conformal Element Series Formulae," Ibid.

5. Jiang Heyang [5592 0725 3152], "Utilization of Quasi-Conformal Element Methods To Derive High Precision Triangular-Shaped Plate Bending Elements," Ibid., Vol 20 Supplement 2, 1981, pp 21-28.

6. Stummel, F., "The Generalized Patch Test," SIAM J. NUM. ANAL., No 16, 1979, pp 449-471.

7. Feng Kang [7458 1660], "On the Theory of Discontinuous Finite Elements," JISUAN SHUXUE [COMPUTATIONAL MATHEMATICS, Vol 1 No 4, 1979, pp 378-385.

8. Stummel, F., "Basic Compactness Properties of Nonconforming and Hybrid Finite Element Spaces, RAIRO, ANALYSE, SUMERIQE, NUMERICAL ANALYSIS, Vol 4 No 1, 1980, pp 81-115.

9. Ciarlet, P.C., "Finite Element Method for Elliptic Problems," North-Holland, Amsterdam, New York, Oxford, 1978.

10. Yoshida Kozo [0679 3944 5087 0155], HAN [3131] KAN BUNSEKI [FUNCTIONAL ANALYSIS] in Japanese, translated by Wu Yuankai [0702 0337 1956], People's Education Press, 1980.

12966/9365
CSO: 4008/1068

INFLUENCE OF METAMORPHISM ON CHEMICAL COMPOSITION OF MAGNO-FERROMICAS IN PRE-CAMBRIAN REGIONAL METAMORPHIC AREAS, NORTH CHINA

Guiyang KUANGWU XUEBAO [ACTA MINERALOGICA SINICA] in Chinese No 1, 1987
pp 27-36

[English abstract of article by He Yixing [6320 5030 5281], et al., of Changchun Geological College]

[Text] The areas studied include Anshan (Liaoning), East Hebei, Miyun (Hebei) and Nei Monggol. The types of host rocks of magno-ferromicas include meta-sedimentary rocks and meta-volcanic rocks.

The Al_2O_3 content and $Mg/Mg/(Mg+Fe^{2+})$ ratio in magno-ferromicas vary with the composition of the magno-ferromicas, especially the $Mg/(Mg+Fe^{2+})$ ratio, and show regular variations with the grade of metamorphism.

The authors' investigations show that the grade of metamorphism (mainly the temperature) tends to increase from Anshan through East Hebei, Miyun, and on to Nei Monggol. In the Shuichang mining area, East Hebei, the grade of metamorphism tends to increase from south to north. The chemistry of magno-ferromicas may provide valuable information for stratigraphic correlation, recognition of geological structures and ore exploration.

9717
CSO: 4009/43

PHASE RELATIONS IN SYSTEMS Ag_2S-Cu_2S-PbS AND Ag_2S-Cu_2S-Bi_2S_3 AND THEIR MINERAL ASSEMBLAGES

Guiyang KUANGWU XUEBAO [ACTA MINERALOGICA SINICA] in Chinese No 1, 1987
pp 9-18

[English abstract of article by Wu Daqing [0702 1129 3237] of the Institute of Geochemistry, Chinese Academy of Sciences, Guiyang]

[Text] The phase relations in the ternary systems Ag_2S-Cu_2S-PbS and Ag_2S-Cu_2S-Bi_2S_3 have been studied using the silica vacuum technique.

In the system Ag_2S-Cu_2S-Bi_2S_3 the phase relations are dominated by join-lines from galena to f.c.c. ($Ag_xCu_{2-x}S$) and b.c.c. ($Cu_xAg_{2-x}S$) at 500°C. With decreasing temperature, galena can coexist with all phases on the Ag_2S-Cu_2S join.

There are six solid solutions and one new phase, i.e., "C" with a composition of $Ag_{1.1}Cu_{4.8}Bi_{3.8}S_{12}$, in the system Ag_2S-Cu_2S-Bi_2S_3 at 500°C. Pavonite ($AgBi_3S_5$) contains 14 mol percent Cu_2S in solid solution, but only 3.0 mole percent Ag_2S in $CuBi_3S_5$ solid solution. The $Cu_3Bi_3S_9$ s.s. and wittichenite (Cu_3BiS_3) s.s. can form join-lines with pavonite s.s., having the maximum content of 9.0 and 18 mole percent Ag_2S. The most striking feature is the presence of bejaminite as a stable phase with a chemical formula of $Ag_2Bi_4S_7$ on the Ag_2S-Bi_2S_3 join. $AgBiS_2$ of the PbS type occupies a fairly large field, with a maximum of 23 mole percent Cu_2S.

9717
CSO: 4009/43

PHASE RELATIONS IN THE SYSTEMS Cu_2S-PbS-Bi_2S_3 AND Ag_2S-PbS-Bi_2S_3 AND THEIR MINERAL ASSEMBLAGES

Guiyang KUANGWU XUEBAO [ACTA MINERALOGICA SINICA] in Chinese No 1, 1987 pp 19-26

[English abstract of article by Wu Daqing [0702 1129 3237] of the Institute of Geochemistry, Chinese Academy of Sciences, Guiyang]

[Text] The phase diagrams of the systems Cu_2S-PbS-Bi_2S_3 and Ag_2S-PbS-Bi_2S_3 have been investigated. This paper studies the complete solid solution between bismuthtite and aikinite above 300°C in the system Cu_2S-PbS-Bi_2S_3. The synthetic phases $CuBi_3S_5$ and $Cu_3Bi_7S_{12}$ have solid solution ranges in the ternary system with 9 and 26 mole percent PbS at the maximum, respectively.

A complete solid solution between PbS and $AgBS_2$ divides the phase diagram of the system Ag_2S-PbS-Bi_2S_3 into two parts: Bi-rich and Ag-rich. All sulfosalt minerals and solid solutions, including pavonite s.s., lillianite s.s., heyovskyite and benjaminite, are on the Bi-rich side. In addition, bivariant relationships were found between pavonite s.s.-lillianite s.s., benjaminite and bismuthtite as well as between lillianite s.s.-bismuthtite and galenobismutite.

Synthetic experiments using the LiCl-KCl flux technique show that when a minor amount of copper (less than 1 wt percent) is added, many Ag- and Pb-bismuth sulfosal minerals, e.g., vikingite ($Ag_3Pb_6Bi_{13}S_{28}$), can be synthesized successfully, particularly at 400°C. This was true of heyrovsky-ite, which has a solid solution range with 3.7 mole percent Cu_2S at the maximum in the system Cu_2S-PbS-Bi_2S_3.

9717
CSO: 4009/43

CHARACTERISTICS AND ORIGIN OF FELDSPAR MEGACRYSTS IN CENOZOIC BASALTS FROM SOME LOCATIONS OF EAST CHINA

Guiyang KUANGWU XUEBAO [ACTA MINERALOGICA SINICA] in Chinese No 1, 1987 pp 37-46

[English abstract of article by Qiu Jiaxiang [6726 1367 7534], et al., of Wuhan College of Geology]

[Text] Presented in this paper are field and laboratory data on feldspar megacrysts in Cenozoic basalts from East China, including 76 wet chemical or electron microprobe analyses of feldspars, and these data are compared with those for 53 feldspar megacrysts from abroad.

The mode of occurrence, physical properties, mineralogical chemistry and trace element distribution of feldspar megacrysts are studied using various approaches.

Also presented are the authors' viewpoints on the origin of feldspar megacrysts--a problem which has been involved in controversy for a long time among geologists worldwide.

9717
CSO: 4009/43

INFRARED SPECTRAL STUDY OF COOKEITE

Guiyang KUANGWU XUEBAO [ACTA MINERALOGICA SINICA] in Chinese No 1, 1987
pp 52-57

[English abstract of article by Liu Gaokui [0491 7559 7608], et al., of the Institute of Geochemistry, Chinese Academy of Sciences, Guiyang]

[Text] Presented in this paper are the infrared spectra of cookeite from Henan and Guizhou provinces, China. The frequencies, absorption intensities, assignments of the main bands and infrared spectra of heated samples are given. These spectra are different from those of cookeite reported in the literature, but similar to those of muscovite and illite. By comparing all these spectra, the spectral identifying characteristics of cookeite are proposed. The infrared spectrometric results indicate that the structure of cookeite may be complicated--there is no water in the form of "H_2O" in it and it is close to dioctahedral in structure, but not to tricotahedral. When cookeite is heated to 453°C and kept at this temperature for 30 minutes, all OH groups are lost and its structure begins to transform toward amorphism. When the temperature rises to 800°C, it is transformed into mullite, amorphous SiO_2 and Li_2O.

9717
CSO: 4009/43

DISCOVERY OF Gd-Dy-ESCHYNITE

Guiyang KUANGWU XUEBAO [ACTA MINERALOGICA SINICA] in Chinese No 1, 1987 pp 66-73

[English abstract of article by Cai Genqing [5591 2704 1987] of the Institute of Uranium Geology, Beijing]

[Text] Gd-Dy-eschynite has been found in the U-Th mixed mineralized coarse-grained biotite granite, which is associated with thorite, monazite, zircon, orthite, magnetite, ilmenite, bastnaesite and minor fluorite, calcite, apatite, etc. a:b:c = 0.3851 : 1 : 0.5381. Ten crystal forms have been identified, including {100}, {010}, {110}, {310}, {001}, {021}, {111}, {211}, {311} and {702}. It is resin yellow, strongly resinous in luster and conchoidal to subconchoidal in fracture. Specific gravity = 4.716 and microhardness = 331-566 kg/cm^2. It possesses brittleness and strong radioactivity. It is transparent in polarized light, colorless to yellow, isotropic, N > 2.20 and grayish-white in reflected light. The difference between Gd-Dy-eschynite and eschynite lies in $[Y]_2O_3 > [Ce]_2O_3$ and $TiO_2 > Nb_2O_5$ in the former against $[Ce]_2O_3 > [Y]_2O_3$ and $Nb_2O_5 > TiO_2$ in the latter; that between Gd-Dy-eschynite and priorite in $[Y]_2O_3/[Ce]_2O_3 = 1.5\pm$ against $[Y]_2O_3/[Ce]_2O_3 = 5$ (the former contains higher U and Pb than the latter); that the former contains lower Th but higher U than the latter; that between Ce-Dy-eschynite and sinicite in $[Y]_2O_3 > [Ce]_2O_3$ and $TiO_2 > Nb_2O_5$ and higher U and Th in the former. Since Gd and Dy comprise 72 percent of the total amount of rare earth elements, this mineral is named Gd-Dy-eschynite.

9717
CSO: 4009/43

STUDY OF GENETIC RELATIONSHIP BETWEEN ALABANDITE AND SPHALERITE IN DAWAN Zn-DEPOSIT

Guiyang KUANGWU XUEBAO [ACTA MINERALOGICA SINICA] in Chinese No 1, 1987 pp 74-77

[English abstract of article by Wei Qiying [7614 4860 5391], et al., of the Department of Geology, Beijing University]

[Text] Alabandite, which occurs in the sphalerite ore of the Dawan skarn-type zinc deposit, closely intergrows with dark, high-Mn sphalerite. Other associated minerals are pyrite, pyrrhotite, chalcopyrite and galena, and some Mn-bearing minerals, such as rhodonite, Mn-allanite and rhodochrosite, are also recognized. Under the microscope it is very easy to confuse alabandite with sphalerite. When compared with dark, high-Mn sphalerite, it has a slightly higher reflectivity and lower microhardness. Election probe and X-ray micro-analysis data are in good agreement with those reported in the literature. According to the micrographic texture, the authors consider alabandite to have been exsoluted from dark, high-Mn sphalerite at about 350°C.

9717
CSO: 4009/43

CONICHALCITE DISCOVERED AT PINGGUI, GUANGXI

Guiyang KUANGWU XUEBAO [ACTA MINERALOGICA SINICA] in Chinese No 1, 1987 pp 84-87

[English abstract of article by Lai Lairen [6351 0171 0088], et al., of Guilin Institute of Geology and Mineral Resources]

[Text] Conichalcite occurs in the oxidized ore of Karst accumulated Au-Sn deposits in Guangxi. Electron probe and wet chemical analyses show (percent): CuO (29.45, CaO (23.32), MgO (0.22), FeO (0.08), SiO_2 (0.33), Al_2O_3 (0.87), ZnO (0.60), As_2O_5 (41.49), H_2O^+ (4.12), total (100.48). The formula is (Ca, Mg) (Cu, Fe, Zn) (As, Si, Al) O_4(OH). Ng' = 1.799, Np' - 1.768. Biaxil positive, 2V - 82°. D_{mean} = 4.28, $H_{v(50)}$ = 190 kg/cm^2. Single crystal diffraction yields orthorhombic lattice dimensions a = 7.33 Å, b = 9.12 Å, c = 5.79 Å. Space group $P2_12_12_1$, Z = 4. The strongest lines of the X-ray pattern are 5.69(4), 4.08(4), 3.40(4), 3.12(10), 2.89(4), 2.83(10), 2.60(8), 2.57(5), 2.066(5), 1.727(7), 1.614(8), 1.571(5), 1.469(4), 1.305(4), 1.099(5), 1.002(4).

9717
CSO: 4009/43

FIRST DISCOVERY OF PUMPELLYITE IN WENDUERMIAO GROUP, NEI MONGGOL

Guiyang KUANGWU XUEBAO [ACTA MINERALOGICA SINICA] in Chinese No 1, 1987
pp 88-91

[English abstract of article by Xu Chuanshi [6079 0278 6108], et al., of Hebei College of Geology]

[Text] Pumpellyite is found in the strata of the Wenduermiao Group, Nei Monggol. It occurs in Paleozoic ophiolite and is associated with glaucophane, lawsonite, stilpnomelane, chlorite, albite, epidote and actinolite.

Pumpellyite is grayish green-pale brown in color, and pale yellow green-pale yellow brown in thin sections, showing polychromism. Ng: pale yellow brown, Nm: light yellow green, Np: light yellow. Ng = 1.6899, Nm = 1.6768, Np = 1.6743, Ng - Np = 0.016, 2V(+) = 45°±. The strongest lines in the X-ray diffraction pattern are: 6.98(6), 4.68(3), 3.17(9), 2.97(10), 2.51(4), 2.12(3) and 1.74(2). Electron microprobe analysis shows that this pumpellyite is of a transition type between pumpellyite and ferropumpellyite. Julgoldite continues to increase with increasing metamorphism.

The discovery of pumpellyite of this type has further confirmed the existence of a low-temperature, high-pressure metamorphic belt in the Wenduermiao Group, which is of great importance for further studies of plate tectonics, petrology and tectonics.

9717
CSO: 4009/43

DISCOVERY OF AQUAMARINES IN NORTHEASTERN HUNAN

Guiyang KUANGWU XUEBAO [ACTA MINERALOGICA SINICA] in Chinese No 1, 1987
pp 92-94

[English abstract of article by Zheng Ruifan [6774 3843 0416] of the Institute of Geology, Hunan]

[Text] Aquamarine occurs in rare metal-bearing granite-bearing granite-pegmatites of northeastern Hunan. It is marine blue, transparent and hexagonally prismatic. Its crystal ranges from 2.5 to 6 cm in diameter and 3 to 12 cm in length. Density: 2.71; refractive index: No = 1.5827, Ne = 1.5750; birefringence: 0.0077; cell parameters: a = 9.23 Å, c = 9.25 Å c/a = 1.002, V = 683.27 $Å^3$. The interior of the aquamarine contains minor amounts of small-grained inclusions.

9717
CSO: 4009/43

HANDELSBLATT VIEWS COMPUTER MERGER

Duesseldorf HANDELSBLATT in German No 63, 3 Mar 87 p B18

[Article by Detlef Rehn, East Asia Institute e.V., Bonn: "The U.S. Giant IBM Is the Model for Building Up Their Own Computer Companies"]

[Text] "China's IBM has been founded!" With these words, the Chinese press exuberantly greeted the merger of 67 institutions of the Beijing computer industry, in the middle of December 1986, to form the "Great Wall Computer Corporation Beijing." The new conglomerate comprises 5 universities, 4 research institutes, service and training facilities, as well as production enterprises for the manufacture of computers and integrated circuits. With 50,000 employees, capital assets of about 240 million RMB (about DM120 million)--just about half the total capital assets of the computer business in China--and an estimated production volume of 250 million RMB (= DM125 million), it is the largest computer enterprise in the country.

Corresponding to its composition, the conglomerate covers all important areas of the computer industry: development and production of new hardware and software, training of technical people, furnishing and services, support for computer applications, etc. The Chinese leadership places great hope in the enterprise, which will take the form of a corporation. Primarily, the leadership assigns to the corporation a locomotive function and hopes that, with its aid, the still very backward computer industry of the country will get a start and will gradually catch up with developments in the industrial states.

Reforms are indeed necessary in a branch that is decisively important for the Chinese modernization program. At this time the Chinese computer industry consists of about 130 institutions with about 100,000 employees. The centers are situated in the coastal areas. Besides Beijing, these centers are in Tianjin, Shanghai, Jiangsu, Fujian, and Guangdong. In 1985, the production value of the computer industry was 1.76 billion RMB (= DM855 million); this corresponded to only a fraction, 6.2 percent, of the total production volume of the electronics industry.

For comparison: In Japan, for example, the computer industry contributes 20 percent to the total production of electronic equipment. China can indeed point to a broad spectrum of its own computer developments in recent years, starting with supercomputers of the "Galaxy" series up to the

IBM-compatible "Great Wall" microcomputers. This does indeed document their increased technological capability, but on the other hand these positive developments are again put in proper perspective by other phenomena: For example, the Chinese computer market is almost completely dominated by foreign enterprises as far as large and medium systems are concerned, and even with microcomputers the domestic market share, according to Chinese data, is at most 40 percent.

Just as serious is the fact that even where import substitution would already be possible, domestic computer manufacturers generally still fall back on foreign components. In the view of the persons in charge, this has a negative effect on the creation of a technological and economic base for the Chinese computer industry. But this means that the true local portion of value creation at this time makes up only a fraction of the production volume of Chinese computer production.

In similar fashion, reports concerning the penetration of computers into all areas of the Chinese economy and society, and China's entry into the information age, must be regarded in differentiated fashion. By the middle of 1986, about 7,000 medium and small computer systems as well as 130,000 microcomputers were installed in China. In comparison to 1980 (2,900/600), these figures represent impressive rates of increase. But in this connection one must also see that, in a leading business center such as Shanghai, the degree to which computers have spread among industrial enterprises is only 10.2 percent, and the efficiency of utilization of the computers employed is frequently very low.

Against this background, the Chinese leadership has developed a computer development strategy for the current Seventh 5-Year Plan (1986/1990). By means of this plan, the main weaknesses of this sector are supposed to be eliminated by the end of the decade, working from various sides.

--Computer application receives top priority. In the future the relevant guideline here will be that application determines the production volume. This approach reflects the Chinese leadership view that the competitiveness of their own products can be raised only with a consistent marketing direction, and that the desired computerization can be implemented step by step. Computers are to be used especially in the technical reformation of so-called traditional industries, for example the textile industry. Marketing direction in this connection also means striving for close cooperation among software houses, service facilities, and users, in order to secure a high use efficiency for the computers.

--The product spectrum of the Chinese computer industry likewise should change fundamentally according to market requirements. Up to now there was a supply of an assortment of the widest variety of computers, which generally were produced only in very small numbers. By 1990, production will be more streamlined. Microcomputers (also called personal computers such as e.g., the IBM-compatible "Great Wall" 0520) will be developed and produced preferentially; as need demands, minicomputers (32-bit superminis) and larger systems will also be produced. The objective is to reach international quality standards within 3 years and to reach international price levels within 5 years.

Computer peripherals is a branch that is very neglected in China, and it too is supposed to gain in importance. What is planned here is primarily the production of technologically demanding products, which presently must largely still be imported: diskette drives, monochrome and color monitors, as well as 24-pin matrix printers.

--In view of the large technological gap of the Chinese computer industry with respect to the international level, China by 1990 wants to penetrate into the area of the fourth computer generation, which uses very large scale integrated circuits (VLSI). The gap would thus diminish to about 8 to 10 years.

But implementing this project presupposes a plethora of measures. Especially in the area of chip development and production, the jump into mass production of technologically high-grade and cheap circuits and the solution of the associated technological and economic problems (automation of production, quality control, etc.) are all required.

--The foundation of the "Great Wall Computer Corporation" as well as further major mergers indicate that the Chinese leadership is particularly set on major conglomerates, which are supposed to cover the entire spectrum from the development of new systems through production of both new hardware and software up to and including after-sales service.

The responsible planners expect from these conglomerates on the one hand that they will overcome the system-based barriers between research and development and production. Another expected positive effect is that the conglomerates will be able to secure mass production on the basis of their personnel, material, and financial capabilities. Finally, the conglomerates should form the technological and economic backbone for the march into the "fourth computer generation."

IBM, the world's largest computer manufacturer, is a model for the Chinese in founding their own computer conglomerates, especially in view of its role in influencing markets and products. In contrast to Western countries, the multiplicity of computer developments in China does not express sharp competition and fast innovation, but rather the conceptual emptiness of their computer policy and the lack of businesslike market orientation. In view of this multiplicity, the responsible parties hope especially that one or more of these new conglomerates will succeed in influencing the domestic market in such a fashion that its products will emerge as industrial standards.

Quasi-private computer enterprises--which, for example, were founded by former scientists of the Academy of Sciences--represent an entirely new development in the Chinese computer industry and accordingly are given positive treatment. Because these enterprises are relatively small compared to the major conglomerates, and because of their operational organization, they are quite flexible. They can help establish entrepreneurial competitiveness. As spin-offs from universities and institutes of the Academy of Sciences, they are also useful in creating high-tech centers.

The import of production engineering and know-how continues to be the focus of the development strategy for the computer industry. But protectionist trends are appearing in connection with imports of finished products, especially microcomputers with a word length of 16 bits and less, which form the central focus of the Chinese computer development strategy. With these computers, they are striving to increase the "guochanhua," i.e., the portion of local production, to 80 percent of the main components by 1990.

For West German enterprises, it follows from this that the best market prospects in the Chinese computer industry (as also in other branches) will result from readiness to deliver know-how and equipment. They will focus on the weak points of China's computer industry, i.e., drive mechanisms, hard-disk memories, diskettes, all types of components, etc. The Chinese computer market is hotly contested. But an expected market volume of 10 billion RMB by 1990 should be attraction enough to enter the competition.

8348/8309
CSO: 3698/394

HELIUM PRODUCTION SITUATION DISCUSSED

Tianjin TIANRANQI GONGYE [NATURAL GAS INDUSTRY] in Chinese No 4, 28 Dec 86 pp 96-100

[Article by Tang Wenjun [0781 2429 0193], Xinan Institute of Industrial Chemistry: "The Future of Helium in China as Viewed from the World Helium Situation"]

[Excerpts] Abstract: This paper describes the circumstances regarding the production, consumption, and supply and demand of helium outside this country, and also compares the levels of production and marketing in China with those abroad. This makes clear the gaps between the helium industry and application technologies in this country and those abroad. The paper proposes how we can learn from foreign experiences, and provides a long-range forecast and planning for helium production in China.

The industry in this country that extracts helium from natural gas has a certain basis, but from the point of view of scale and level of technology there is not only a great disparity with advanced nations, but it is also far from suitable for the pace of development of modern science and technology and of production in this country, especially in regard to its high cost and expensive selling price. In recent years, China has made definite advances in aspects of airship research, but great quantities of helium are used in doing so. Because the price of helium is too high, this keeps some units from going forward.

The levels of production and consumption of helium in this country are very low. There is not only great disparity in comparison with developed countries, but we cannot even compare with the levels of India and Sweden. According to statistics, nonmilitary helium consumption in developed countries is not less than 5 cubic km per 1 million residents (not including helium used for welding). Figuring from this, each 100 million in population should consume 500 cubic km of helium, or in this country of 1 billion, there should be consumption of 5 million cubic meters per year. When military needs are added to this, the demand for helium should be much greater than that figure.

The price of helium in this country has always been high, the reasons being that the helium component in the raw material natural gas is not very high,

our techniques are backward, energy consumption is high, and the costs are high. The high price of helium has terrified many science research departments, limiting the development of application technologies and is of no use to the modernization of science and technology. This is a problem in urgent need of resolution, but for the present we can only adjust the price of helium appropriately on the existing cost basis. The basic methods are to build facilities on a greater scale, use more advanced technologies, lower the indices of energy consumption, and greatly decrease costs. Another way would be to import technology, using the method of jointly funded operation with foreign enterprises.

There is already a certain basis to the helium industry in this country, but from the perspective of scale of production, the quantities sold are just too much out of line. As far as technology is concerned, the cryogenic method has been industrialized, but because the energy consumption is rather high, costs cannot come down; the thin-film penetration method is under research and development, but it needs to be made more powerful to promote the industrialization process; the varying-voltage-adsorption technique is already at a certain level, but how that is to be integrated with helium extraction techniques awaits research and experimentation.

Based on the actual situation in this country, I now propose the following recommendations and measures:

1. Request consideration by relevant departments of the government, and in terms of organization, adopt measures to strengthen the management of natural gas resources, actively develop efforts at surveying helium resources, and formulate helium-protection planning that can truly be implemented.

2. Select an area that has natural resources and build a second helium production base, and promote technological transformation, reductions in energy consumption, and reductions in cost to greatly reduce the selling price.

3. Strengthen capacities and resolutely pay attention to the research and development of new technologies, especially the membrane separation technology, the (Kongfen) helium extraction technique, etc.

4. Establish a Chinese industrial gas company, under which set up a helium branch company to uniformly manage all industrial gases in this country and uniformly manage helium resources, production, and marketing, which will vigorously promote the development of the helium industry in this country.

In China, we are currently working for the four modernizations, and as the wave of the new technological revolution is coming to engulf us, this strategic material that is helium has its own particular importance. The dominant position of American helium can be maintained for 30 to 50 years, and the helium production capacity of the Soviet Union has now vaulted into second place in the world. When to that is added the natural resources of Poland, the countries of Eastern Europe can satisfy the current and future demands for helium. China's economic leap is still in its initial stages, and based on the experiences of countries like Japan, future demand for helium is certain to grow 100-fold. Looking at this from the perspective of the situation in this country regarding natural resources and technological development, if we do not now pay close attention to this problem, it is certain to bring serious consequences in the future.

12586
CSO: 4008/2067

CONFERENCE LECTURE ENCOURAGES WORK IN SOFT SCIENCES

Tianjin KEXUEXUE YU KEXUE JISHU GUANLI [SCIENCE OF SCIENCE AND MANAGEMENT OF S&T] in Chinese No 12 Dec 86 p 1

[Article prepared from lecture by He Zhongxiu [0149 6988 4423]: "I Hope that the Cause of the Soft Sciences Will Flourish and Develop in China"]

[Text] Today, more than 300 workers in the soft sciences have come from all over this country and from more than 10 nationalities to gather here to discuss the problem of youth in soft science research. This occasion makes us all tremendously excited.

When I say that "this makes us tremendously excited," this is no exaggeration, and everyone feels the same. More than 2 months ago, the majority of those participating in the All-China Soft Sciences Research Working Conference were middle aged or older. More than 80 comrades spoke and many achievements were exhibited, all of which unequivocally proved that soft science research truly has a special and important role to play in the socialist modernization of this country. A lecture by Vice Premier Wan Li elicited a great response throughout this country. At present, everyone is calling for the creation of conditions in which a new generation of workers in the soft sciences can mature. As we open our conference here today, more than half of you are young comrades in your twenties and thirties, and how can this not excite us?

Someone asked, what is the aim of calling this conference? It is just in hope that we can create the conditions for our young comrades that will provide the opportunity of a gathering in which to exchange ideas, so that we might promote the development of the cause of the soft sciences in this country.

There are a minority of middle-aged and elder co-workers among us, and we came to the practice of the soft sciences after the breakup of the "gang of four." We have labored for nearly 10 years, and most of us are in our forties and fifties. I am sure you all remember that at that time any proposal to engage in the soft sciences was not understood: what are "soft sciences"? That is too obscure and cannot solve any real problems; when you think about it, distant water cannot quench a nearby thirst; and it was even believed that that was "not a real occupation." But it was in just that kind of atmosphere that some comrades said: "Let us proceed from the actual situation in this country. Let us study the role of science and technology in the economy and in society. Let us explore the rules for the development of science and

technology to understand the basis for development principles and governmental policies regarding efforts in science and technology. Let us review the fundamental experiences of successful management, and let us ascend to the heights of scientific principles to guide our practice. This will allow science and technology to serve the development of socialist modernization, which is, after all, the pressing matter." They said that "even though they are soft sciences, they will still require hard effort," and "even if kept waiting for 10 years, I will still carry on with China's soft sciences!" Classes have gone beyond renouncing the pen for the sword and have instead "renounced hard for soft," "left specialties to take up management," and have resolutely taken up a life work in the soft sciences.

Today, research in the soft sciences is not likely to be seen as "not a real job." We at this conference have the support of so many leading units, the mass media, and research organizations that these are then the conditions created for young skilled personnel in the soft sciences to make their mark. But we cannot say that for these reasons there will be no difficulties for the young in studying and researching the soft sciences. There are in fact various new obstructions, as for example, "Are the soft sciences things that you young people can do?," and "Getting involved in fads!" ... are often-heard opposing views. When some comrades received the invitations to this conference, their unit would not support them, so they could not come. I have heard that some of the younger comrades at the conference today have come on their own expenses by requesting a rotation of their holidays. They have made a long, arduous journey to seek teachers and visit with friends, and they have not flinched in the face of adversity, which deeply moves us.

The soft sciences are necessary for our modernizing development. Comrades who are determined to take up the cause of the soft sciences must have the spirit to be persistent and dauntless and to not be swayed by repeated setbacks. I believe that both we middle-aged and elder comrades and our young comrades should have this drive: be resolute, fear no pressure, and persevere; be tenacious, be not in awe of any hardship or danger, and you will be able to persist; be enthusiastic, take no advantage of anyone, and be willing to commit yourself; be true, engage in no fraud, and seek real results. As long as the direction is correct and we have these four determinations, we can be all-conquering.

In recent years, there have appeared in all fronts throughout the country a group of youth who have set their minds on soft science research, and who are full of life and vitality. They have their own ideas and their own determination, and have produced many achievements, but there has been little in the way of lateral relations, and they have yet to constitute a contingent. If we can create the conditions for them, can provide an opportunity of a gathering in which to share ideas, then not only will we allow them to become known to each other, to strengthen their relations, and to form into a contingent, but also we can allow those who are middle aged to meet the next crop and have each gain from the other. With mutual cooperation, the cause of the soft sciences is certain to flourish even more.

12586
CSO: 4008/2067

CHONGQING UNIVERSITY RAISES OWN RESEARCH FUNDS

Beijing GUANGMING RIBAO in Chinese 20 Jan 87 p 1

[Article by reporter Li Jiajie [2621 1367 2638]: "Creases Competitive Environment, Encourages Faculty to Go Off-Campus to Open Up Sources of Funds for Scientific Research; Last Year Chongqing University Raises Over 13 Million Scientific Research Funds On Its Own; Exceeds Overall All-University Scientific Research Funds by 90 Percent"]

[Text] A fundamental change has taken place in Chongqing University's source of scientific research funds. Statistics up to the end of 1986 indicate that the self-raised funds exceeded overall all-university scientific research funds by 90 percent.

An important reason why the university was able to increase self-raised scientific research funds by such a large amount is that the school did its utmost to create a competitive environment for the faculty and when allocating scientific research funds provided by the state it was not unbiased. Whichever department obtained more results received more scientific research funds next year.

Another important reason is that the school was fully aware that the faculty are in the position of masters of the school. As long as the faculty firmly believe that they can undertake a scientific research topic, even if it will be a big risk, they will firmly support the faculty setting up the topic. After obtaining results for such risky topics, they also firmly support the faculty going into the factories for carrying on further applications research. Through just this one move the university approved investing 700 thousand yuan in resources to mount 50 topics and won back from the factories 240 topics and 6 million yuan in scientific research funds.

In those instances when it cannot be commercialized, research results which win prizes off-campus, the school always awards the faculty school prizes and encourages the faculty to go off-campus to find sources of funds for scientific research.

In 1986, the state appropriated only 1 million yuan in scientific research funds to Chongqing University but the faculty themselves found over 13.5 million yuan.

8226/12624
CSO: 4008/2057

BEIJING JOINT RESEARCH-PRODUCTION ORGANIZATIONS PROLIFERATE

Beijing GUANGMING RIBAO in Chinese 20 Jan 87 p 2

[Article: "Seven Types of Joint Research and Production Appear in Beijing Area; Joint Research and Production Organizations Expand to 450 Including 181 Which Have Spread Beyond the Region"]

[Text] According to information from persons concerned, joint scientific research and production in Beijing Municipality is showing new development momentum. The number of joint organizations is constantly increasing and the area covered is becoming larger. In addition, there is a tendency to develop from casual forms to semi-close and very close forms. Up to the present joint research and production organizations have increased to 450, 181 of which extend across regional boundaries.

Concerned persons also told reporters that 7 models of joint research and production have appeared in Beijing Municipality.

Long-term Comprehensive Technical Cooperation Type
As market competition increases, to improve their technological development ..lity and absorb into their own sphere social and science and technology forces in a variety of forms, many enterprises have formed long-term comprehensive technical cooperation relationships with scientific research units and institutions of higher education. This type of cooperative relationship generally involves the enterprise supplying the topic and certain conditions and the scientific research unit is responsible for attacking the problem and supplying results. The enterprise arranges for intermediate testing and putting it into production. This method of close linking of research, intermediate testing, and production has shortened the research cycle so that scientific and technological results are rapidly converted into productive forces. For example, the polyacrylic high effect catalyst successfully developed by the Yanshan Petrochemical Company in a three-way cooperation with the Academy of Science's Institute of Chemistry and Institute of Chemical Engineering in just a year passed (Xiaoshi) appraisal and in terms of quality achieved international advanced levels. They are now constructing an intermediate testing shop at the Yanshan Petrochemical Company and after going into production it can save 1.8 million dollars a year.

Technical or Intellectual Shares Type
Treating their scientific and technical results or intellectual work as investment in an enterprise, scientific research institutes have increased earnings and rationally divided it among the two parties. This is a new form which has developed on the foundation of past technical transfer. It avoids the difficulty of the enterprise having to pay transfer fees before it has earned any income and at the same time it opens for the scientific research institute a rather stable source of funds and is beneficial for mobilizing the initiative of both sides.

Joint Venture Type
This consists of a plant managed jointly by a research institute and a relevant enterprise, the leadership and management is by agreement between the two sides and both sides provide personnel. The research institute provides the technical results and some of the technicians, and some are also responsible for marketing and market development; the enterprise supplies the plant building, equipment and labor, and the earnings are divided by agreement. The experience of many enterprises proves that once a joint venture relationship is established with a research institute it's like adding wings to a tiger. For example, the Haidian Agricultural Machinery Manufacturing Plant had been losing money for several years and was on the verge of closing down. After joining in a venture with the Iron and Steel Institute they began producing a special type of alloy steel tubing it was in great demand. In 6 years it created a value of production of 23 million yuan, last year the value of production grew 14-fold over the period before the joint venture and profits grew 11.7-fold. The profits handed over to the state increased 45-fold, and labor productivity increased 13-fold.

Complete Technological Development and Engineering Contracts Type
By focusing on development of complete technology and engineering contracts, this type combines research, design, manufacturing, and construction units to form a new technological economic entity which has legal standing. Although there are not many of this type of joint organization at present, they are rather special and have very good prospects for development. For example, the China Recreational Vehicle Joint Company in which the Ferrous Metals Design Institute took the lead and in which over 20 enterprises in Beijing and other areas participate, since its construction it has provided 28 provinces and municipalities with over 1,300 recreational vehicles in more than 80 types and has saved a great deal of foreign exchange.

Industrial Comprehensive Development Type
Comprehensive development focussed on one industry combines laterally research and production units which are scattered in other systems. Generally a casual type alliance is formed first then as needed many semi-close and close type alliances are formed. For example, the dried and fresh fruit improved variety breeding technology and deep processing connected alliance formed by 12 units, including the Academy of Agricultural Sciences' Orchard Institute, Forestry Bureau, Agricultural Academy and some counties and districts has formed 13 joint organizations from formulating dried and

and fresh fruit comprehensive development plans and beginning to promote scientific and technical results, has established municipal, county and key rural specialized fruit tree centers, has propagated 5,100 mu of nursery, 25,000 mu of demonstration orchards, and a demonstration system of 20 million jin of storage and processing capacity. Direct income from just the excellent nursery stock provided in 1986 reached 2.6 million yuan. It played an important role in promoting fruit products production in the Beijing suburbs.

Jointly Run Collective Scientific and Technical Development Agency Type
In the past few years a large group of scientific and technological development agencies owned by collectives and individuals have appeared in the Beijing area, mostly in the Haidian district which has over 100 of them. Many of them are run jointly by the Haidian district, research units of the Chinese Academy of Sciences and various departments of the State Council, and institutions of higher education, and there are also many which are operated by scientific and technical personnel who have voluntarily thrown away "iron rice-bowls" and formed partnerships. Sitong, Kehai, Haihua, and Xintong have already obtained interesting results which have won praise from various areas of society. The value of output of these few companies reached an unprecedented 200 million yuan in 1986.

Joint Scientific Research and Production Group Type
This is a new type which has suddenly appeared. It generally relies on a tap industry and has as its goal developing new technology, new products, new systems, starting new industries, and bringing along old industries, it breaks through boundaries, develops regional advantages, and links research, production and applications units into a group company. For example, the Great Wall Computer Group Company recently approved by the State Council and has 67 participating units is new type enterprise group which is a combination of research, development, production management, applications service, and training which encompasses 50,000 employees and over 1,500 scientists and technicians. Its establishment will promote development of a northern electronics industry base and provide new technological material foundation for development of the economy of the capital and even entire nation.

8226/12624
CSO: 4008/2057

TECHNOLOGY MARKET SURVEY

Tianjin JISHU SHICHANG BAO in Chinese 3 Jan 87 p 1

[Article: "Like the Constancy of the Moon, Like the Rising of the Sun; A Technology Market Survey Report"; first paragraph is source-supplied introduction]

[Text] Editor's note: In the last half of last year, the National Technology Market Survey Directorate organized a survey group jointly with the State Science and Technology Committee, the State Council's Legislation Bureau, State Industry and Commerce Administrative Management Bureau, and the Tianjin Municipal Science and Technology Committee carried out a nationwide technology market survey. They visited 4 provinces, 1 district, and 12 cities (Liaoning, Heilongjiang, Zhejiang, Hunan, Guangxi, Shenyang, Liaoyang, Harbin, Tianjin, Shanghai, Hangzhou, Guilin, Nanning, Zhuzhou, Liling, Yiyang, Changsha) and in 4 months visited research institutes, plants and permanent technology markets and held dozens of informal discussions of different types. Their survey is offered to the reader below.

Quick Action on the Reform of the Science and Technology System Has Had a Big Impact; Science and Technology Market's Have Put Down Firm Roots in China

Since the CPC Central Committee announced their decision on reform of the science and technology system, the commercialization of technological results and opening up of the technology markets has moved rapidly nationwide. According to incomplete statistics from 34 ministry committees, 29 provincial, municipal and autonomous district and 7 cities with province-level economic decision-making authority, there are over 5,000 agencies engaged in technology trade and the volume of trade actually conducted in 1985 in the technology market was over 2.3 billion yuan. In the reform of the science and technology system, the technology market moved the fastest and was influenced the greatest. It has put down firm roots in China.

However, the technology market is something new. Since the last half of 1985 it has encountered conflict several times and since they did not fully understand the documents from upper echelons, some departments and local areas were not clear about the dividing lines between some policies

and confused opening up technology markets with the incorrect style of party and government agency engaging in trade and treated them as "fly-by-night companies." Some scientific and technical development and technological product management agencies were subjected to various kinds of pressure. The Central Committee promptly discovered and corrected these phenomena so that the vigor of nationwide technology markets would develop again and the technology market is now steadily advancing.

Currently, nationwide various types of technology trade exchange agencies have been springing up like bamboo shoots after a spring rain. Science committees, economic committees science associations, industrial societies, industrial offices, academies of sciences, education committees and democratic parties, mass organizations, and civilian organizations have established their own technology trading agencies and various areas have formed preliminary multi-level, multi-channel, multi-form technology trading network. Various "armies" have formed their own powerful "front armies," which have both horizontal alliances and mutual competition and promoted the development of technology markets.

According to Tianjin's statistics of a year ago, the entire municipality had over 570 various types of technology grading agencies, involving over 60,000 persons, distributed in various industries and trades and cities, districts and counties to form a close alliance of science and technology and the economy and an important force for promoting economic development. The technology development business agencies and branches now established in Shenyang number over 6,000. The Shanghai technology market is nicknamed "8th Route Army": i.e., Shanghai Technology Development Exchange Center, Shanghai Industrial Foundation, Starfish Technology Development Company, Science and Technology Consulting Service Center, Shanghai Higher School Science and Technology Service Center, Employees Technology Association, and Civilian-run Technology Development Agency. With their own solid strength they form an enormous rank. According to incomplete statistics from markets in Guangxi, over 200 technical trade agencies for technical development and technical consulting have been established. Hunan Province has also established 574 technical development, technical service, and technical consulting agencies. The provinces have preliminary technical market networks of different levels.

Technology trade forms are now developing profoundly in multiple functions and multiple directions. 1) Transferring pure technology to lower levels as a package. For example, the Tianjin Technology Association and a light industry bureau helped the Dagang Tool Works No 6 to start an imported loop cable production line, and accepted and completed such mission as translating blueprints, checking equipment, installation and testing, and connecting the machinery and producing and ensuring that the production line would go into production and operate normally. 2) Intermediate service agencies developing in-depth service, gradually changing the method of purely picking up service expenses. The Shanghai Science and Technology Development Exchange Center stressed intensifying the creation of "talent banks" and management

of civilian-run science and technology agencies, exchanged various types of talent so that civilian-run agencies could make a contribution to national economic construction. 3) Vigorous development of lateral connections between scientific research and production. Through technology market mechanisms many areas have established allied cooperative organizations of scientific research, education, and production in many forms and according to incomplete statistics, over 9,800 allied organizations of scientific research and production have been established nationwide. 4) Developing technological cooperation internationally. Some have developed series of products through joint investment with foreign factories and merchants, some have arranged technology exports, some units in cooperation with foreign merchants have entered the international market with advanced technology. 5) Assisting enterprises to develop technological demonstrations so that they will change from reckless importation of technology will change to consultation and verification and scientific policy determination which promoted enterprise development.

Stimulate the Economy, Science and Technology Relieve Inadequacy, Train Talent, the Social Benefits Produced by the Technology Market Are Clear

Practice of the past few years has shown that development of the technology market has promoted technology transfer, stimulated the local economy, and brought obvious social benefits and economic benefits. On the basis of the Shanghai Municipal Science and Technology Development Exchange Center's tracking analysis of 104 technology contracts signed in 1985, each yuan of contract increased the value of production by 16 yuan, increasing income 8.6 yuan, scientific and technical personnel receive 1 yuan, and the state increased revenue by 36 yuan. Seen from the perspective of the 31 Center projects checked and accepted in 1985, invested expenses were 7.5 million yuan, value of annual output was 62.792 million yuan, equivalent to 2.6-fold the total investment. The results of some single projects the benefits were even higher. The instances of factories and mining enterprises in other areas such as Liling City and the Yiyang District in Hunan and even Huayuan County in western Hunan making up deficits and increasing surpluses, coming back to life from the dead, increasing output and income and escaping poverty and becoming rich through importing technology and development new products are too numerous to mention.

News also keeps coming in of the victory of the technology markets in expanding science and technology to relieve poverty and to organize and implement "spark plans." For example, around a "spark plan", the Hunan Provincial Science Association's technology market broadcast technology supply and demand information, held 2 large information meetings, printed 4 volumes of material, issued over 8,000 items of information and abstracted 417 information items on "short even and quick" technology results. The Yiyang District technology market actively supports the Yiyang County Microbiology Institute's implementation of the state's "spark plan" new technology for cultivating black tree ears, it has improved technical training, set up demonstration plants, and has helped

10 cultivation specialists to escape poverty and become rich. In the past few years, the Zhuzhou City Technical Association has sent out 118 specialist technical service brigades for technical assistance to over 80 enterprises in Guizhou, Yunnan, Guangxi and the border areas of western Hunan, they saved 31 enterprises which were on the verge of closing, with new increases in the value of output of over 70 million yuan. The Guangxi Science and Technology Development Center undertook such tasks as the formulation and implementation of a "spark plan" for the entire district and the technical development of the mountain region. They helped the counties in the mountain region formulate and develop overall plans, arranging technical development projects for 17 mountain regions with an investment of 16.78 million yuan.

To suit the needs of technical market development, technical markets have trained a large number of technical administration management personnel and various types of specialist technicians. The Shenyang Technical Market Research Association has been assigned by the municipal science committee the task of standardizing and giving specialized training to middle level personnel in various agencies and technical market management personnel city-wide, beginning in June, 1986, and has already held 4 classes and trained 240 persons, and by the end of the year will have trained over 1,000 persons. In the past few years, the Tianjin Municipal Science and Technology Consulting Service Company has trained over 2,000 specialized technicians. The Yiyang Regional Technical Market in Hunan has held 36 specialized training classes and trained 2,670 technicians. The Zhuzhou City Employees Technology Association has begun specialized technical training in which over 10,000 persons have participated and over 600 lectures on technology have been held providing a solid foundation for technical market development.

8226/12624
CSO: 4008/2057

FATIGUE STRENGTH TEST ROOM DEVELOPED

Beijing KEJI RIBAO in Chinese 16 Jan 87 p 2

[Article by Wang Wergvo [3769 5898 0948]: "Aircraft Fatigue Strength Test Room Constructed; Brings Glad Tidings For Aviation Industry and Air Units"]

[Text] China's first aircraft fatigue strength test room of 1980's level was formally established on 30 December 1986 at an Air Force Research Institute.

The aircraft fatigue strength test room is a new facility for testing and studying the life and reliability of air force aircraft currently in service. In the past, the "lead" aircraft method was used to determine the useful life of domestically manufactured aircraft, i.e., first an aircraft was test flown and if no trouble occured with the aircraft in 300 hours then the other aircraft of the same type were provisionally considered to have a useful life of 300 hours. Then the "lead in" aircraft continued to be flown. To a considerable degree this method was a risk.

The birth of the aircraft fatigue strength test room is glad tidings for the aviation industry and flying units. In this test room various types of aircraft can be fastened to the test frame completely and various inflight load maneuvers simulated. Deformations and cracks produced in a part measured by monitoring of the aircraft through 512 channels can be accurately recorded in the control system display and the useful life of the aircraft determined.

The test room is not only suited for use in measurement and research on various types of aircraft but also has broad civilian use for testing force-bearing parts of motorized vehicles, metallurgical machinery, agricultural machinery and small ships.

8226/12624
CSO: 4008/2057

CAS SHANGHAI EARNS FOREIGN EXCHANGE THROUGH EXPORTS

Shanghai WEN HUI BAO in Chinese 11 Jan 87 p 1

[Article by Zhou Yuan [0719 0955]: "Open up the International Technology Market, Establish Joint-Venture Companies; Chinese Academy of Sciences Branch Creates New Path Using Science And Technology To Create Foreign Exchange; High Tech Products Marketed All Over The World, Last Year Export Volume Exceeded Import Volume"]

[Text] The research institutes of the Shanghai Branch of the Chinese Academy of Sciences have opened up the international technological market and have signed with foreign plants and merchants for cooperative development projects and established joint venture companies. Many high tech products are marketed throughout the world, last year creating a record of export volume exceeding import volume. This new road using science and technology to create foreign exchange clearly has a bright future.

In some cooperative research and development project, the achievements of the Shanghai Institute of Pharmacology are striking. This institute has signed 7 contracts with 6 pharmaceutical companies in Japan and the United States to develop new medicines cooperatively. They include antineoplastic drugs, gastric ulcer drugs, new antibiotics, and health beverages that can treat melituria. Generally, after the other side has screened the preliminary research results provided by our side, they have priority production rights and apply for a patent in the relevant country but the inventor's rights belong to us. Foreign pharmaceutical companies annually provide scientific research expenses to the Shanghai Institute of Pharmacology, and once patent results have been spread, the profit is divided between the two sides. Clinical tests on an anti-cancer drug jointly developed by the Institute of Pharmacology and the Japanese Zenyaku Co., Ltd joint stock company have already been completed and 10 companies in Europe and America have applied for patents and many famous foreign pharmaceutical companies have expressed interests in buying it. So that Chinese medicines can better benefit mankind, this institute and the Japanese Yamanouchi joint stock company has signed a joint 5-year development contract and has also made advances.

Since last year, in Shanghai the first joint ventures companies between institutes and foreign merchants have been born in the Chinese Academy of Sciences system. Last July, the Shanghai Institute of Technical Physics

set a precedent in establishing a joint venture with a Japanese company--(Nisaila) Company Ltd.--in which both sides will provide technology, equipment and funds, and most of the products will be sold in the international technology market. This joint venture is currently installing equipment in Shanghai and is about to go into trial production, The Shanghai Silicate Institute has established a joint venture with the Yongqing Company of Singapore primarily to produce new types of energy-saving insulating materials and will construct a petrochemical industry enterprise in Southeast Asia to take care of pipeline design and materials supply.

From the recent data of the Shanghai Branch of the Dongfang Scientific Instruments Import-Export Company of the Chiense Academy of Sciences, the Shanghai branch has thoroughly turned around the past situation of "only use foreign exchange, not create foreign exchange". Last year's export volume exceeded import volume by one-third. The BGO crystals of the Shanghai Silicate Institute are the highest in output volume in the world and a high tech product of the highest quality. The large order from the cooperative group of the Western European Nuclear Center headed by Professor Ding Zhaozhong [0002 5128 0022] will be used in key parts of the world's largest electron-positron collider. Last year the Silicate Institute produced over 2,000, creating over 2 million yuan in foreign exchange. The Shanghai Optics and Fine Mechanics Institute's YAG crystal began to enter the U.S. market and is used by world famous scientific instrument companies.

8226/12624
CSO: 4008/2057

END

END OF FICHE

DATE FILMED

12 Aug. 1987